Republic of Iraq
Ministry of Higher Education & Scientific Research
University of Kerbala
College of Engineering
Department of Civil Engineering

CLIMATE CHANGE EFFECT IN STORM WATER NETWORK SYSTEM: CASE STUDY IN KERBALA

A Thesis Submitted to the Department of Civil Engineering, University of Kerbala in Partial Fulfillment of the Requirements for the Degree of Master of Science in Civil Engineering (Infrastructure Engineering)

By

Ghofran Abdul-Alhussien Mohamed

BSc. in Civil Eng. / University of Kerbala (2015)

Supervised by

Prof. Dr. Basim Khlail Nile

Assist. Prof Dr. Waqed Hammed Hassan

2019

بسم الله الرحمن الرحيم

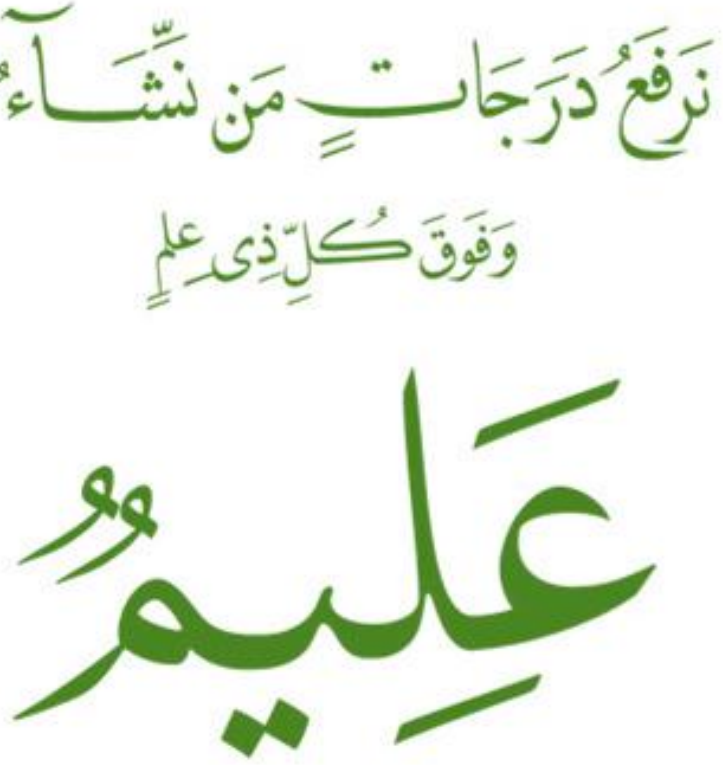

صدق الله العلي العظيم

سورة المجادلة - الآية ﴿١١﴾

ABSTRACT

The flooding of the storm water network is caused by climate change, land use change, increase in urbanization, and the wider population. This study deals with the development of models to extrapolate future change in rainfall events in order to protect the infrastructure of the storm water network from flooding. The Al-Abbas quarter in Karbala city, Iraq was selected as a case study. For the first analysis, the effect of climate change on the predicted rainfall intensity for the future period (2017-2070) depends on historical data for the period of 1980- 2016. This was conducted using the artificial neural network (ANN) model. The input layers that enter to ANN model include climate change parameter include (monthly rainfall, min. temperature, max. temperature, wind speed, humidity, and sunshine). This data divided to training data represent 95% of the data and testing data represent 5% for calibration process. Output parameter include rainfall intensity. Following this, a Storm Water Management Model (SWMM) model is constructed in order to assess the flood conditions of the study area for expected rainfall intensities. The results indicate that the maximum rainfall intensity will reach 46.48 mm/h. in 2067. This value represents three time of the design intensity. The percent of the flooding manhole increase with progress of time. At the end of the design period (2070) stage 1has been decrease with rate about 39.2%, stage 2 has been increase with rate about 14.2%, stage3 has been increase 6 time, stage has no change, and stage 5 increase with rate about 6% compared to beginning period (2017).

SUPERVISOR CERTIFICATE

We certify that this thesis entitled **"**CLIMATE CHANGE EFFECT IN STORM WATER NETWORK SYSTEM:CASE STUDY IN KERBALA**",** which is prepared by " Ghofran Abdul-Alhussien Mohamed ", is under our supervision at University of Kerbala in partial fulfillment of the requirements for the degree of Master of Science in Civil Engineering (Infrastructure Engineering).

Signature:

Name: Prof. Dr. Basim Khalil Nile

(Supervisor)

Date: 20 / 9 / 201٨

Signature:

Name: Assist. Prof Dr. Waqed Hammed Hassan

(Supervisor)

Date: 20 / 9 / 201٨

LINGUISTIC CERTIFICATE

I certify that this thesis entitled **"**CLIMATE CHANGE EFFECT IN STORM WATER NETWORK SYSTEM: CASE STUDY IN KERBALA**"** which is prepared by Ghofran Abdul-Alhussien Mohamed under my linguistic supervision. It was amended to meet the English style.

Signature:

.....

Linguistic Supervisor:

……

Date: / / 2018

EXAMININATION COMMITTEE CERTIFICATION

We certify that we have read the thesis entitled **"**CLIMATE CHANGE EFFECT IN STORM WATER NETWORK SYSTEM: CASE STUDY IN KERBALA**"** and as an examining committee, we examined the student **"**Ghofran Abdul-Alhussien Mohamed **"** in its content and in what is connected with it, and that in our opinion it is adequate as a thesis for degree of Master of Science in Civil Engineering (Infrastructure Engineering).

Signature:
Name: ……..
Date: / / 2019
(Supervisor)

Signature:
Name: ……
Date: / / 2019
(Co-Supervisor)

Signature:
Name: …….
Date: / / 2019
(Member)

Signature:
Name: …….
Date: / / 2019
(Member)

Signature:
Name: ……..
Date: / / 2018
(Chairman)

Approval of Civil Engineering Department

Signature:
Name: Assist. Prof. Dr. Waqed H. Hassan
(Head of civil Engineering Dept.)
Date: / / 2018

Approval of Deanery of the College of Engineering - University of Kerbala

Signature:
Name: Asst. Prof. Dr. Basim Khlail Nile
(Dean of the College of Engineering)
Date: / / 2018

This thesis is dedicated to:

My parents and my family, brothers, sisters, uncle and cousin for their love and continuous prayers

ACKNOWLEDGMENTS

Praise and Glory be to **Almighty ALLAH** for bestowing me with health and power to complete this work and to achieve something that might serve humanity. I would like to thank my parents for their continuous support to complete my research work.

The author would also like to thank, in particular, his director of the study and main academic supervisor, **Dr. Basim Khalil Nile, Dr. Waqed Hammed Hassan** for there valuable assistance, suggestions, advice, continuous guidance and encouragement throughout the research.

Special thanks are also to those who provided help and support for completing the research work, especially my husband, Eng. Mostafa Amari for always hortative to completing the research work.

Ghofran Abdul-Alhussien Mohamed

CONTENTS

LIST OF FIGURES

LIST of TABLES

ABBREVIATIONS

Abbreviation	Description
ANN	Artificial Neural Network
D.S.K	Directorate of the Stream of Karbala
DC	Determination Coefficient
DEM	Digital Elevation Model
G.A.M.S.O	General Authority for Meteorology and Seismic Observation
GIS	Geographic Information System
IPCC	Intergovernmental Panel on Climate Change
M.C.H.PM	Ministry of Construction and Housing and Public Municipalities
R	Correlation coefficient square
RMSE	Root Mean Square Error
SPSS	statistical package for the social sciences
SSA	Storm and Sanitary Analysis
SWMM	Storm Water Management Model
TIN	Triangular irregular network
USGS	U.S Geological Survey

Chapter One

INTRODUCTION

1.1 Introduction

The growth of cities worldwide is associated with an increasing demand for sanitation and drainage infrastructure in the context of the water cycle .combined with the effect of climate change ,which alter the rainfall patterns ,the situation of these system in urban environmental is critical .part of the existing sewer network required an imminent renovation ,other must be constructed in developing area, where as storm water runoff becomes as threat in terms of flooding because of soil impervious .in this part should be determine the best practices aimed at reducing these issues from innovative environmental and economic view point and at the same time adapt cities to climate change.(Boix, 2017)

Climate change significant impact on precipitation, when the rainfall increase this led to urban flooding in storm network. Global warming causing all over the globe increase in temperature and sea level , this increase causing rise in rainfall intensity and frequency, then this led to flooding.(Jung et al., 2015).

Increase population and urbanization led to increase improvise area this decrease infiltration and increase runoff quantity, so this also led to flooding.

To reduce the hazard of flooding would be predict the rainfall intensity, artificial neural network (ANN) model used to predict rainfall intensity under the effect of climate change.

The origins of artificial neural networks (ANN) are in the field biology. The biological brain consists of billions of highly interconnected neurons forming a neural network. Human information processing depends on this connectionist system of neurons cells. Based on this advantage of information processing, neural networks can easily exploit the massively parallel local processing and distributed storage properties in the brain. (Jeng et al., 2003)

Storm water management model (SWMM) has ability to link many of parameter on the performance of storm network to get many of option such as water flooding and water depth.

The model is widely used for planning, analysis and design related to drainage systems in urban areas. The model, provides an integrated Windows environment for editing input data, running simulations, and viewing the results in the form of thematic maps, graphs, tables, profile plots and statistical reports.(Gironás et al., 2010)

The study area is Karbala, Iraq is faster urbanization city because it's characterize by religious nature and also the political conditions in the country caused immigration thousands of citizens from different cities to it. The urbanization in the study area [al-Abbas quarter, Karbala] converts the most of the lands from pervious into impervious area where that increase the urban flooding. Due to that the control of the urban flooding quantity become an important issue to reduce the cost of infrastructure damage..

1.2 Statement of the problem

Al-Abbas section located at the north-east of the center of Karbala. Urban flooding of the storm network is the problem of the study area. This problem growth with climate change and increase of population, urbanization. The climate change led to increase of rainfall intensity higher

than design intensity of the storm network of the study area and this led to flooding. The study area suffering from flooding during rainy season.

1.3 Objective of the study

The aim of this research is to study the impact of climate change on expected rain intensities in the study area and to determine the expected flood ratios in rainwater drainage networks.

1.4 Methodology of the study

Methodology of the study summarized as steps follow:

1. Collection of metrological data from the General Authority for metrology and Seismic Observations (G.A.M.S.O) for period from 1980 to 2016 include (monthly rainfall (mm), mean maximum temperature(c°), mean minimum temperature(c°), mean relative humidity (%), mean wind speed (m/s), mean sun shine (hr./day),and the data collected for period from 1981 to 1990 include rainfall intensity for Karbala station in (mm) for 1 hr.
2. Collection the field data for the Al-Abbas quarter from Directorate of the Streams of Karbala (D.S.K) include pipe and manhole and its properties for storm water networks.
3. Built artificial neural network (ANN) model to predicted rainfall intensity for 53 years next.
4. Made calibration for the ANN model to choose the best model by many statistical indicators.
5. Application expected rainfall intensity on the storm network for the study area by using SWMM model to estimating the flooding ratio.

1.5 Thesis Structure

This thesis consists of five chapters as follows:

- Chapter 1, illustrates the objectives and methodology of the thesis.
- Chapter 2, shows the previous studies for the various parts, the first parts deals with climate change, the second parts deals with flooding and it is reason, the third parts deal with ANN model, and the final parts deals with SWMM model.
- Chapter 3, description ANN model, SWMM model and description the study area and the properties of all data collection.
- Chapter 4, display the result of rainfall intensity model, result of flooding model and display suggestion scenario for the future.
- Chapter 5, contain the conclusions for the present the study and recommendations for future work.

Chapter Two

LITERATURE REVIEW

2.1 Introduction

This chapter include previse study for the flowing object: climate change, reason of flooding (include: climate change, urbanization, population, CO2 concentration and land use), ANN model to predict rainfall intensity depend on historical climate change, and simulation rainfall intensity by SWMM to determine flooding for the study area.

2.2 Climate change

Climate change include changing in the parameter of climate such as rainfall, temperature, wind speed, humidity , sun shine, so rainfall and temperature significant impact parameter on flooding for example increase of temperature and sea level causing increase in rainfall intensity and frequency.

The Middle East is largely arid to semi-arid and fresh water is often a scarce and precious resource. The combination of a stressed fresh water resource and rapid population growth, substantially increases the vulnerability of the region to future climate change. Simulating the climate of the region is a challenge for climate models (Evans, 2009)

The Intergovernmental Panel on Climate Change (IPCC) state that an increase in temperature of between 1˚C and 3.5˚C due to rising in

greenhouse gases by the end of this century (Houghton, 1996) and (Bijlsma et al., 1996) state that is rising in sea level between 13 and 94 cm.

Denault et al. (2006) Studied the effects of increased rainfall intensity and evaluated infrastructure future drainage capacity in Mission/Wagg Creek watershed in British Columbia, Canada by utilising the SWMM technique. The result concluded that, in future, rainfall intensity with short duration may be slightly increased. However, this does not happened as sharply in the Mission/Wagg Creek system.

Sansom and Renwick (2007) evaluated the impact of future climate change, this effect can causing both floods and droughts. Using general circulation models (GCMs) to estimate climate change in New Zealand, the result that found increase in rainfall intensity due to increases in rainfall with climate change.

Evans (2009) studied prediction of future climate change in the middle East by using 18 global climate models in the Intergovernmental Panel on Climate Change, the study conclude the temperature rising (1.4 ˚C at mid century_4 ˚C at the end century) and lower in precipitation epically in, Turkey Syria, Northern Iraq, Northeastern Iran and the Caucasus.

Nie et al. (2009) Studied effect of climate change on urban drainage systems at Veumdalen catchment in Fredrikstad, Norway as case study. By using predicted and artificial climate scenarios to evaluate climate change. The result conclude the number of flooding manholes and number of surcharging sewers may change hugely and irregularly with a small change of precipitation, and change with events and periods.

Hassan et al. (2017) evaluated the behavior of storm networks of the Middle East region (Karbala city, Iraq) to predict future flooding hazards caused by climate change, specifically in case of inadequate sewer connections. The study utilized the SWMM model for Karbala's storm drainage network simulation by using continuous hourly rainfall intensity data from 2008 to 2016. It was concluded that, without consideration of additional sewage due to an illegal sewer connection, the system was sufficient as designed. The results indicated that the SWMM was efficient for modelling urban flood forecasting, and without surface runoff routing, the urban flooding might not perfectly forecast.

Osman (2017) Studied climate change effect on precipitation in the dry medium of Iraq by using Seven Global Climate Models (GCMs) for three period selected 2011-2030, 2046-2065 and 2080-2099. The study reported that annual mean precipitation decrease for most region of Iraq at end of the 21st century.

2.3 Flooding model

2.3.1 Introduction

Flooding can be define as incapability of storm water network to accommodating of incoming of water. So there are many reason of causing flooding include: change in climate ,change of land use, and increase of urbanization, population, CO2concentration.

The EPA Storm Water Management Model (SWMM) is simulation model utilized to simulation of runoff quantity and quality from primarily urban,it is first develop in 1971 (Rossman, 2010). The network simulated in SWMM containe of pipe, manhole ,and subcatchment connected to nearest manhole.

2.3.2 SWMM Modeling capabilities

SWMM calculations for various hydrological processes that produce runoff from urban areas.These include(Rossman, 2010):

- Precipitation of varying time.
- Evaporation of permanent surface water.
- Snow melt and accumulation
- Intercept the rain from storing depression
- Rainfall leakage phenomenon in unstable soil layers
- percolation the water that infiltrated into groundwater layers.
- Mixing happened between the drainage system and groundwater.
- Directed the nonlinear reservoir to the wild flow.

The study area was subdivided into a group of smaller and homogeneous sub-regions to achieve spatial change in all of these processes. Each subclass contained its own part of previous sub-sub-regions. The land flow can be directed between the entry points of the drainage system or between the sub-zones, between the subregions.

SWMM also include an elastic group of hydraulic modeling apilities used to guid external inflows and runoff through the drainage system network of pipes, channels, storage/treatment units , and conversion structures. These containe the ability to:

- Dealing with networks of unbounded size.
- A various collection of open conduit and standard closed forms as well as natural channels are use.
- Special modular items like pumps , openings, dams, flow separators, and storage / processing units.

- apply groundwater, water quality inputs from surface runoff ,and external flows .
- Dry weather sanitary flow, interflow, rainfall-dependent infiltration/ inflow, and userdefined inflows.
- Using either full dynamic wave flow routing or kinematic wave methods.
- model different flow regimes, like surcharging, backwater, surface ponding, and reverse flow.
- apply user-defined dynamic control basics to simulate the working of pumps, weir crest levels, and orifice openings.

SWMM can also evaluation the production of pollutant loads associated with this runoff, In addition to modeling the generation and transport of runoff flows,. The following operations can be designed for any number of user-defined water quality components:

- Accumulation of pollutants in dry weather on different land uses.
- Pollution gases from land use during storm events - direct contribution to rainfall precipitation.
- Reduction buildup in dry-weather due to street cleaning.
- Due to BMPs the washoff load is reduction.
- To any point in the drainage system can entry of user-specified external inflows and dry weather sanitary flows.
- Directed of water quality compenents out of the drainage system.
- Decrease the compenent focus out of natural processes in pipes and channels or by treatment in storage units.

2.3.3 Typical Applications of SWMM

SWMM has been utilized in thousands of sewage and rainwater surveys worldwide. Typical applications include (Rossman, 2010):

- Flooding control by design and sizing of drainage system components
- Determine the size of retention facilities and their appendixes for water quality protection and flood control.
- Normal flood mapping of natural channel system.
- Reducing the combined sewer overflowsby designing control strategies.
- Assess the effect of infiltration and inflow on sewage nozzles.
- Production of non-point-of-point contaminated loads for trash distribution studies.
- minimizing wet weather pollutant loadings by assess evaluating the effectiveness of BMPs .

Schreider et al. (2000) reported how a significant amount of CO2 concentration in the atmosphere could contribute to the extent of flooding. The study features two main sections. Firstly, the modelling of frequency and magnitude of the flood in the context of global warming is assessed. This phenomenon is associated with rainfall intensities. The second section involves the estimation of changes in the susceptibility of flooding that appears in urban areas with the use of greenhouse effect-related flood data. The results of modeling for all cases indicated that when CO_2 conditions were dual this led to a rise in the magnitude and frequency of the flooding events and these vary from one place to another.

Reynard et al. (2001) discussed the effect of climate and land use changes on the flood regimes of large U.K. catchments by using continuous flow simulation model (CLASSIC). They concluded that in the 2050s, climate change would increase the frequency and magnitude of flooding events in these catchments. However, land use changes show a marginal impact on the flooding.

Denault et al. (2006) studied the effects of increased rainfall intensity and evaluated infrastructure future drainage capacity in Mission/Wagg Creek watershed in British Columbia, Canada by utilizing the SWMM technique. The result concluded that, in future, rainfall intensity with short duration may be slightly increased. However, this does not happened as sharply in the Mission/Wagg Creek system.

Nirupama and Simonovic (2007) studied hazard of flooding due to raising urbanization in the City of London in the province of Ontario in Canada. Quantitative assessment for the hazard of river flooding to London by analysis meteorological and hydrological data in additional to analysis land use classification. The study found that between 1974 and 2000 there has densely urbanization in the watershed of the top Thames River, the City of London is section of it so this led to increase hazard of floods.

Semadeni-Davies et al. (2008) estimated for storm water flow the climate change effect and urbanization in Helsingborg, south Sweden. using special drainage simulations for present situation moreover two climate (medium and high), run period of simulations were 15 month. The result found raise in heavy rainfalls this led to increase volumes of peak flow peak flow volumes and raise risk of flooding.

Saghafian et al. (2008) Studied flooding cause by climate change, land use change due to roof roughness and infiltration in the Golestan watershed located northeast of Iran. using trend analysis for three stations inside the watershed showed that two stations were subject to human change on the yearly maximum flood record. To build model for rainfall-runoff Using a calibrated event-based, the study found land use changes

more effectively on the flood peak discharge from that some sub watersheds.

Huong and Pathirana (2013) assesed effect of climate change and Urbanization on future urban flooding in Can Tho city, Vietnam. Built future scenario by using group of simulation model include: using a land use simulation model (Dinamica EGO), atmospheric model (WRF). The study concluded that the worst situation happened when a sea level reach to 100 cm and the flow from upstream and Variation in river level.

Jiang et al. (2015) Utilized planning and management models for urban flooding, in the Dongguan City in southern China, an area which rapidly became urbanized. (SWMM) is a tool used for this application. The results indicate that the area studied will not experience flooding when the return period precipitation is one year. However, the area studied will be submerged when the return period precipitation is 2, 5, 10 and 20 years.

Jung et al. (2015) studied climate change effects on urban flooding in the drainage basin of Gunja, utilizing the SWMM model to make a single event simulation of runoff quantity. The results conclude that when there were increases in the short duration rainfall intensity, this led to the rising of the simulated peak discharge from SWMM.

2.4 Artificial neural network (ANN)

An artificial neuron network (ANN) is a computer model based on the functions and structure of biological neural networks.

ANNs are modeling tools for nonlinear statistical data where complex relationships between inputs and outputs are formed or patterns are found. ANN is also famous as neural network.

ANN is used as a random function approximation tool because it has one of the most recognized features that it can actually learn from controlling data sets in addition to having many other features. . ANN takes

data samples instead of full datasets to access solutions, saving money and time.

ANNs have three interconnected layers. The first layer consists of entered neurons. These neurons send data to the second layer, which in turn sends neurons to the third layer, as can be seen in Figure (2.1). And to clarify the idea better, Figure (2.2) describe how ANN internally working and gives the best results.

The training of the artificial neural network includes a selection of permitted models with several associated algorithms. (Cybenko, 1989, Hornik, 1991)

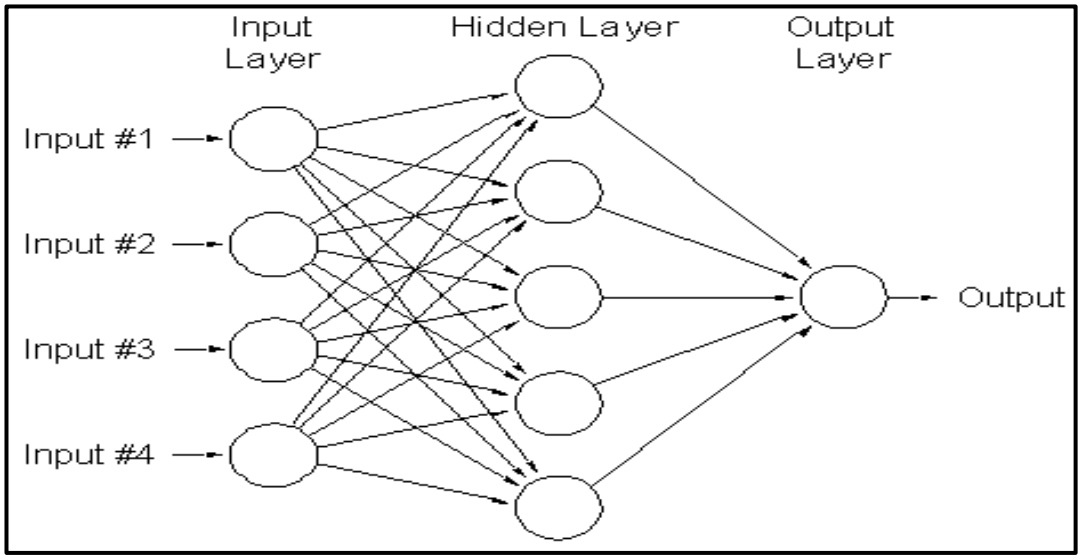

Figure 2-1 A schematic presentation for ANN methodology

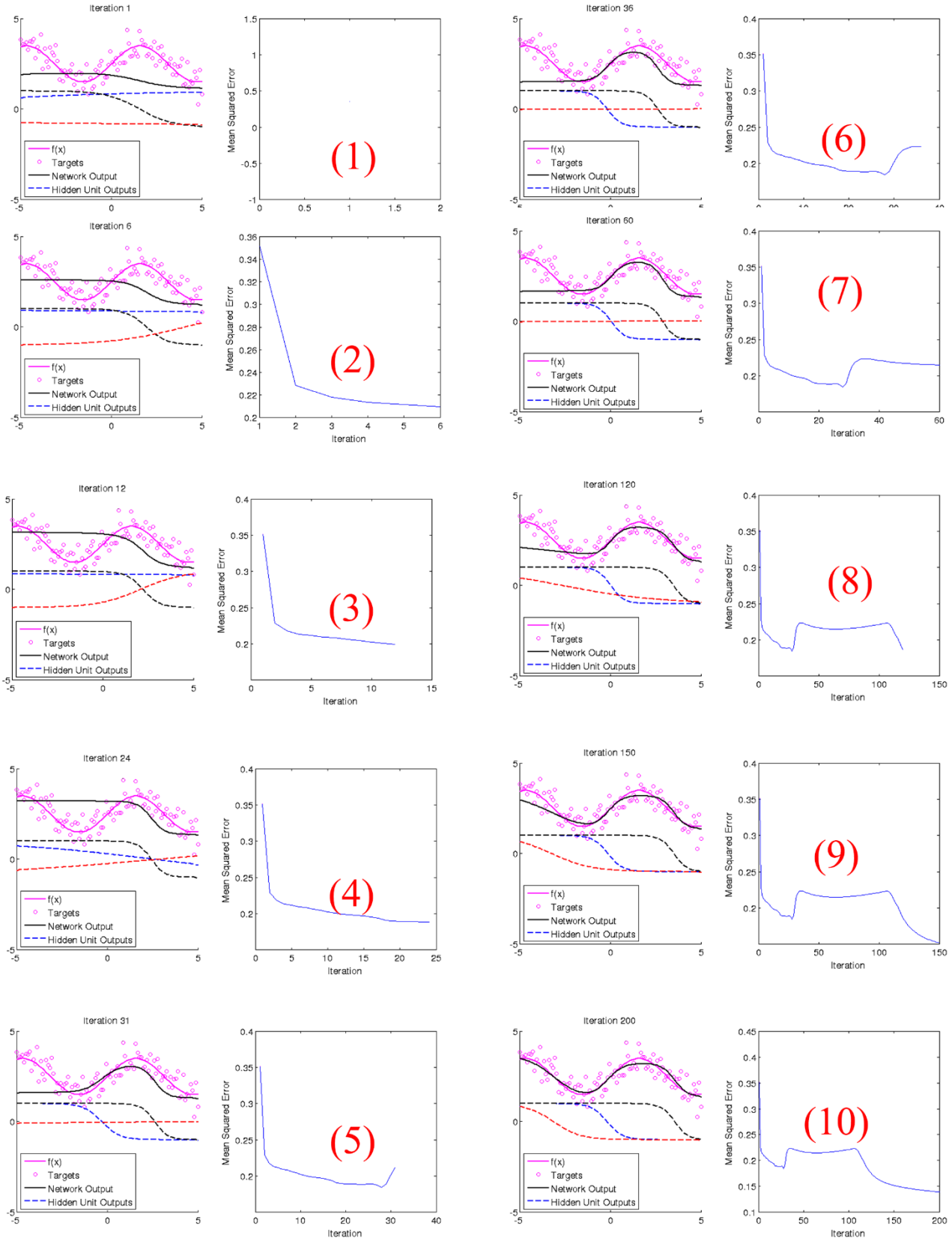

Figure 2-2 example of ANN working methodology

2.4.1 ANN components

Artificial neural networks are typically composed of input layers, hidden layers and output layers, as can be summarized below(Hinton et al., 2006):

1- Input Layer: The input layer of a neural network is composed of artificial input neurons, and brings the initial data into the system for further processing by subsequent layers of artificial neurons. The input layer is the very beginning of the workflow for the artificial neural network.
2- A hidden layer in an artificial neural network is a layer in between input layers and output layers, where artificial neurons take in a set of weighted inputs and produce an output through an activation function. It is a typical part of nearly any neural network in which engineers simulate the types of activity that go on in the human brain.
3- The output layer in an artificial neural network is the last layer of neurons that produces given outputs for the program. Though they are made much like other artificial neurons in the neural network, output layer neurons may be built or observed in a different way, given that they are the last "actor" nodes on the network.

2.4.2 ANN and Civil engineering applications

A reliable model for any storm or sanitary network is essential in order to provide a tool for predicting its performance and to form a basis for controlling the operation of the process.

ANN Technique has the ability to build prediction model, there are many application used ANN technique such as : rainfall intensity , coefficient of discharge ,inflow of reservoir, water quality index (SUJANA PRAJITHKUMAR et al.), sedimentation load (Bouzeria et al., 2017). It is

consist of three layers input layers, hidden layers (Treatment layers), and output layers.

Dawson and Wilby (1998) studied prediction of flow using actual hydrometric data in two flood-prone UK areas by using artificial neural network (ANN). The result found the prediction similar goodness to that obtain from operational systems for the River Amber.

Tokar and Johnson (1999) evaluated the prediction of daily rainfall as a function of daily precipitation, temperature, and snowmelt for the Little Patuxent River watershed in Maryland by using artificial neural network (ANN). The study conclude that prediction data from ANN more accuracy and flexibility, and the study conclude that using of ANN shortens calibration data, and reduces the length of the time spent in calibration of the models.

Jain et al. (1999) predicted inflow for the reservoir and operation it by using artificial neural network (ANN) in the state of Orissa, India as case study, The study found that the ANN is using in effect for operation of reservoir and prediction of inflow of it and ANN strong device for mapping of input –output.

Luk et al. (2001) Studied extrapolate of the rainfall. By using artificial neural network ANN that represent nonlinear mapping between inputs and outputs. Case study in the western suburbs of Sydney, the study conclude the result of forecasting by realization of ANN.

Al-Ansari et al. (2014) Evaluated the rainfall quantity for long term(winter , spring , summer , autumn) by using artificial neural network (ANN). The study were take Sinjar area, northwest of Iraq as a case study. The result discover that the average rainfall decrease.

Alfatlawi and Alshakli (2015) forecasted coefficient of discharge for stepped morning glory spillway by using artificial neural network

(ANN). The study show that the coefficient of discharge of stepped morning glory Spillway reduce as rising (head/length) and/or (head/radius) ratios.

2.5 Summary

The previous study indicate that ANN gave prediction result has similar quality to field result (Dawson and Wilby, 1998) , ANN gave prediction result has more accuracy and flexibility(Tokar and Johnson, 1999).

Most previous studies consider climate change to be a change in temperature and rainfall but we will consider climate change as change in wind speed, humidity, sunshine in addition to change in rainfall and temperature.

Chapter Three

MODELING AND CASE STUDY

3.1 Introduction

This chapter involves three main stages. In each stage, all required data, parameters, and characteristics shall be discussed in next subsections.

The first stage shall involve the Artificial Neural Network technology (ANN), brief description, its work methodology, and characteristics of the input parameters. The ANN technique shall be performed utilizing the ANN program version. It is worth to mention that although used ANN version has stopped supporting by the created company nowadays, but it can overcome the required model. The ANN technique has approved its efficiency and accuracy in model prediction that generated from any input multiple variables. The input parameters shall include climate change independent variables (monthly rainfall, min and max temperature, humidity, wind speed, and sunshine) and depended variable (rainfall intensity). The outcome of this stage shall include one model relating between rainfall intensity and time for future periods.

While in the second stage, shall include steps of applying the resulted model of ANN on the studied network area. The selected network components (pipes and manholes) data have been taken as GIs Arc Map shape file. The data have been smoothed and refined using the same program. The output data of GIS and ANN programs have been input to Storm Water Management Model (SWMM) program to presents the final results (flooding accordance and ratio)

The third stage shall consist of properties of the case study like, location, topography, land use, and subcatchment area. Also, the collected data shall be presented in this stage. Description of case study area are generated with the help of GIS ARC Map program. Methodology of the research plan can be seen in Figure (3.1)

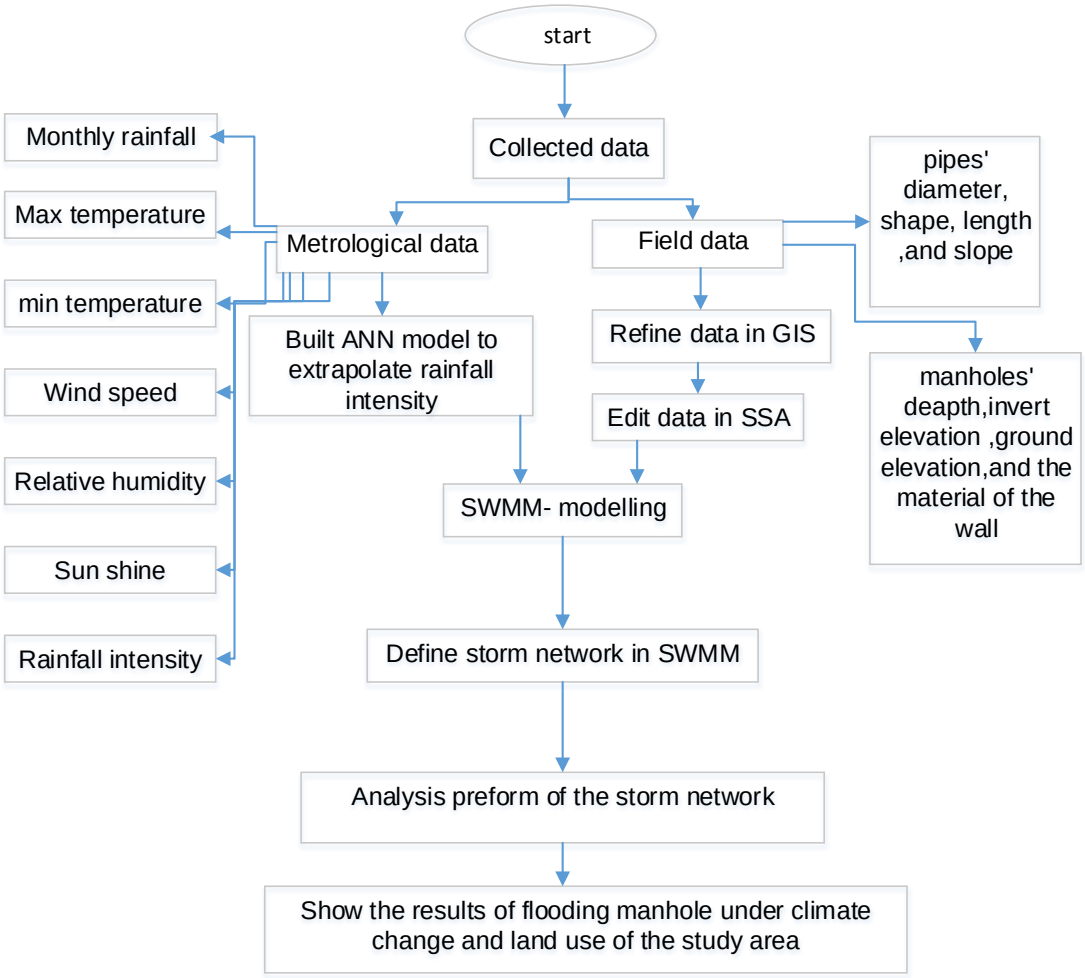

Figure 3-1 Flowchart of the research methodology.

3.2 Description of the research plan

Work stage include working with two main program: artificial neural network (ANN) and storm water management model (SWMM5.1) so, the hydraulic data analyze by ANN program and built model to

extrapolate rainfall intensity to enter it to SWMM then made simulation and prediction the flooding of the study area.

3.2.1 Artificial neural network (ANN)

This part include description of ANN and how to build ANN model.

3.2.1.1 Description of ANN model

The ANN system consists of as minimum three main parts, the first Part define as input layer, the second part define as hidden layer at least one layer and this layer processing of input layer and the third define as the output layer. The number of input nodes, I, and the number of output nodes, O, in an ANN are dependent on the problem to which the network is being applied. the number of hidden layer depending on training(Murata et al., 1994). There are nothing fixed to choose nodes of hidden layers ،the network have difficulty generalizing to problems when the numbers of nodes too few in the hidden layer, the network takes an unacceptable period when there are too many nodes in hidden layers. (Dawson and Wilby, 1998). The structure of neural network can showed in Figure (3.2).

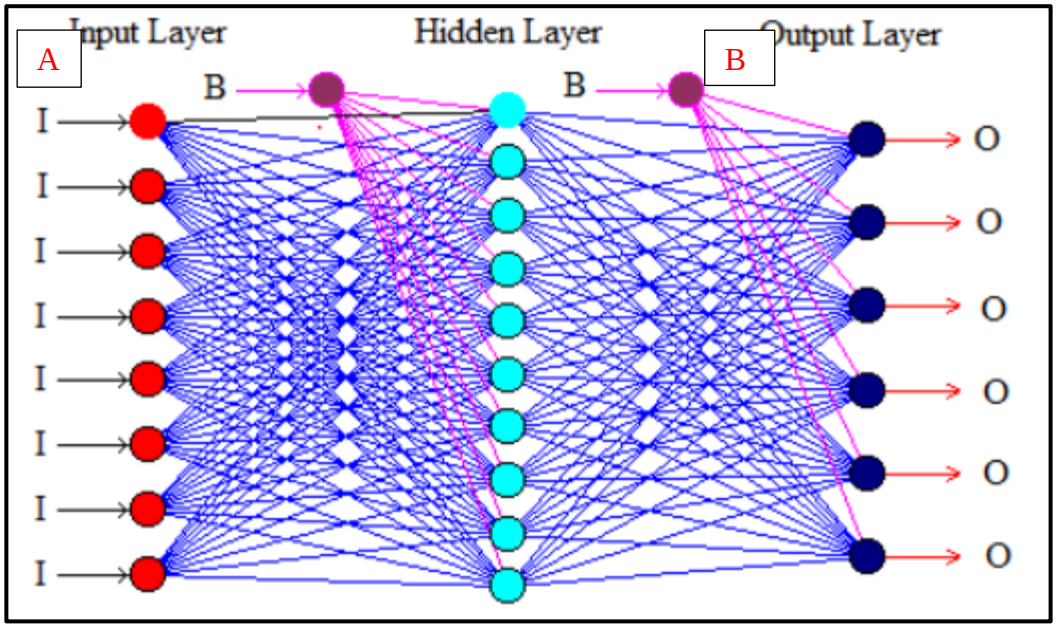

Figure 3-2Structure of neural network system.

3.2.1.2 Description of ANN program

The data enter to ANN divided to training data 95% and testing data 5% to validation the result of program. The program used to application ANN is neural power.

The sequence of process in ANN program can be briefed as follows:

1. Preparing data file that involve input and output layers.
2. For Learning settlements step, and to add learning files after that go to learning configuration to add hidden layers and determine node number and transfer function for each layer, ,there are six type of transfer function display below .

The ANN program contains several Types of transfer function in hidden layer, and can be summarized as follows (Giuseppe Ciaburro and September, 2017

)

1- Sigmoid function: This function, as clarified in Equation (3.1) is frequently chosen, due to comfortable, differentiable, monotonic, and limited this mean the sigmoid function well done

$$\boldsymbol{f(x) = \frac{1}{(1+exp^{(-x)})}} \text{..... (3.1)}$$

2- Tanh function: Tanh function, as presented in equation (3.2), is comfortable, differentiable, monotonic, and limited so it is similar to sigmoid but subsequent functions, don't have this properties so this limit the use of this function.

$$\boldsymbol{f(x) = \tanh x} \text{ ..... (3.2)}$$

3- Gaussian function: The Gaussian function as shown in Equation (3.3) used when the input data less probably to contribute to final result. it is even function so it gave the same output for input value for positive or negative

$$\boldsymbol{f(x) = exp^{(-x*x)}} \text{ ..... (3.3)}$$

4- Linear function: Linear function, as demonstrated in Equation (3.4), used when the output wanted without applying any limitations, the answer gave without any further modification expect doing the input × weight ,the linear function do not used in the hidden layer.

$$\boldsymbol{f(x) = x} \text{ ..... (3.4)}$$

5- Threshold linear function: Threshold linear function, as presented in Equation (3.5), need difficult limitation when the function applies the output either exactly single value or not. So this function don't used.

$$\boldsymbol{f(x) = if(x < 0, 0, if(x > 0, 1, x))} \ldots\ldots\ldots (3.5)$$

6- Bipolar linear function: as clarified in Equation (3.6), This function type has the capability to release node above limitation but it have adopt in lower region.

$$\boldsymbol{f(x) = if(x < (-1), (-1), if(x > 1, 1, x))} \ldots\ldots\ldots (3.6)$$

the sigmoid function is the best transfer function ,The description of all transfers function from (MLNnotebook, 2017)

The error between outputs of the network and target outputs are computed at the end of each process, then the Processing continues to training until the error less than selected.

There are important factors in learning process (Weights and biases):

Weights are very significant factor in ANN program to converting an input to impact the output. It is like to slope in linear regression, wherever a weight is multiplied to the input to add up to form the output. Weights are numerical parameters which determine how strongly each of the neurons affects the other.

For example, if the inputs are $\mathbf{x_1}$, $\mathbf{x_2}$, and $\mathbf{x_3}$, then the synaptic weights to be applied to them are denoted as $\mathbf{w_1}$, $\mathbf{w_2}$, and $\mathbf{w_3}$,

The Output is:

1. $\boldsymbol{y = f(x) = \sum x * w}$ ..... (3.7)

Bias is similar the intercept added in a linear equation. It is an additional parameter which is used to adjust the output along with the weighted sum of the inputs to the neuron.

The processing done by a neuron is thus denoted as :

$$\boldsymbol{output} = \boldsymbol{sum}\,(\boldsymbol{weight} * \boldsymbol{input}) + \boldsymbol{bias} \quad \ldots\ldots\ldots \quad (3.8)$$

The abstract of ANN learning process can be presented in Figure(3.4).

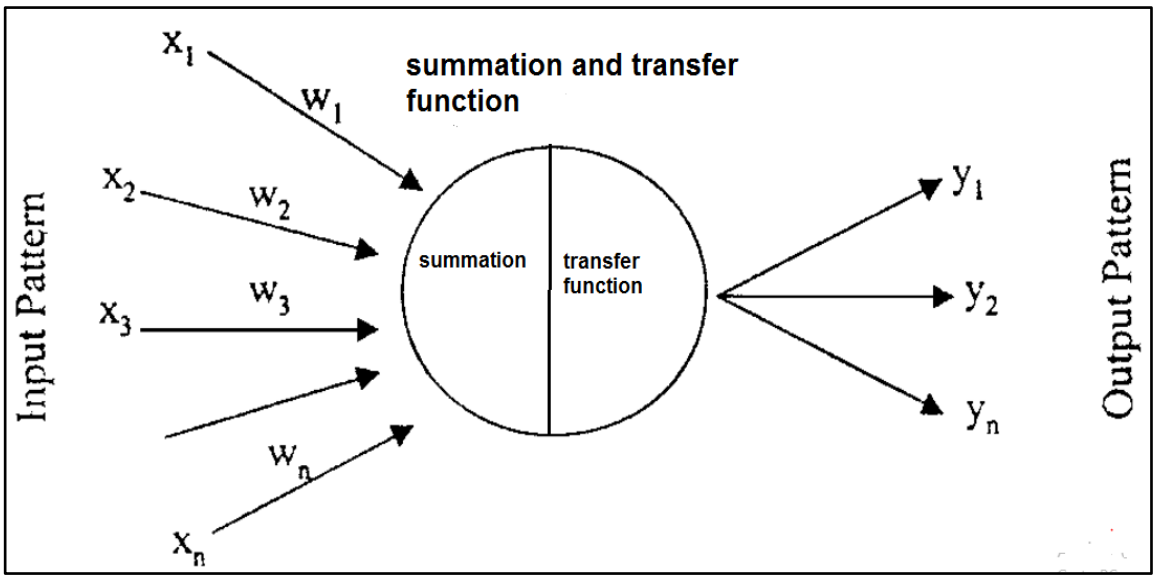

Figure 3-3 learning process of artificial neural network (Xn: input, Wn: weights, Yn: outputs).

3.2.1.2 Determining the number of hidden layers

When looking at the structure of dense layers, there are really two decisions to make about these hidden layers: the number of hidden layers in the neural network and the number of neurons in each of these layers. At the first We'll look at how to determine the number of hidden layers to use with the neural network.

Before deep learning problems that require more than two hidden layers were rare .simple data sets will often require two or fewer layers. However, additional layers can be useful with complex datasets include

time-series or computer vision. Table (3.1) summarizes the ability of several common layer architectures.

Table 3-1 Determining the Number of Hidden Layers.

Number of Hidden Layers	**Result**
>2	Extra layers can learn complex representations of layers (a type of automatic feature geometry).
2	Can represent arbitrary decisions that are arbitrarily defined with rational activation functions and can round any smooth layout of any accuracy.
1	Round any function that contains a continuous layout from one distance to another
none	Represent only deterministic decisions or functions.

3.2.1.3 The Number of neurons in the hidden layers

Overall for neural network structure determine the number of neurons in the hidden layers is a very important part . although these layers do not directly react with the outer environment, they have a large influence on the final output. Both the number of neurons and the number hidden layers in each of these hidden layers must be carefully considered.

Under fitting will happened when the neurons in the hidden layers too few. Over fitting happened when the number of neurons in the hidden layers too many. Several problems occur with the over fitting. First, more than installation occurs when the neural network has a large amount of information processing capacity that the limited amount of information in the training group is not enough to train all the neurons in the hidden

layers. A second problem can occur even when the training data is sufficient. A large number of neurons in hidden layers can increase the time it takes to train the network. The amount of training time can be increased to the extent that it is impossible to train the neural network adequately. Generally the number of neurons should be moderate between too many and too few in the hidden layers Figure (3.3) illustrates the above mentioned problems.

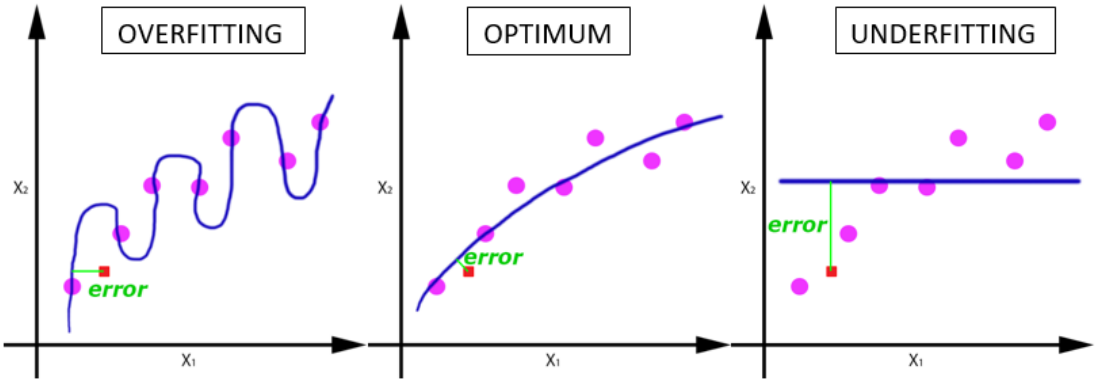

Figure 3-4 an example for effect of number of neurons on ANN model accuracy {Murata, 1994 #18}.

A few rules of thumb that suggested to choose hidden layers. There are many rule-of-thumb methods for determining an acceptable number of neurons to use in the hidden layers, such as the following:

1- Determining the number of neurons in the hidden layers that should be between the size of the input layer and the size of the output layer.
2- The number of hidden neurons should be 2/3 the size of the input layer, plus the size of the output layer.
3- The number of hidden neurons should be less than two time the size of the input layer.

It is uncertain to start throwing random numbers of layers and neurons at the network this led to very time consuming, so the selection of the layers and neurons depend on the trial and error , three rules upon provide a starting point to consider.

3.2.1.3 Building the ANN model

artificial neural network model (ANN) built depended on input layers and out put layers, input layers include (year, month, monthly rainfall total (mm), mean max temperature (℃), mean min temperature(℃), mean relative humidity (%), mean wind speed (m/s), mean sun shine (hrs./day) ,output layer include (rainfall intensity (mm) for 30 min). month and rainfall intensity(I) input to program by formula (N+1 , N-1) means for each neuron took before neuron and after neuron to determine location of it Accuracy as shown in Table(3.2).

Table 3-2 formula of data that using in ANN.

y	N	N+1	N-1	R	min.tem	max.tem	hum	wind	sun.sh	I	I+1	I-1
			1									1.6
1981	1		2	12.5	5.3	17	75	2.7	6.8	1.6		2
1981	2	1	3	4.9	7.5	19.3	63	2.8	7.2	2	1.6	2
1981	3	2	4	12.8	11.1	24.7	59	3	8.3	2	2	0.7
1981	4	3	5	4.3	14.5	29.1	44	3.2	8.4	0.7	2	0
1981	5	4	6	0.001	19.2	34	36	3.6	8.8	0	0.7	0
1981	6	5	7	0.001	24.9	40.5	33	4	12.1	0	0	0
1981	7	6	8	0	28.6	44.1	27	4.5	11.9	0	0	0

The sequence of prediction of rainfall intensity was done by ANN include the steps:

1. Building ANN model for 10 yrs. (first model) due to rainfall intensity available (output layer) from General Authority for meteorological and Seismic Observation (G.A.M.S.O) only for 10 yrs. for period (1981-1990).

2. ANN model for 10 yrs. (first model) used to predict rainfall intensity for period (1991 – 2008).
3. From Iraqi Agromet Center Data (I.A.C.D) the rainfall intensity from 2008 to 2016 was found.
4. Built ANN model (second model) for period (1981-2016).
5. SPSS program made simulation to find input layer (climate change) for future period (2017-2070).
6. Input data found from step 5 into second model to found rainfall intensity for period (2017-2070).

There are five model built depend on number of hidden layers after that chosen the best depend on several statistical index include root mean square error RMSE and correlation coefficient Square R^2 ,so the best model chosen that has least RMSE(nearest to zero) and greater R^2(nearest to 1)

3.3 Storm water management model (SWMM)

This subsection includes description of SWMM simulation, flow routing, and infiltration model and how to build SWMM.

3.3.1 Description of SWMM

Storm Water Management Model (SWMM) developed by US EPA , first developed in 1971, SWMM is a model used to simulation runoff quantity and quality from urban areas, It is used for single event or long-term (continuous). The runoff component of SWMM run on a collection of sub catchment areas that receive precipitation and produce runoff and pollutant loads, this runoff transports during a system of pipes, channels, storage/treatment devices, pumps, and regulators. SWMM5.1 keeps track of the flow rate, flow depth, runoff volume generated within each sub-catchment, and the quality of water in each pipe and/or channel at

different time steps of the simulation. SWMM Version 5.1, which is running under Windows is used in the current study as in the present study as it provides an integrated environment for editing, inputting data of the study area, running hydrologic, hydraulic and water quantity simulations, and viewing the results in a variety of formats. These include color-coded drainage area and conveyance system maps, time series graphs and tables, profile plots, and statistical frequency analyses (Rossman, 2010).

3.3.2 System flow routing

The process of determine the time and magnitude in any point of the drainage system based on known or assumed hydrographs at one or more point in upstream called the flow routing. There are three level of sophistication used in SWWM for flow routing to solve the conservation of mass and momentum equations for conduits of open channel and this equation is the comprehensive one-dimensional (Rossman, 2010).The SWMM lets the modeler to select the level of sophistication to solve the equations. The three level of flow routing in SWMM are steady flow routing, kinematic flow routing and the dynamic flow routing. In this study the dynamic flow routing has been used because it has the ability to account for pressurized flow, channel storage, flow reversal, backwater and entrance/exit losses so the dynamic flow routing consider the most theoretically precise consequences. In dynamic routing the full flow closed pipe represent as Aeron pressurized flow and the flooding happens when the water depth skips the maximum available depth at the node.

For the Saint-Venant the flow can be represented by the two partial differential equations. First the momentum [eq. 3.9]:

$$\frac{1}{A}\frac{\partial q}{\partial t}+\frac{1}{A}\frac{\partial}{\partial x}\left[\frac{q^2}{A}\right]+g\frac{\partial y}{\partial x}-g\left[S_0\text{-}S_f\right]=0 \qquad \ldots.[3.9]$$

Second the continuity [eq 3.10]:

$$\frac{\partial A}{\partial t} + \frac{\partial q}{\partial x} = 0 \quad \text{....[3.10]}$$

Where:

q = The flow rate in the system (m^3/sec).

g = The acceleration due to gravity (m/s^2).

y = The depth of flow (m).

$S_\circ$ = The bed slope (m/m).

S_f = The friction slope (m/m).

A = The cross-sectional area (m^2).

x = The distance along the channel (m).

and **t** = The time (sec) (Pitt et al., 1999).

The terms in the momentum equation describe as follow:

$\frac{1}{A}\frac{\partial q}{\partial t}$ = The change in momentum due to the change in velocity over time.

$\frac{1}{A}\frac{\partial}{\partial x}[\frac{q^2}{A}]$ = The change in momentum due to the change in velocity along the channel.

$g\frac{\partial y}{\partial x}$ = the change in the water depth along the channel.

$g\ [S_0-S_f]$ = gravity force term, proportional to the bed slope and friction force term, proportional to the friction slope.

While the terms in the continuity equations represent as follow: -

$\frac{\partial A}{\partial t}$ = The rate of change of area with time.

$\frac{\partial q}{\partial x}$ = The rate of change of channel flow width distance.

The two partial differential equations solve numerically as done for runoff surface routing. The dynamic flow routing used manning equation to determine flow rate [Q]. the Hazen-Williams or Darcy-Weisbach equation is used for circular force main shapes under pressurized flow(Rossman, 2010).

3.3.3 Infiltration model

The infiltration in SWMM can model in three different formulas Horton, Green-Ampt and SCS curve number method. In this research the Green-Ampt model has been used. There is no unified vision for preference one way for others and the Green-Ampt model is more physically-based (Gironás et al., 2009)The Green -Ampt method is a simplify, empirical model to represent the infiltration process. It develops from the application of Darcy's law and the law of conservation of mass. Green-Ampt suppose that a sharp wetting front exists in the soil column separating the soil where the above wetting front is fully saturated and the soil below is at the initial moisture content (Rawls et al. (1983)). This method is a function of the soil's hydraulic conductivity, soil suction head, porosity and initial moisture deficit of the soil. The general [eq.3.11,3.112]of the Green-Ampt is given below (Rawls et al., 1983):

$$f = K^* \{ [\frac{\Psi * n}{F}] + 1 \quad \ldots [3.11]$$

$$F = K * t + \Psi * n * \ln \{1 + [\frac{F}{\Psi * n}]\} \quad \ldots [3.12]$$

Where:

f = Infiltration capacity [mm/h].

K = Saturated hydraulic conductivity [mm/h].

Ψ = Suction head [mm].

n = Available porosity which is calculated as the effective porosity [θ_e] minus initial soil water content saturated [θi] for initially dry soil or it is the difference between the soil's porosity [**ϕ**] and its field capacity [**FC**] for completely drained soil [where θ_e estimate as the total porosity[ϕ] minus residual saturation, θ_r].

F = Mass infiltration [mm].

Rawls et al. (1983) has been considered these equations was under the assumption that the depth of ponding on the soil surface is negligible and analyzed approximately 5000 soils samples through the United States and published values for the Green-Ampt parameters as shown in Table (3.3):

Table 3-3 Parameters of Green-Ampet for different soil type, Rawls et al. (1983).

Soil texture class	**K**	**Ψ**	**Φ**	**FC**	**WP wilting point**
Sand	4.74	1.93	0.437	0.062	0.024
Loamy Sand	1.18	2.4	0.437	0.105	0.047
Sandy Loam	0.43	4.33	0.453	0.19	0.085
Loam	0.13	3.5	0.463	0.232	0.116
Silt Loam	0.26	6.69	0.501	0.284	0.135
Sandy Clay Loam	0.06	8.66	0.398	0.244	0.136
Clay Loam	0.04	8.27	0.464	0.31	0.187
Silty Clay Loam	0.04	10.63	0.471	0.342	0.21
Sandy Clay	0.02	9.45	0.43	0.321	0.221
Silty Clay	0.02	11.42	0.479	0.371	0.251
Clay	0.01	12.6	0.475	0.378	0.265

3.3.4 Building SWMM model

The result of climate change scenario represent as rainfall intensity from (ANN) model for predict period (2017-2070) were used on Al-Abbas quarter in Karbala city.

So, the following steps are followed in SWMM to model rainfall intensity on a study area:

1. Collection of Field data for the Al-Abbas section from Directorate of the Streams of Karbala (D.S.K) include pipe and manhole and its properties.
2. Assign set of option and properties of object were used as default.
3. Refine data in GIS.
4. Edit data and connect area to nearest manhole in storm and sanitary Analysis (SSA), which as program of AutoCAD civil3d Package.
5. Enter in SWMM and make analysis performs.
6. Show the results of the simulation.

3.4 Study area and data

In this subsection, description of the study area, land use, topography of the case study, field and metrological data shall be presented with details.

It worth to mention that the raster map of GIS has been provided by Ministry of Construction, Housing, Municipalities and Public Works (M.C.H.M.PW). The map has been captured in year 2016, which is the last version has been taken for study area.

3.4.1 Description of the study area

Geographically, the study area (Al-Abbas quarter) is located to the north-east of the center of Karbala city , Iraq, between latitudes

32°37'56.7"N - 32°38'15.9"N ,and longitudes 44°02'39.8"E-44°03'08.9"E, as shown in Figure (3.5). The distance is 2 km between center of the study area and center of Karbala city. The total area approximately is 0.373 km², total impervious area approximately is 0.257 km², (70% of total area) including (roofs and paved area), previous area approximately is 0.116 km², (30% of total area) including (green area and unpaved area). It is a flat surface with low slopes and sandy, clay soil. Regional elevations range from 34 m to 41m above sea level. The network of the case study is storm water network divided into 64 sub-catchment. Some new developments is expected to take place surrounding the case study according to Kerbela master plan. The climate of the case study show in Table(3.4).

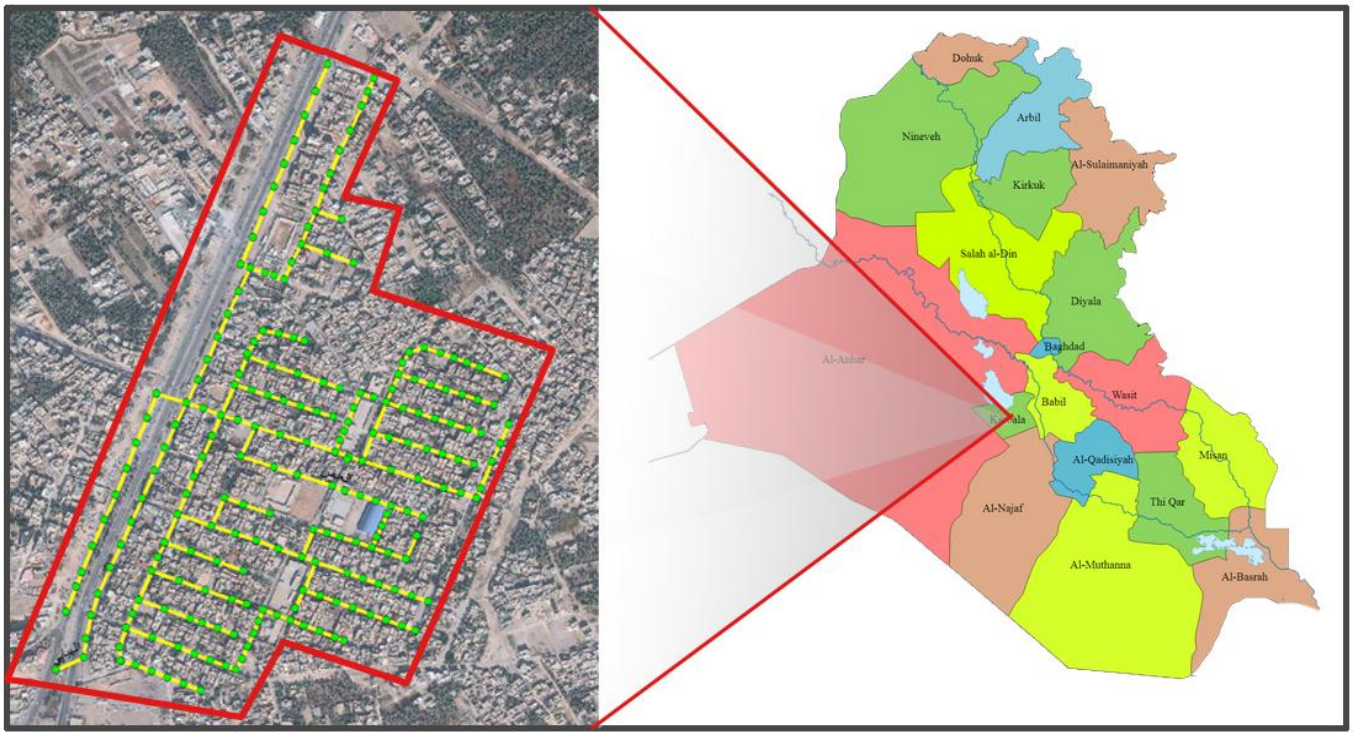

Figure 3-5 Geographical location of the study area according to Iraqi map(M.C.H.M.PW).

Table 3-4 clarify min and max value of climate of the case study.

Climate	Min value	Max value
Temperature (c˚)	1.6	46
Monthly rainfall (mm)	0	48
Humidity (%)	23	83
Wind speed (m/s)	1.9	5.2
Sun shine (hrs./day)	5.2	12.6

3.4.2 Land use

Identifying characteristics of land use of a specific location is necessary to assign quantity of water runoff that con not be absorbed by land media. Land use area of the case study divided into three main parts; paved area, gardens and service building, and houses. The paved area occupied about 8% from total land use area, which consider the smallest portion. The second part, which occupies about 12% from total land use area, consists of gardens and service buildings, such as schools and hospitals. While the third part, which occupied by houses, forming about 80% from total land use area. Figure (3.6), clarifies land use area of the selected case study. It worth to mention that the previous figure has been created utilizing ARCMAP program of GIS package.

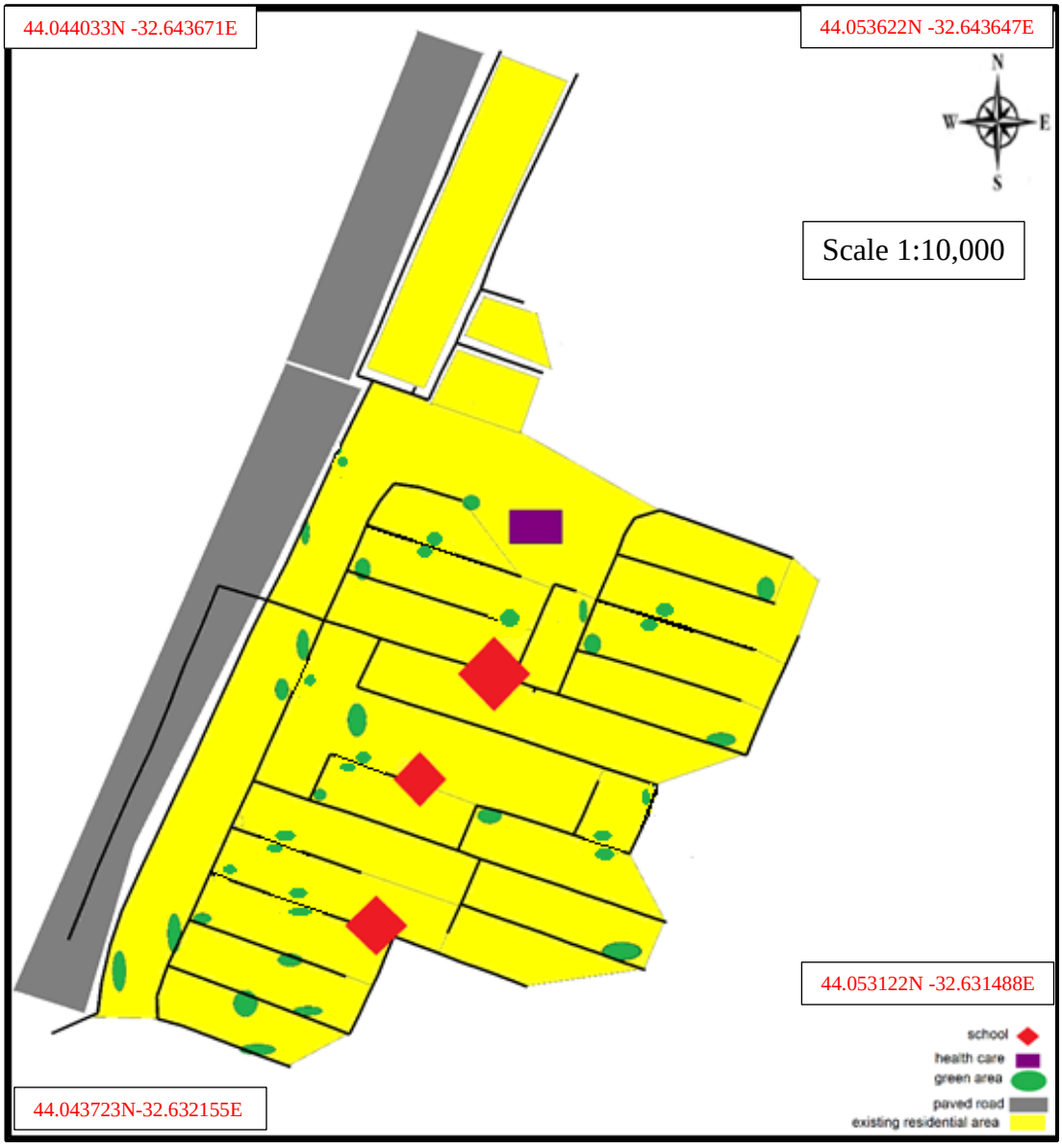

Figure 3-6 land use of Al-Abbas quarter.

3.4.3 The topography

The contour map of the study area has been generated with 0.5 meter contour interval using GIS (geographic information system) software. The map has been created utilizing from the DEM (Digital elevation model) surface raster file that provided from the USGS (U.S Geological survey**)** (USGS, 2018). After importing the DEM file in GIS (ARC MAP V10.4.1), a random points has been generated for the study area only, after that, the Z elevation was extracted from the DEM file to the

generated Radom points. The resulted processes were point's data with XYZ information. Finally, the contour map has been generated utilizing ARC tool box that provided as a package with the GIS software. It is worth to mention that Karbala city has a flat ground and the earth topography is ranged from 28-34 m of the steady area. This illustrate in Figure (3.7).

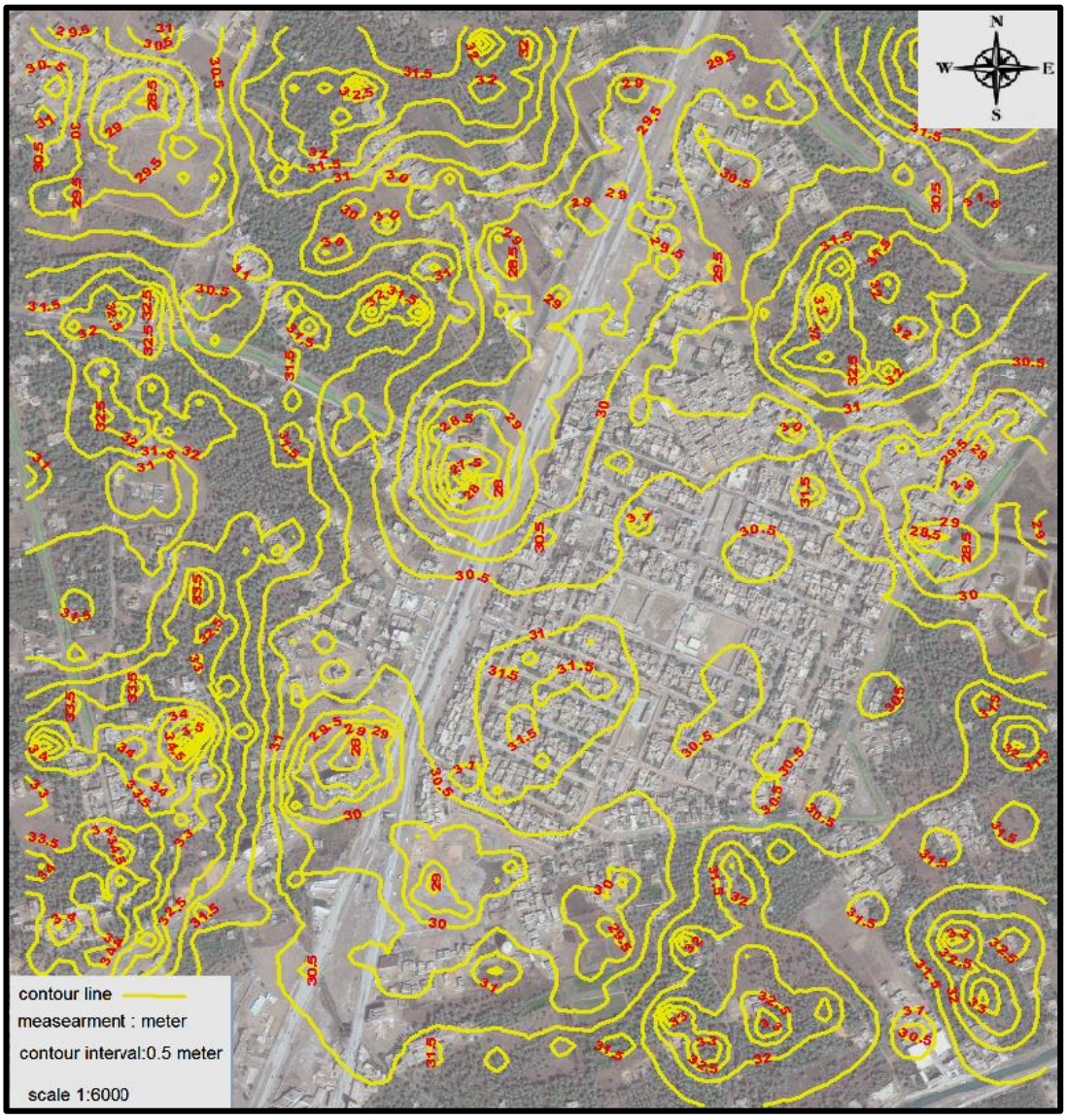

Figure 3-7 topography of the study area (USGS, 2018).

3.4.4 Sub catchment

Sub catchments divided into pervious and impervious sub areas. Surface runoff of the pervious subarea can Infiltrate into the upper soil zone, but not through the impervious subarea. Impervious areas can be divided in two type: sub catchment have depression storage and sub catchment do not contain depression storage. Runoff flow either routed from sub area in sub catchment to another sub area, or both sub catchment can drained to the sub catchment outlet. The total area approximately to 0.373 km² and it divided into 64 sub catchments as shown in Figure (3.8).

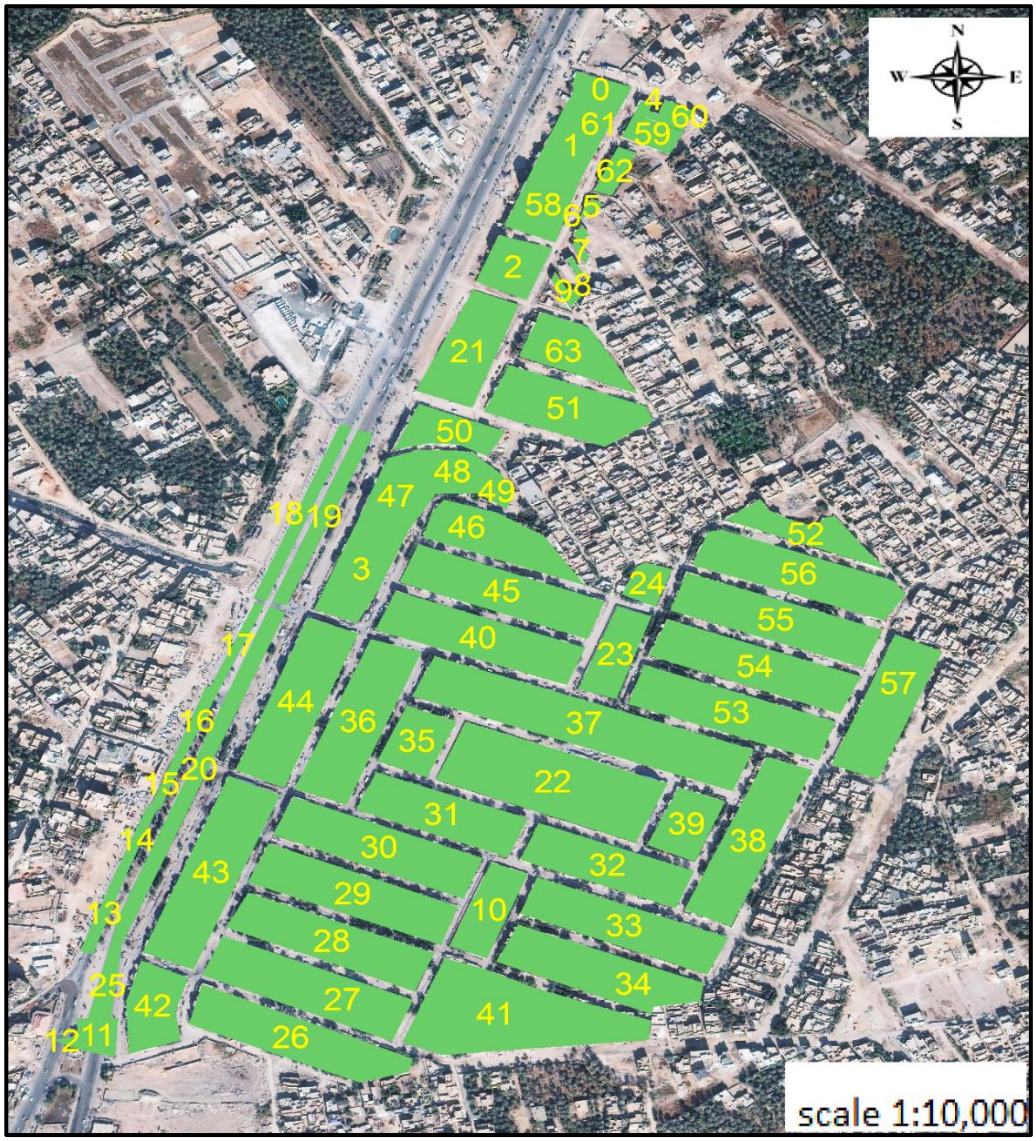

Figure 3-8 sub catchment areas distrbution of the study area.

3.4.5 Field data

Field data collection for the case study Al-Abbas quarter from (D.S.K) includes pipe and manhole and their properties. The collected data has been drawn in GIS ARCMAP as point and line shape files. After drawing and refining data, the network has been imported to SWMM program.

3.4.5.1 Pipes properties

Pipe is a type of Conduits that using move water from one node to another in the conveyance system. The spatial distribution and the upstream and downstream altitude must be supply for each pipe in the model to gain the slope and to set the flow direction of the fluid. The study area contain 222 pipes that have circular shape, the length of the pipes between (2-68) m and the diameter of the pipe of the network between (315-600) mm as shown in Figure (3.9) The pipes made from polyvinyl chloride [PVC] and the manning roughness coefficient values for the pipes are shown in the Table (3.5) below where the manning value for the PVC pipe [plastic pipe] is 0.009.

Table 3-5 Values of Manning roughness coefficients for different materials of pipes.

The material of pipe	N
Plastic pipe	0.009
Well-planed timber evenly laid	0.009
Neat cement. Very smooth pipe	0.01
Unplanned timber. Cast-iron pipe of ordinary roughness	0.012
Well-laid brick work. Good concrete. Riveted steel pipe. Well-laid vitrified clay pipe	0.013
Vitrified tile and concrete pipe poorly jointed and unevenly settled. Average brick work	0.015
Rough brick. Tuberculation iron pipe	0.017
smooth earth or firm gravel	0.02
Ditches and rivers in good order , some stones and weeds	0.03
Ditches and rivers with rough bottoms and much vegetation	0.04

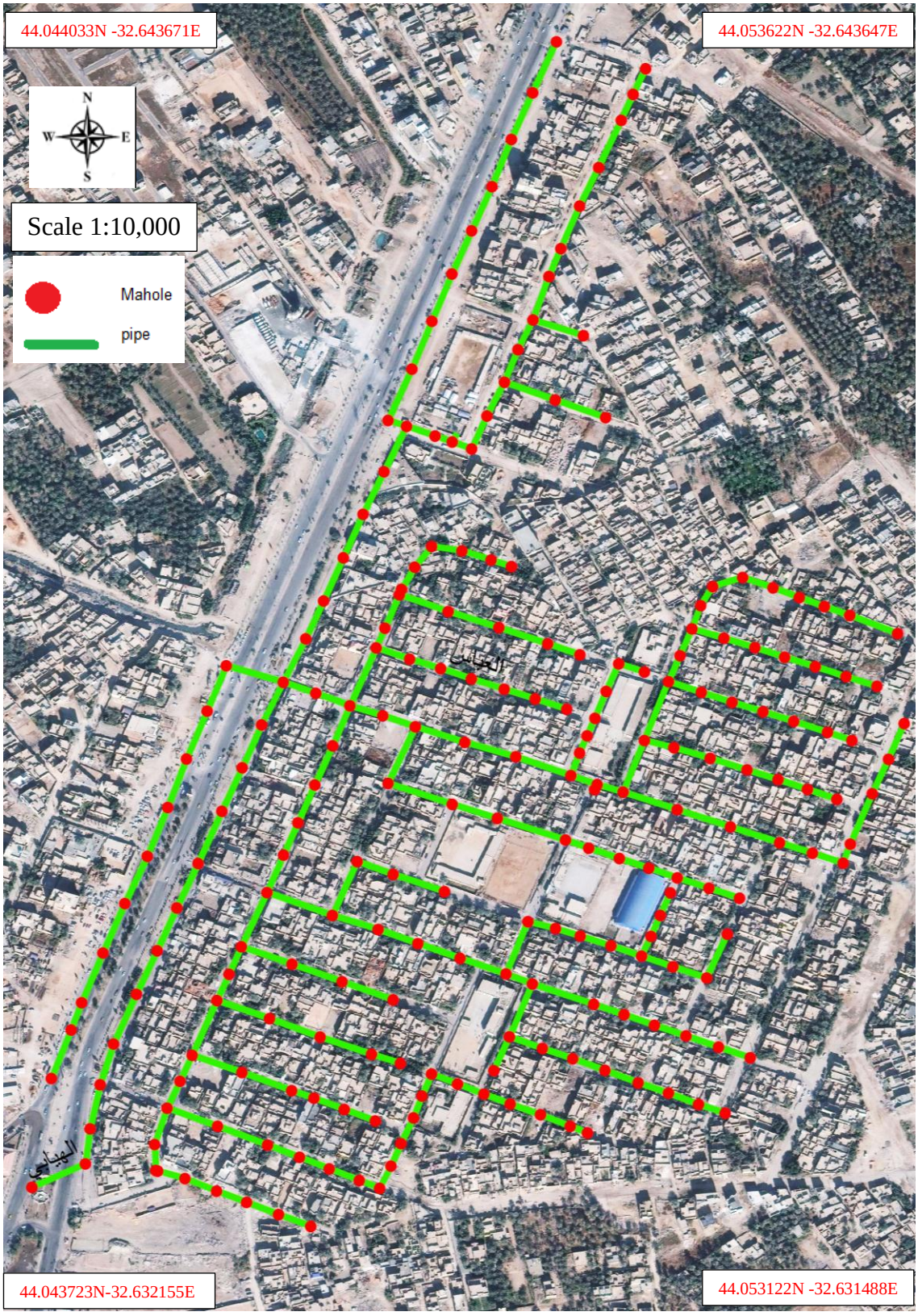

Figure 3-9 the storm drainage network of Al-Abbas quarter.

3.4.5.2 Manholes properties

The Wall of the manholes has been made with concrete materials. The maximum depth of manholes is 3.632 m, and the maximum invert elevation is 27.225 m. Maximum ground elevation of the manholes is 28.81 m. three types of manholes shapes were found in the network and summarized below:

- AS type: a rectangular manhole shape having dimensions 150 cm length and 110 cm width. It is used for shallow depths and can connected with 250 mm pipes diameter.
- BS type: has a circular cross section area of 110 cm, used for medium depths. Three pipes diameters can be connected to such manhole, are, 250 mm, 315 mm, and 400 mm.
- CD type: has a circular cross section area of 150 cm, used for deep cases. Four pipes diameters can be connected to such manhole are, 400 mm, 600 mm, and 715 mm.

3.4.6 Metrological data

metrological data has been collected from the (G.A.M.S.O) for period from 1980 to 2016 including; monthly rainfall (mm), mean maximum temperature (℃), mean minimum temperature (℃), mean relative humidity (%), mean wind speed (m/s), mean sun shine (hr. /day). While the collected data for period from 1981 to 1990 included rainfall intensity for Karbala station in (mm) for 1 hour. This data use in ANN program. Figures (3.10) through (3.16) shows the average of (monthly rainfall, mean

max temperature, mean min temperature, mean relative humidity ,mean wind speed, mean sun shine) for 36 yrs., and the average of rainfall intensity for 10 yrs, consequently.

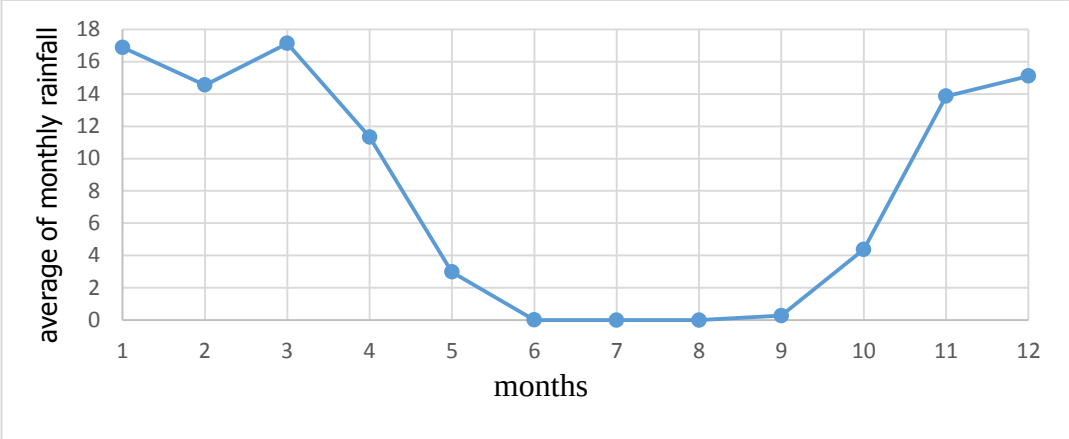

Figure 3-10 the average of montly rainfall for period (1980-2016).

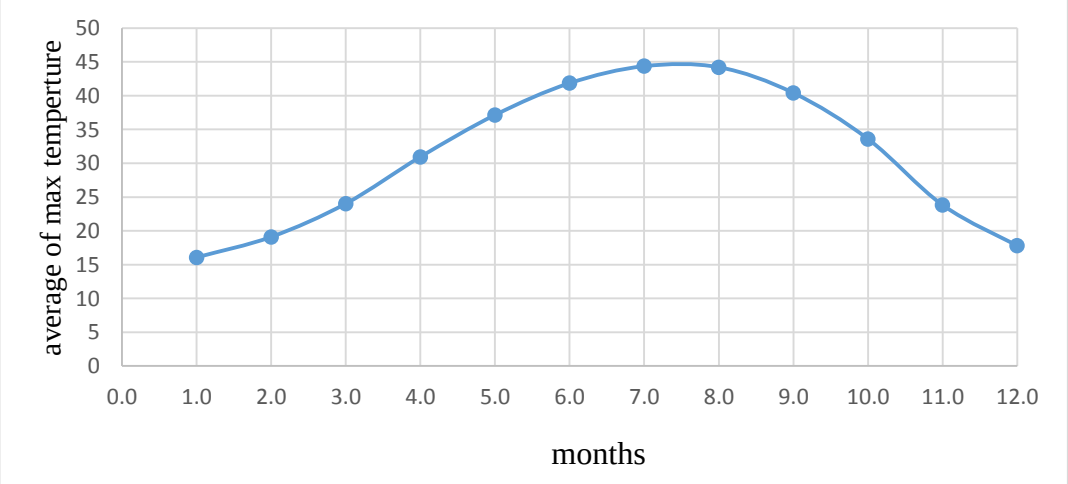

Figure 3-11 the average of max temperture for period(1980-2016).

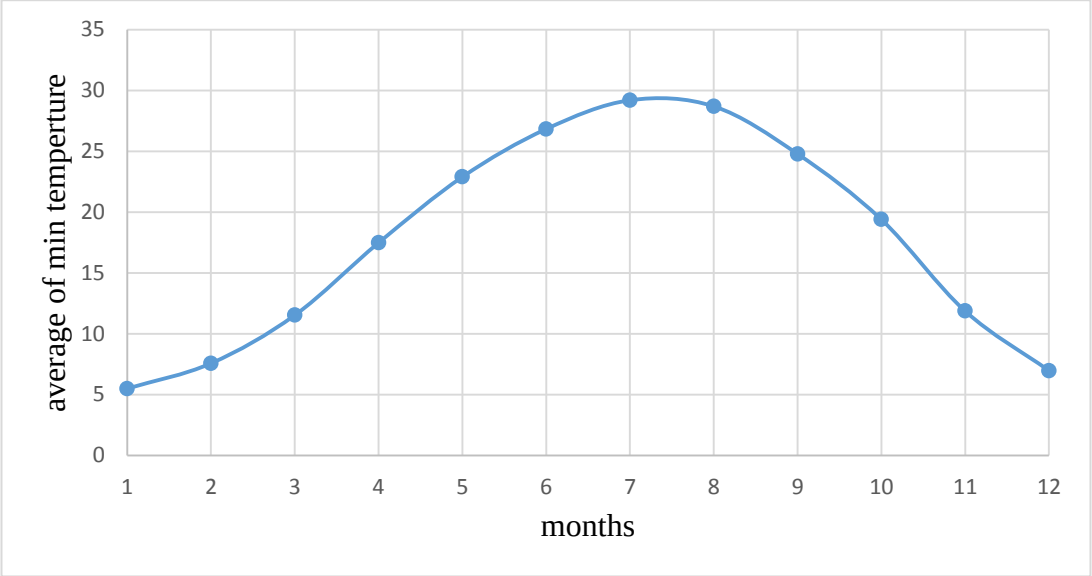

Figure 3-12 average of min temperture for period(1980-2016).

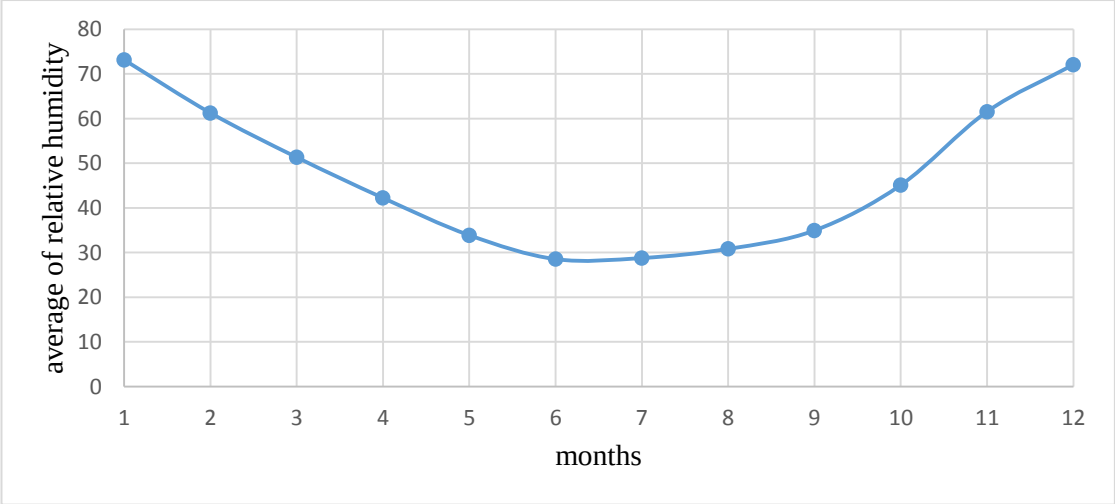

Figure 3-13 average of relative humidity for period(1980-2016).

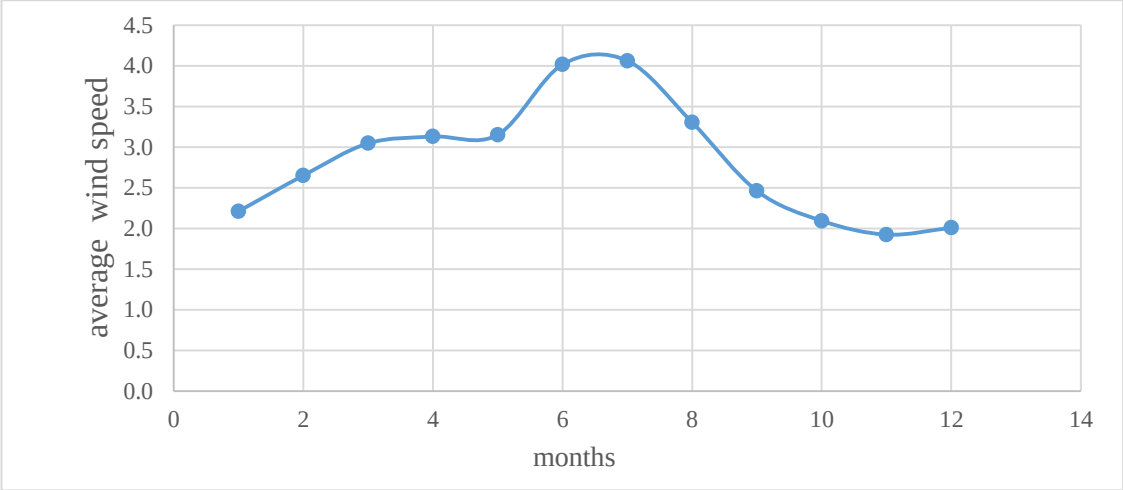

Figure 3-14 average of wind speed for period(1980-2016).

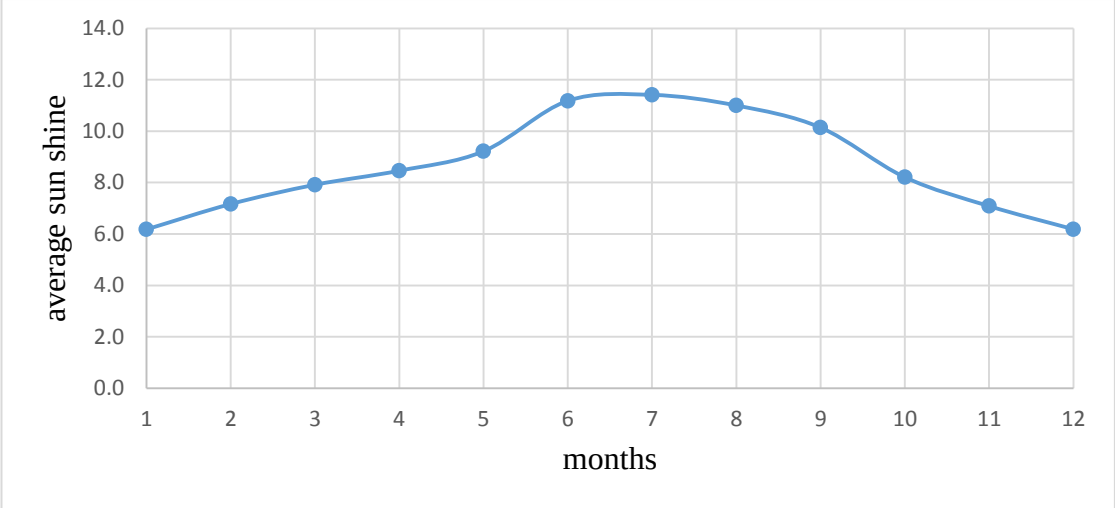

Figure 3-15 average of sun shine for period(1980-2016).

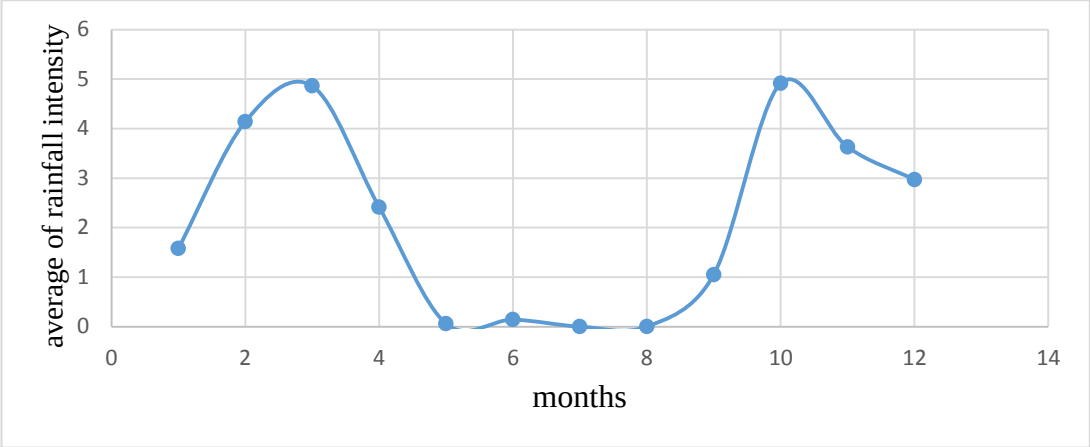

Figure 3-16 average of rainfall intensity for period (1981-1990).

3.5 Suggestion scenario

Land use is an important factor that should be taken into account for future prediction of flooding occurrence, in addition to the change of rainfall intensity. Therefore, In case of forecasting period of the study plan until 2070, any developed area within the study area should be taken into account. The previous analysis of flooding occurrence has been considered only the current land use area.

In the previous suggested scenario, the rational method has been used to calculate flooding discharge. It is the simplest method to determine peak discharge from drainage basin runoff. Equation (3.13) describe rational method parameters:

$$Q=CIA \quad \text{(3.13)}$$

Where:

Q = Peak discharge, m^3/sec

c = Rational method runoff coefficient from Table (3.6)

i = Rainfall intensity, mm/30 min

A = Drainage area, m^2

Table 3-6 Rational Method Runoff Coefficients.

Ground Cover	**Runoff Coefficient, c**
Lawns	0.05 - 0.35
Forest	0.05 - 0.25
Cultivated land	0.08-0.41
Meadow	0.1 - 0.5
Parks, cemeteries	0.1 - 0.25
Unimproved areas	0.1 - 0.3
Pasture	0.12 - 0.62
Residential areas	0.3 - 0.75
Business areas	0.5 - 0.95
Industrial areas	0.5 - 0.9
Asphalt streets	0.7 - 0.95
Brick streets	0.7 - 0.85
Roofs	0.75 - 0.95
Concrete streets	0.7 - 0.95

Chapter Four

RESULT AND DISCUSION

4.1 Introduction

This chapter display the result obtained from the models. This chapter divided into three parts: the first parts display the result of rainfall intensity model and its calibration, the second parts display the result of flooding model and calibration of it, and the third parts display suggestion scenario by calculation the effect of future land use on the storm network of the case study.

4.2 ANN Rainfall intensity model

This part display calibration of ANN model, weight distribution, and effect of climate change on ANN model.

4.2.1 Learning process of ANN models functions

Learning ANN program to predict rainfall intensity function requires several input parameters. One of the most important parameters are, type of transfer function and number of hidden layers. No universal accepted criteria for selecting type of transfer data or number of hidden layers, but several researchers adopted sigmoid function in their research since it can learning faster, and gives optimum results.

In this study, and to ensure that sigmoid function works correctly in test for training data, several trials has been made for years from (1981-1990) to predict some missing data. Different functions types such as, sigmoid,

Tanh, Gaussian, and bipolar has been testes to select the best one. Also, for each trialed function, optimum number of hidden layer was also checked out, as can be seen in Table (4.1).

Table 4-1 present effect different training function and number of hidden layers on the strength of the correlated function.

function type	No. hidden layer	R (correlation coefficient)	RMSE (root mean square error)	DC (determination coefficient)	average R	average RMSE	average DC
Sigmoid	**1**	**0.922**	**1.285**	**0.849**	**0.97475**	**0.849**	**0.9515**
Sigmoid	**2**	**0.984**	**1.584**	**0.97**			
Sigmoid	**3**	**0.997**	**0.26**	**0.994**			
Sigmoid	**4**	**0.996**	**0.267**	**0.993**			
Tanh	**1**	**0.959**	**1.25**	**0.92**	**0.95525**	**0.95675**	**0.919**
Tanh	**2**	**0.985**	**0.587**	**0.97**			
Tanh	**3**	**0.977**	**0.53**	**0.975**			
Tanh	**4**	**0.9**	**1.46**	**0.811**			
Gaussian	**1**	**0.646**	**2.4**	**0.42**	**0.646**	**2.4**	**0.42**
Gaussian	**2**	**N/A**	**N/A**	**N/A**			
Gaussian	**3**	**N/A**	**N/A**	**N/A**			
bipolar	**1**	**0.364**	**3.73**	**-0.234**	**0.364**	**3.73**	**-0.234**
bipolar	**2**	**N/A**	**N/A**	**N/A**			
bipolar	**3**	**N/A**	**N/A**	**N/A**			

From the previous table, it can be noticed that the average R and RMSE parameters for sigmoid function type, is higher than other types, as mentioned previously by the researchers. It should be noticed that the lowest value of RMSE reflected the best results. Also, the correlated function is highly dependent on number of hidden layer, for each type of trailed function. It can be noticed that 2 hidden layer for sigmoid function gave better results than other. While increasing hidden layers more than 2 was insufficient in term of time cost and performance of network learning, and this called overfitting.

Therefore, and base on the previous data results, it has been selected sigmoid function with 2 hidden layers as a constant parameters for other to test model learning from (1981-2016).

Figure (4.1), (4.2), and (4.3) clarify ANN learning process of a sigmoid- 2 hidden layers incorporated 9 neurons per layer, relation between observed and correlated data set for the same period, and behavior of RMSE function, respectively. The same consequences are presented in Figures (4.4), (4.5), and (4.6).

For both cases, the learned function tends to fit the observed function through adjusting node weights process. The weights are modified in each iteration process. So, after a numerous number of iterations, finally the function had been learned successfully (the red color function), and with 0.97 and 0.706 of R and RMSE values for Figure (4.1) and the weights have been reached the stability limit. These results are the best reached and has been taken for testing, as can be seen in next subsection (calibration model). The same explanation can be adopted for Figure (4.4).

For the RMSE function as presented in Figure (4.3) and (4.6), it has been noticed a continuous reduction in RMSE values with higher number of iterations. This behavior is reasonable, and sometime after a certain time of process, the values begins to slight increase and decrease for a specific limit without any noticeable improvement achieved.

Overall, the maximum values of R and the minimum values of RMSE, have been taken as the main criteria for accepting models.

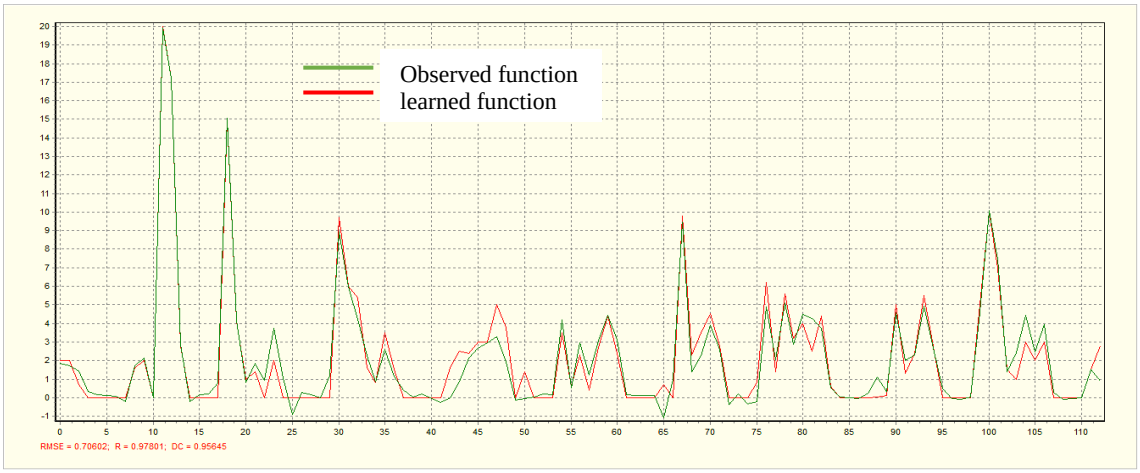

Figure 4-1 ANN learning process of a ten years testing data.

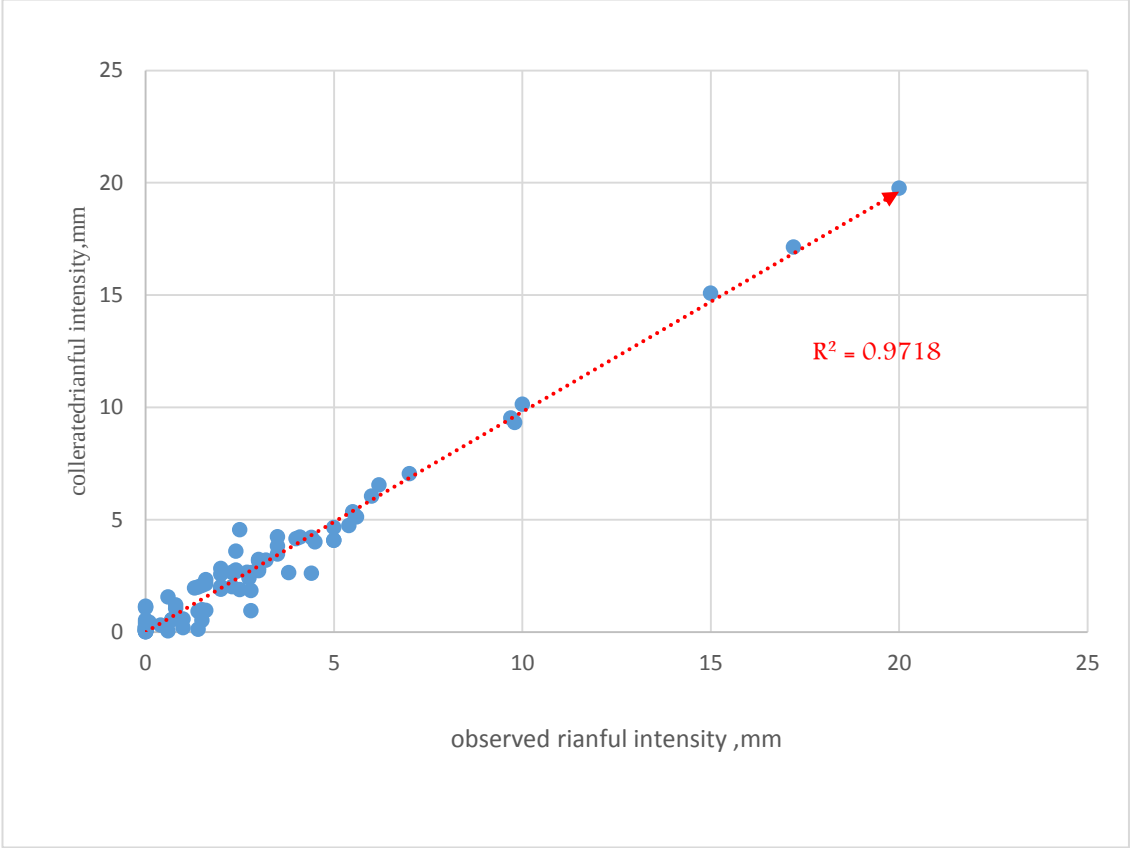

Figure 4-2 correlation strength of the fitting line between observed and learned data for 10 years.

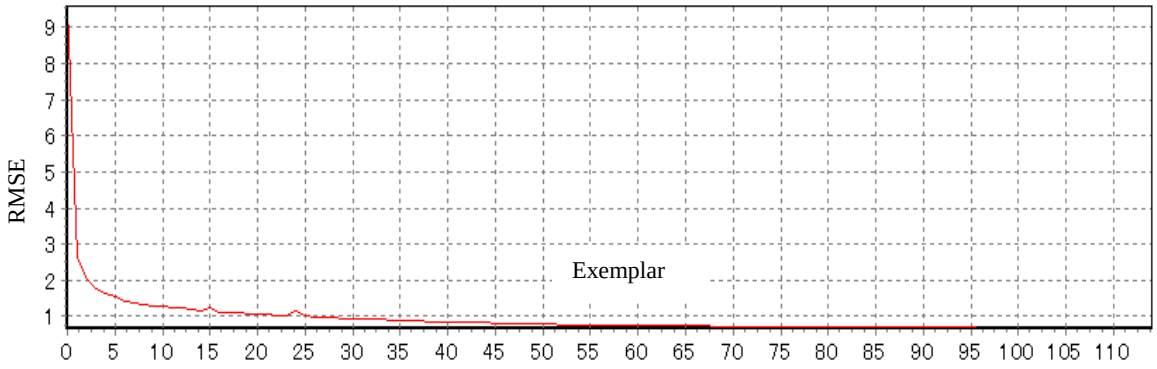

Figure 4-3 RMSE function behavior during function learning process.

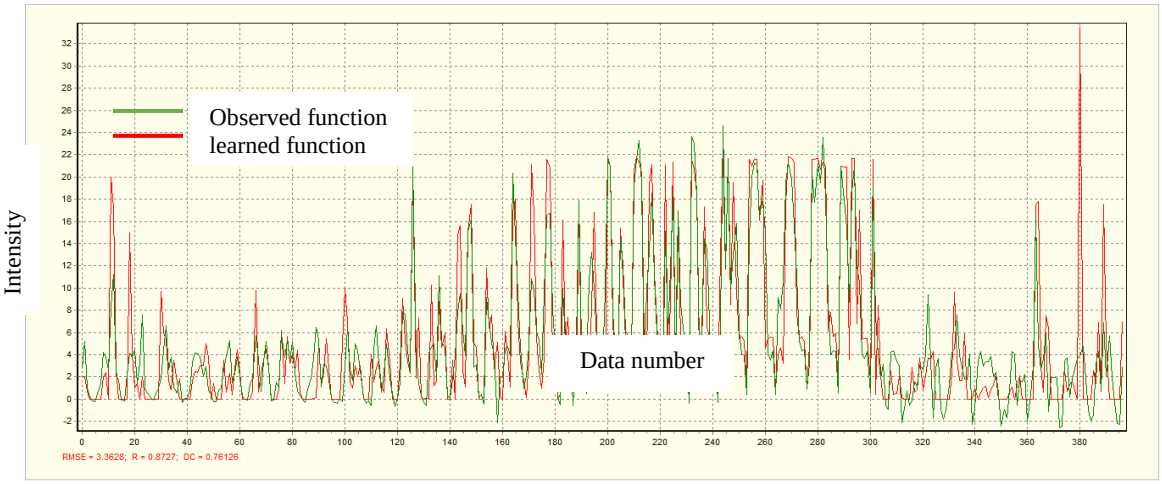

Figure 4-4 ANN learning process for 36 years testing data.

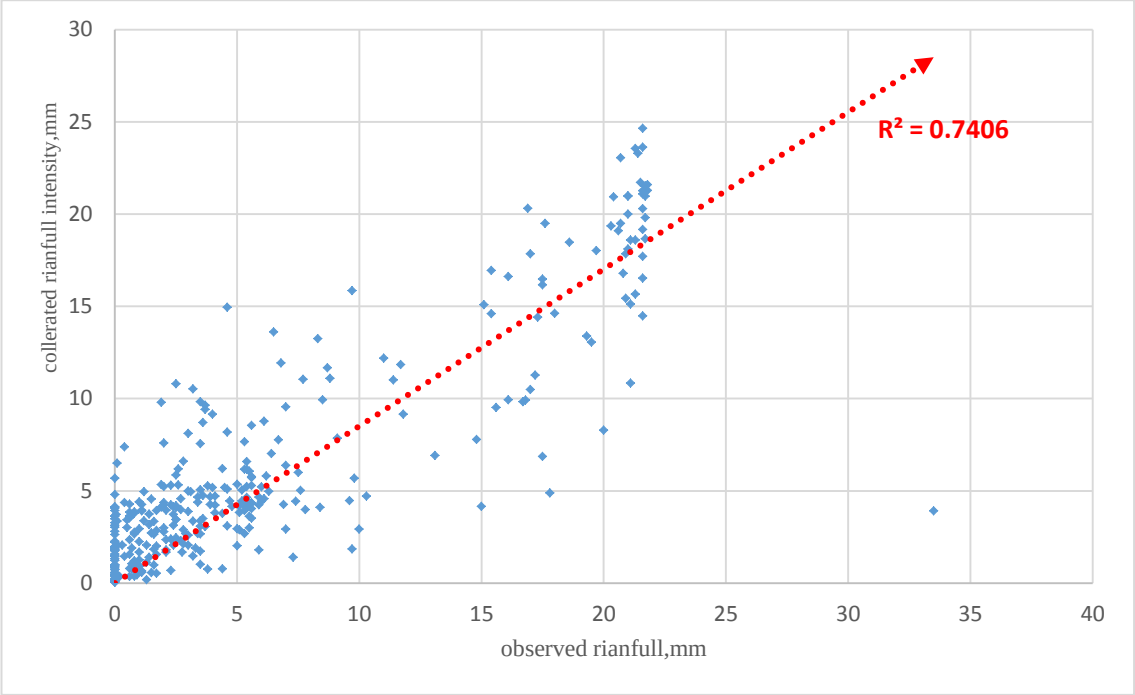

Figure 4-5 Correlation strength of the fitting line between observed and learned data for 36 years.

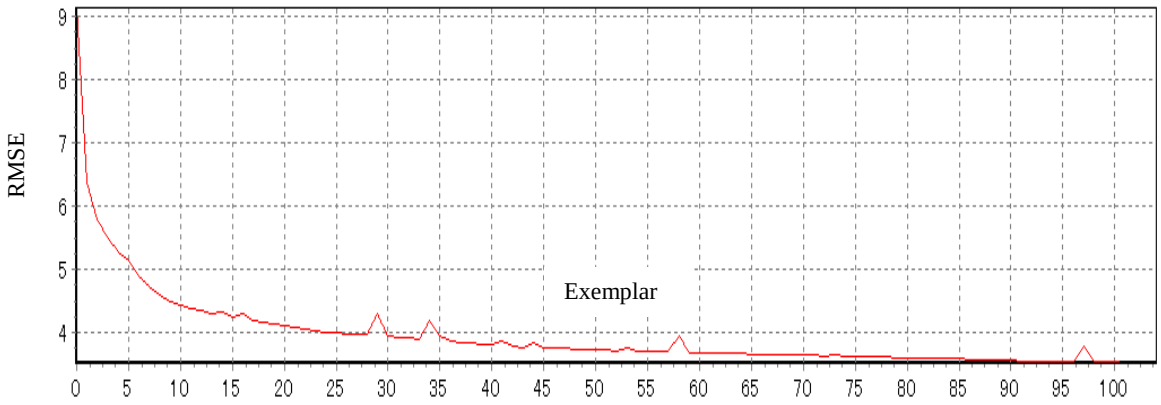

Figure 4-6 RMSE function behavior during function learning process.

4.2.2 Weights distributions of models

Weight is the most important factor in learning process. Each input parameter is connected to all nodes in the first hidden layer, and each node in a hidden layer connected to the nodes of the second hidden layer,

also, each output layer is connected to the nodes of the last hidden layer. In addition to bias number. The total mentioned connections refers to the number of weights. Figure (4.7) illustrates layers connections between them of two different cases.

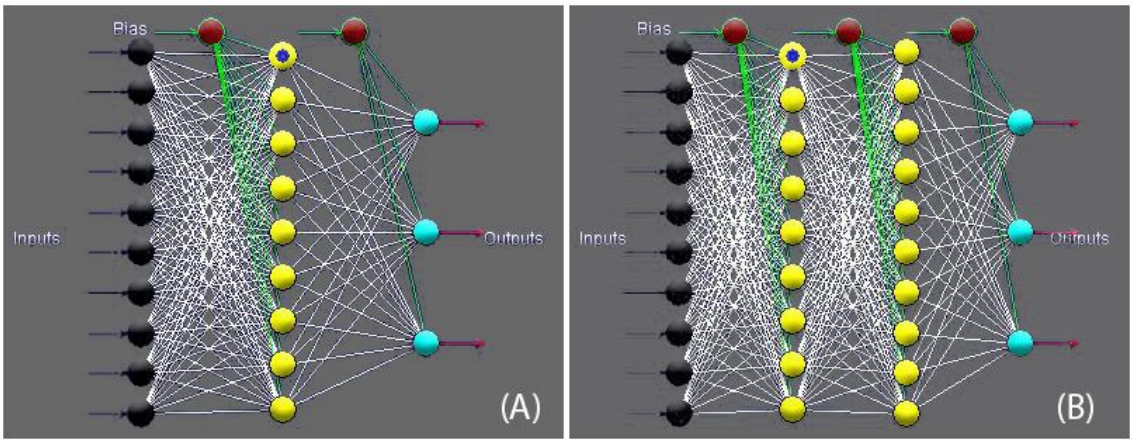

Figure 4-7 weight distribution process, A- for 1 hidden layer contains 9 nodes, B- for 2 hidden layer contains 19 nodes.

The number of weight, maximum and minimum value of it varies from ANN model to another. Figure (4.8) show weight distribution of model 1, the total number of weights are 232 and the most effective value of weight is (33). It should be noted that the horizontal axis refers to number of weights, and the vertical axis refers to weight value, for all weight distribution figures.

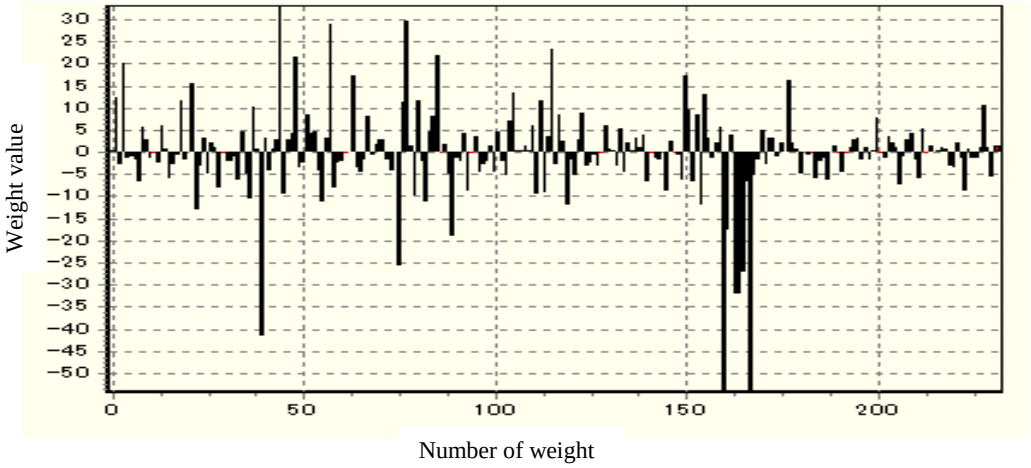

Figure 4-8 show distribution of the weights of model 1.

Figure (4.9) clarifies weight distribution for model 2, the number of weights connection are 356 and the most effective value of weight is (77).

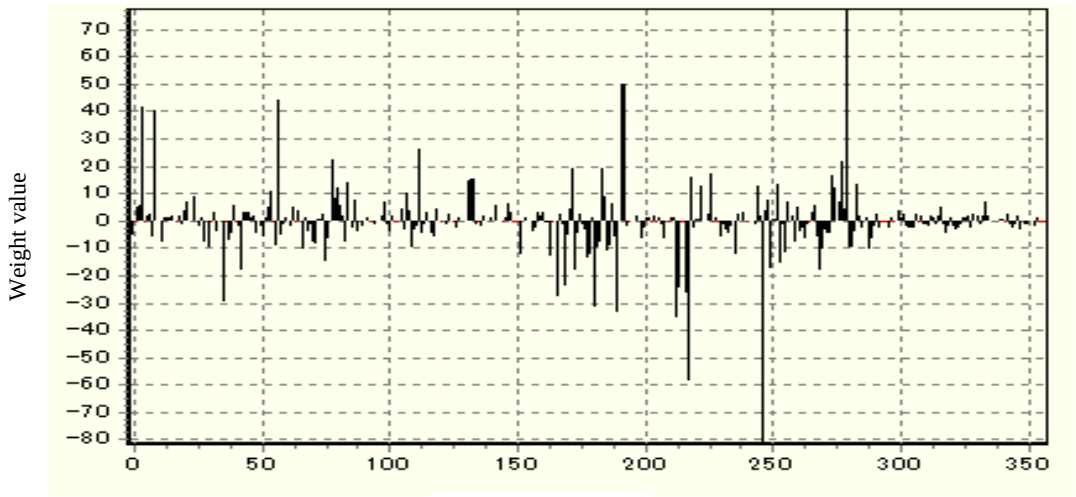

Figure 4-9 show distribution of the weights of model 2.

Figure (4.10) illustrates the weight distribution for model 3, the number of weights connection are 232 and the most effective value of weight is (89).
Figure (4.11) illustrated weight distribution for model 4, the number of weights connection are 129 and the most effective value of weight is (94)
Figure (4.12) show the weight distribution for model 5, the number of weights connection are 356 and the most effective value of weight is (80).

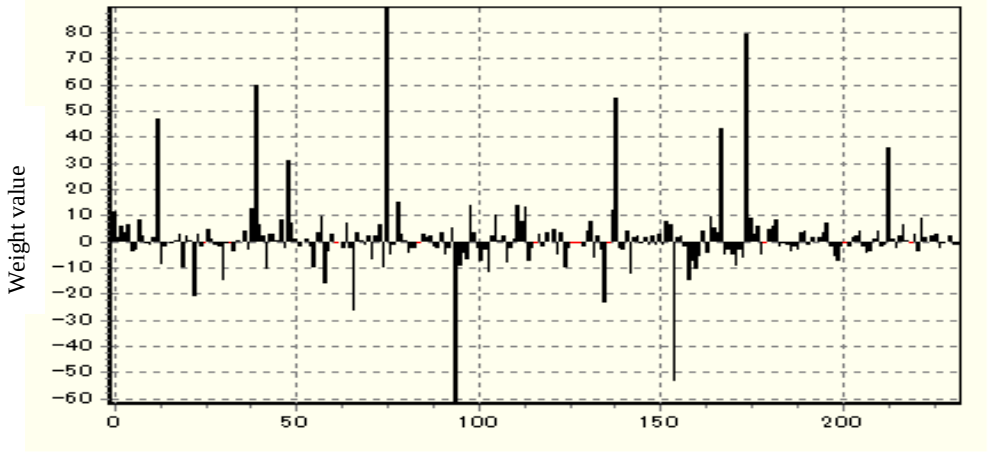

Figure 4-10 show distribution of the weights of model 3.

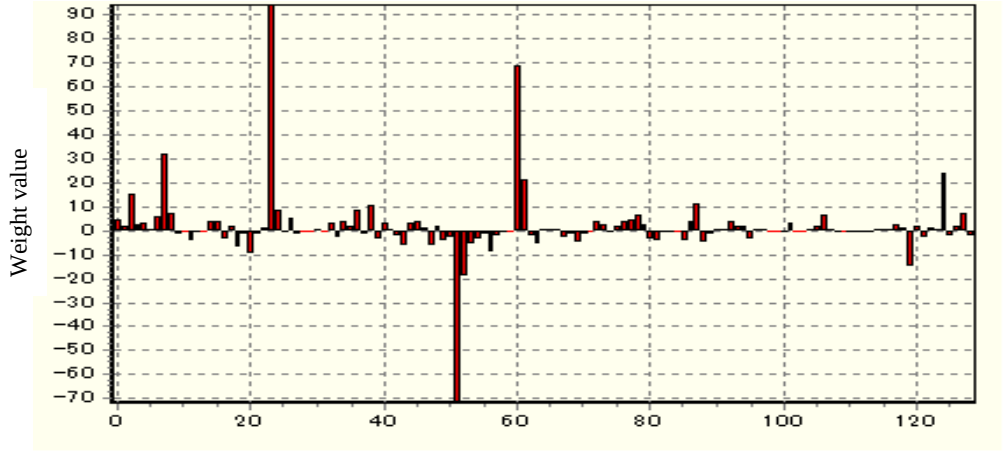

Figure 4-11 show distribution of the weights of model 4.

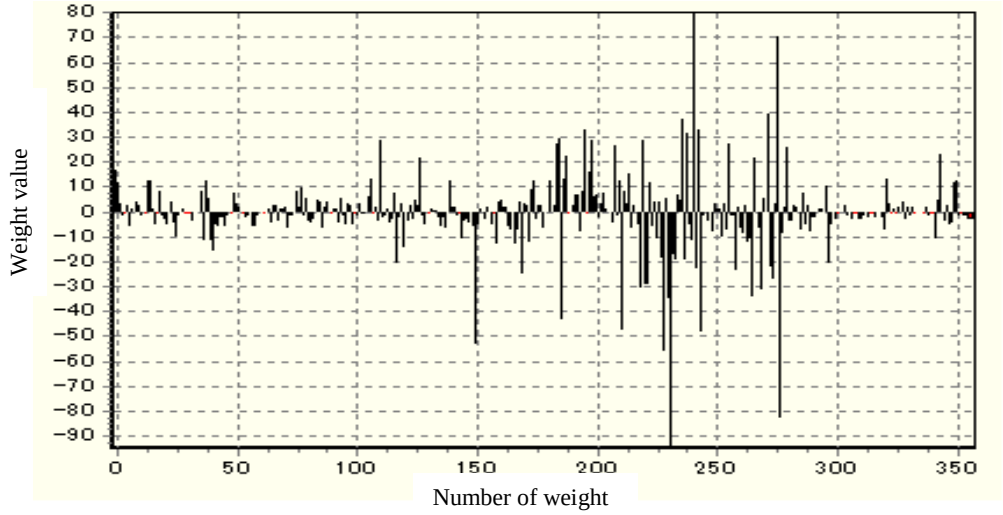

Figure 4-12 show distribution of the weights of model 5.

4.2.3 Calibration of ANN model

The difficulty of predicting rain intensity due to the fact that it is a non-continuous function daily such as temperature and depends on the seasons and rainy periods. After selecting the ANN parameters (function type, number of hidden layers, and number of neurons each layer), Table(4.2) show number of the models, number of hidden layers, R^2, RMSE for ANN models that used to prediction the rainfall intensity in the study area. Model 1 was the first model chose and model 3 was the second model chose, since they have minimum RMSE values (1.67, 3.46), and maximum R^2 values (0.722, 0.64), respectively.

Table 4-2 The model description, number of hidden layers, and its parameter.

number of model	Description	Number of hidden layers	R^2	RMSE
Model 1	First model for 10 years for period (1981-1990)	2	0.722	1.67
Model 2	First model for 10 years for period (1981-1990)	3	0.684	2.68
Model 3	Second model for 36 years for period (1981-2016)	2	0.64	3.46
Model 4	Second model for 36 years for period (1981-2016)	1	0.62	3.68
Model 5	Second model for 36 years for period (1981-2016)	3	0.41	5.25

It is worth to mention that the used data in ANN model has been selected randomly by SPSS program. About 95% of data set has been

selected randomly for generating the training function process, and about 5% of data set has been taken for validation (testing) process. Figures (4.13, 4.14, and 4.15) illustrates the result of calibration process between the observed and the predicted rainfall intensity data for models 3, 4, and 5 respectively.

In Figure (4.13), the Figure clarifies that the mathematical model was able to predict values to an acceptable limit, and can be used to predict in the coming years with some ratios of errors.

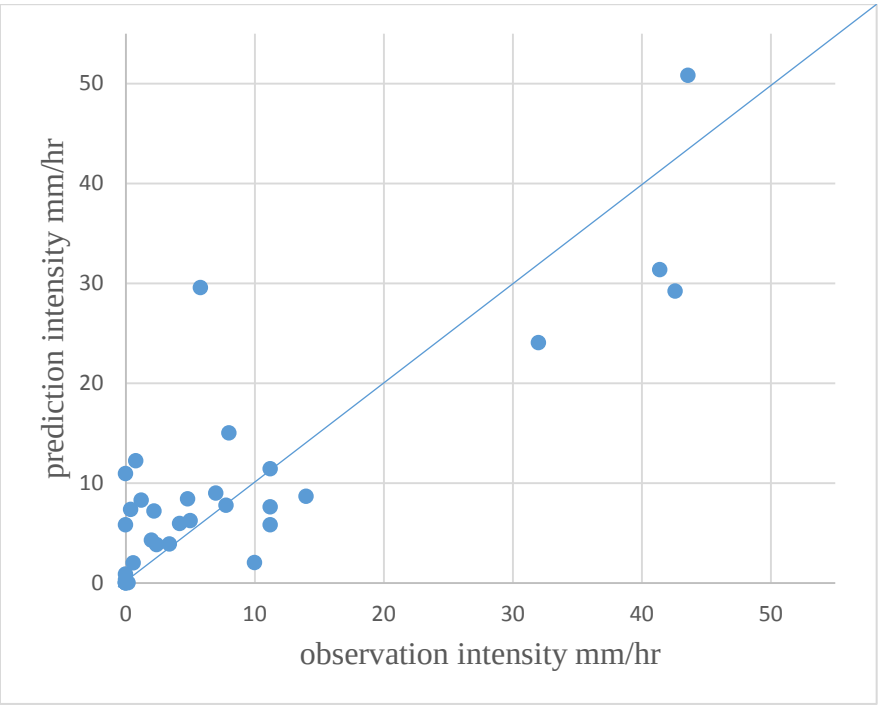

Figure 4-13 predict versus observation intensity values of model 3 ((R^2=0.640, RMSE=3.460).

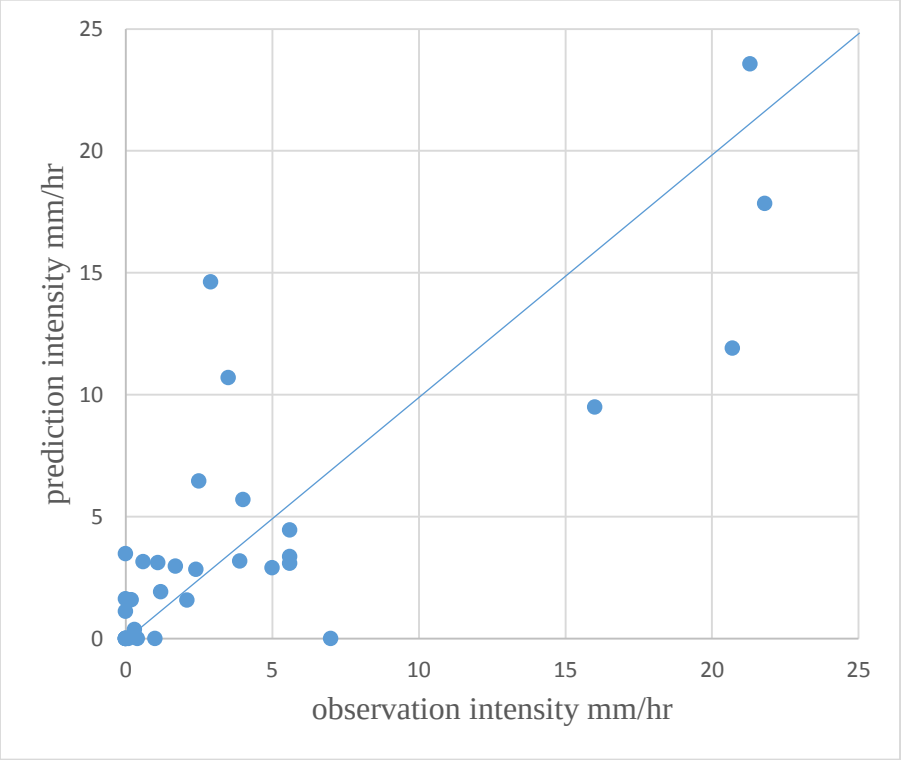

Figure 4-14 predict versus observation intensity values of model 4 (R^2=0.620, RMSE=3.680).

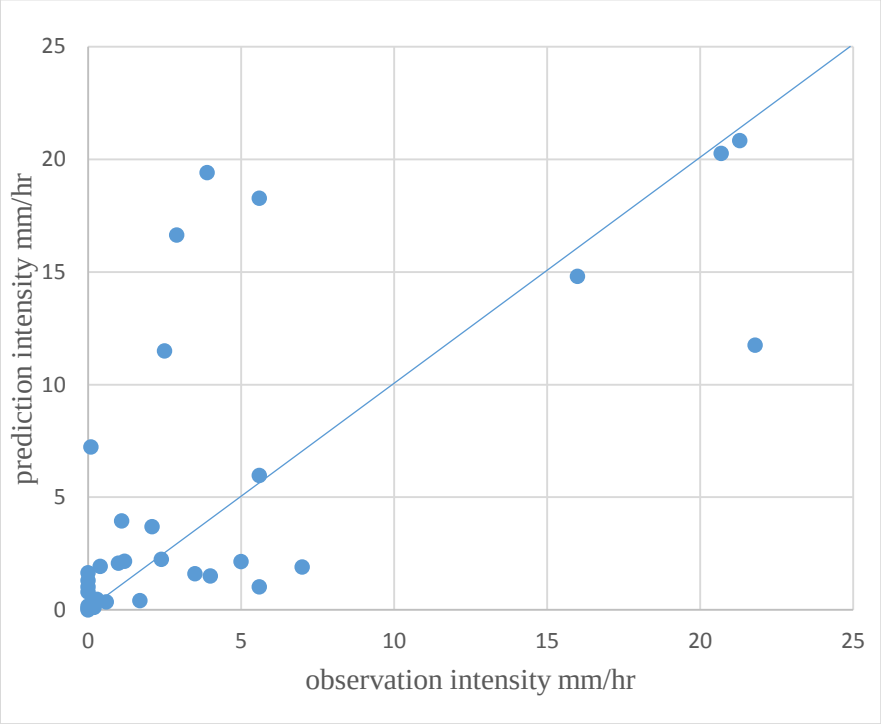

Figure 4-15 predict versus observation intensity for model 5 (R^2=0.410, RMSE=5.25).

Figure (4.16) shows the intensity value for three periods from 1981- 1990 which gated from the General Authority for metrological and Seismic Observations (G.A.A.S.O, 2018), second period (1991-2008) which predicted from the model 1 and the third period (2008-2016) which gated from (I.A.C.D, 2018) the trend line of the intensity increase with the progress of time in general. Using model 3 to predicted rainfall intensity from 2017-2070, in general the trend line of the prediction increase with progress of time this illustrates in Figure (4.17) , the maximum value of each year from Figure (4.17) enter to the SWMM. Model 3 can used to predict rainfall intensity at any period due to it is developed depend on climate change of 36 years.

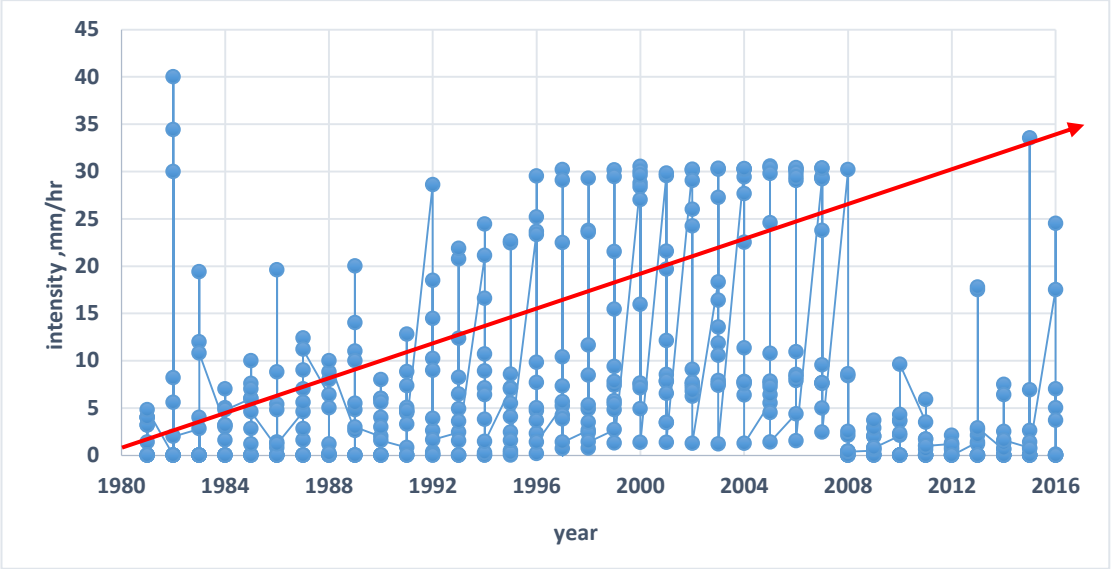

Figure 4-16 observation data of rainfall intensity.

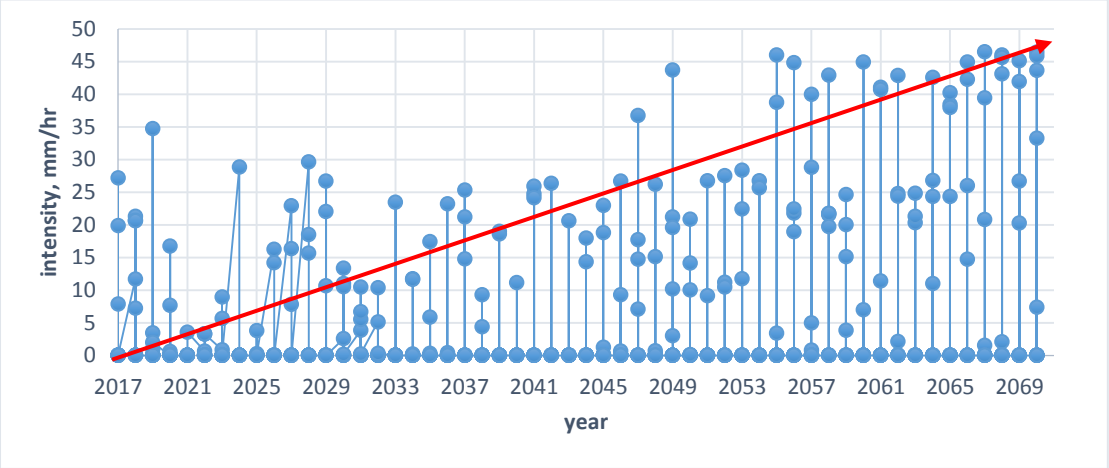

Figure 4-17 Prediction of rainfall intensity by ANN model (model 3).

4.2.4 Effect of climate change on ANN model

There are many factor of climate use to build ANN models include rainfall, max temperature, min temperature, wind speed, humidity, and sun shine. From ANN models it has been concluded that the rainfall more factor effect on the modeling. Rainfall, wind speed, sun shine, min temperature, max temperature, and humidity the sequence of climate factor

that effect on model 1. Rainfall, wind speed, sun shine, min temperature, humidity, and max temperature. The sequence of climate factor effect on model 3.

In each model generation, the priority of climate parameter changing according to their effects. For example, model 1 has parameter priority that differs from model 3. But, it should be noted that rainfall parameter is still the dominant among others. Figures (4.18, and4.19) illustrate model importance of data parameters.

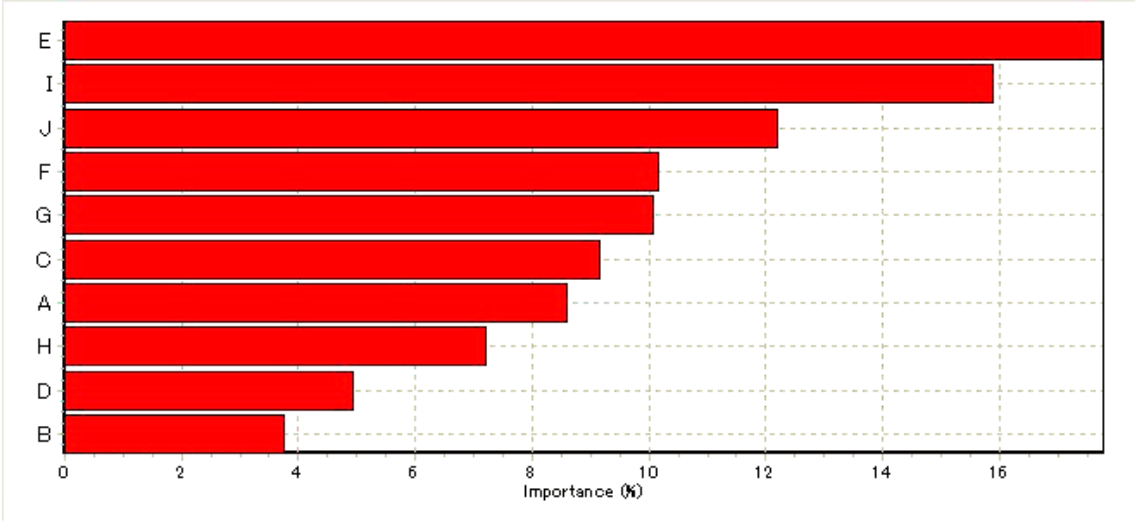

Figure 4-18 model importance distribution parameters of model 1.

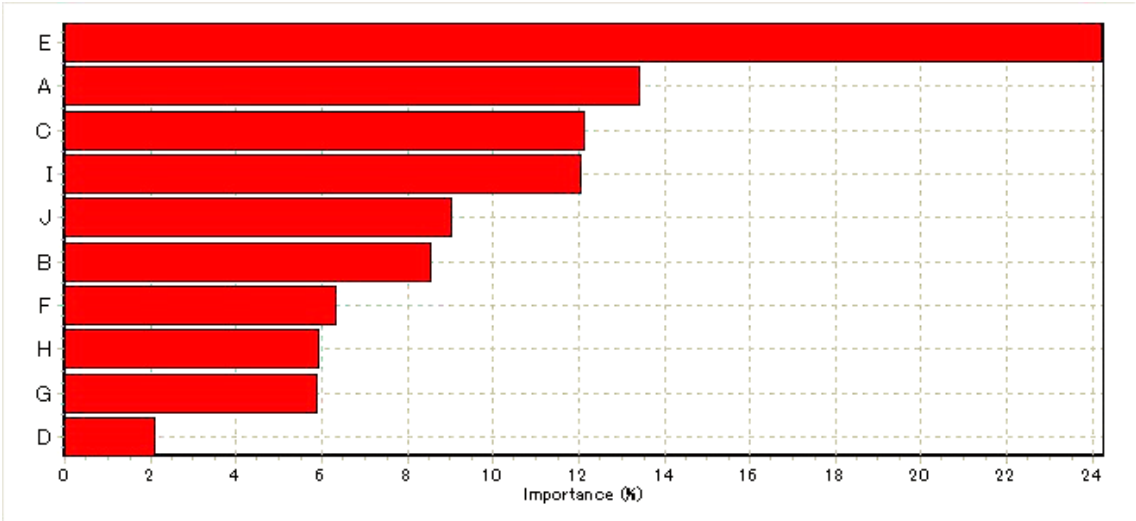

Figure 4-19 model importance distribution parameters of model 3.

Where:

A: is the years parameter

B: number of data N

C: is N-1 parameter

D: is N-1 parameter

E: rainfall intensity parameter

F: minimum temperature parameter

G: Maximum temperature parameter

H: Humidity parameter

I: wind speed parameter

J: is sunshine parameter

4.3 Flooding model

The process of Simulation flooding occurrence is not simple, since many different numbers of parameters should be considered during this step. After generating ANN model and prediction of data for different future periods, and preparing the network geometry and its related parameters, it can be said that simulation process is ready with SWMM. First, SWMM model shall be calibrated with current available data. Also, Simulation process shall cover different time periods.

4.3.1 Model calibration

A manual trial and error method has been used to calibrate the simulation model of storm drainage network of the study area. There was a lack in data that need to calibrate the model. There are six month available as observation data: January 2017, February 2017, November 2017, January 2018, March 2018, and April 2018. Rainfall intensity was using:

(7.86, 27.5, 19.86, 11.66, 21.28, and 7.24) mm/h. the result of calibration shown in figure (4.20).

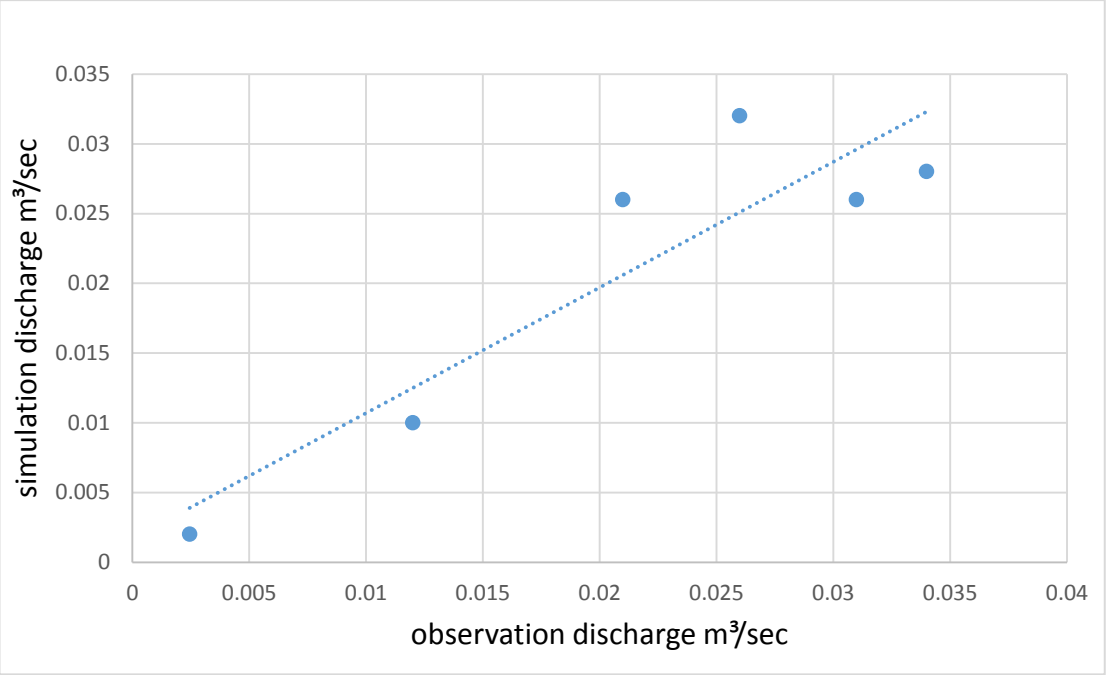

Figure 4-20 model calibration result under different rainfall intensity

In order to check the validity of all the input parameters in the model and estimation of model parameters, cross validation is carried out on the data. The cross validation results show that the mean square error (MSE) for all events are very close to zero (0.000021). Moreover, root mean square error (RMSE) is very low as compared to the variance of the observed data for all events (0.0045).The correlation coefficient (R^2) equal to (0.83). The model can be used after calibration with acceptable result and with the error rate indicate in the Table (4.3).

Table 4-3 the result of calibration of SWMM.

Observed data	Simulation results	MSE	RMSE	R^2	error
0.031	0.026				16.1%

0.026	0.032	0.000021	0.0045	0.83	23%
0.021	0.026				23.8%
0.012	0.01				16.6%
0.034	0.028				17.6%
0.0024	0.002				18.36%

4.3.2 Climate change simulation results by SWMM

The storm drainage network in the Al-Abbas quarter had been designed for a rainfall intensity of 13 mm/h and 2-year return period (D.S.K and 2018). However, the study area has been exposed to the impacts of climate change represent as increase in rainfall intensity reach to max percent in 2067 is three times of design intensity. The study area more exposed to flooding due to increase in rainfall intensity. The climate change of the case study has been simulated for the rainy event (maximum month in each year) for the future period from (2017 to 2070). The flooding discharge amount of the manholes divided into five stages as follows:

- Stage1 [no flooding] range from [0 to 0.001 m^3/sec].
- stage2 [very light flooding] range from [greater than 0.001 to 0.01 m^3/sec],
- stage3 [medium flooding] range from [greater than 0.01 to 0.05 m^3/sec]
- stage4 [high flooding] range from [greater than 0.05 to 0.12 m^3/sec],
- Stage 5 [very high flooding] for [greater than 0.12 m^3/sec].

In order to study this effect on rain intensity change, a set of expected rain intensities will be applied in the next years on the network in the study area. The focus will be on the high intensities expected to determine the extent of the network's ability to deal with these intensities.

Figure (4.21) show the behavior of the storm network in winter 2017 with rainfall intensity equal to 27.5mm/h, this value of rainfall intensity greater than design rainfall intensity with ratio equal to 111%.78% of the manhole had no flooding (stage 1) and 16% of the manhole had very light flooding (stage 2), 3% of the manhole had medium flooding (stage 3), 3% of the manhole flooding had high flooding (stage 4). So, the behavior of the network looks somewhat good for the duration of flooding 50 min.

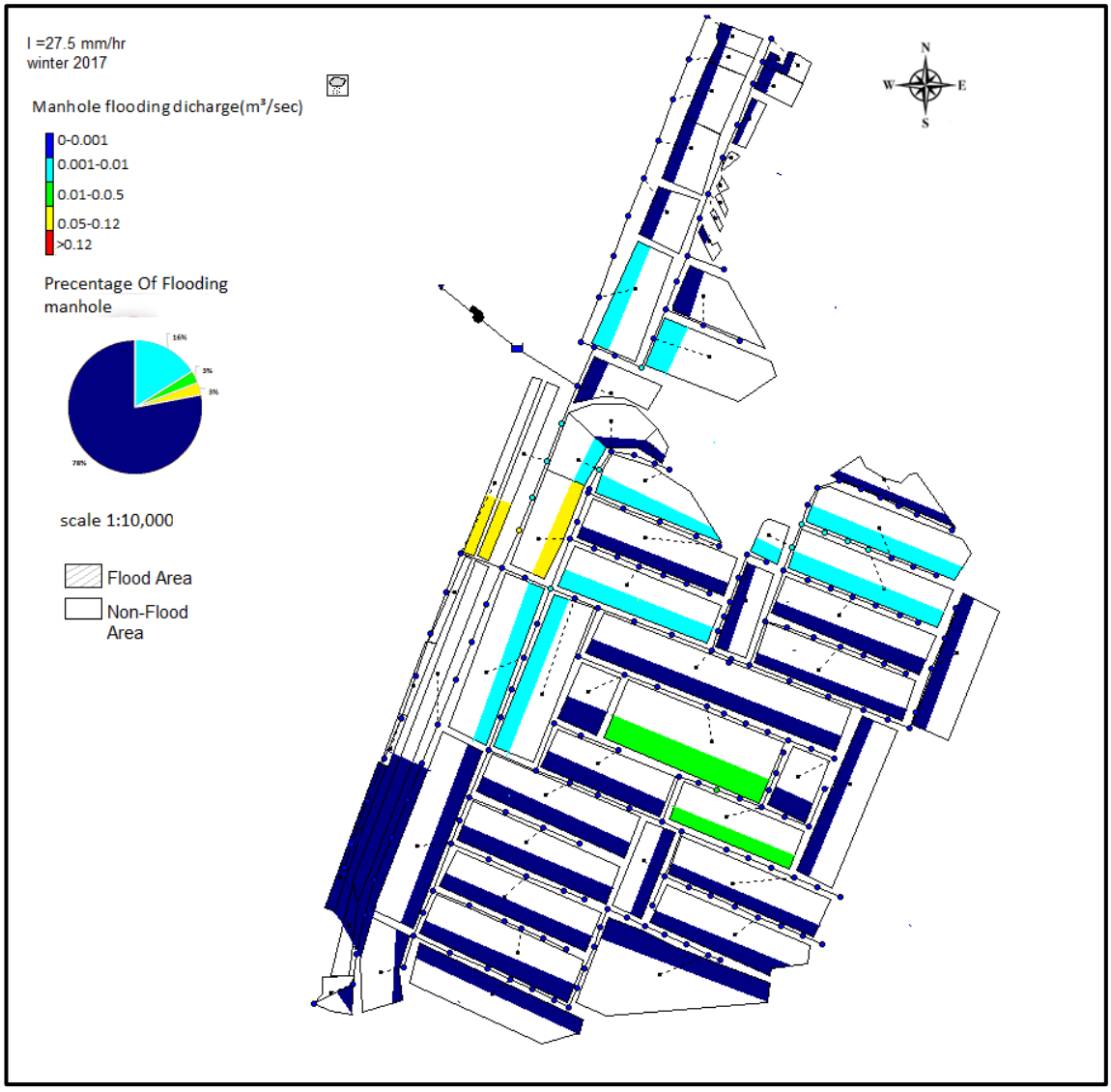

Figure 4-21 The flooding manhole under rainfall intensity (27.5 mm/h) at peak time in winter 2017.

Figure (4.22) show the behavior of the storm network in winter 2019 with rainfall intensity equal to 34.47mm/h, this value of rainfall intensity greater than design rainfall intensity with ratio equal to 165%.81% of the manhole had no flooding (stage 1) and 19% of the manhole had very light flooding (stage 2) so the behavior of the network consider good , the duration of flooding is 45 min.

Also, from the same Figure, it can be observed that flooding discharge condition for year 2019 decrease stage 1 with rate about 21.8%,

stage 2 has no change , stage 3 and stage 4 increase with double compared to year 2017. No significant change has been occurred during this interval since the period too close.

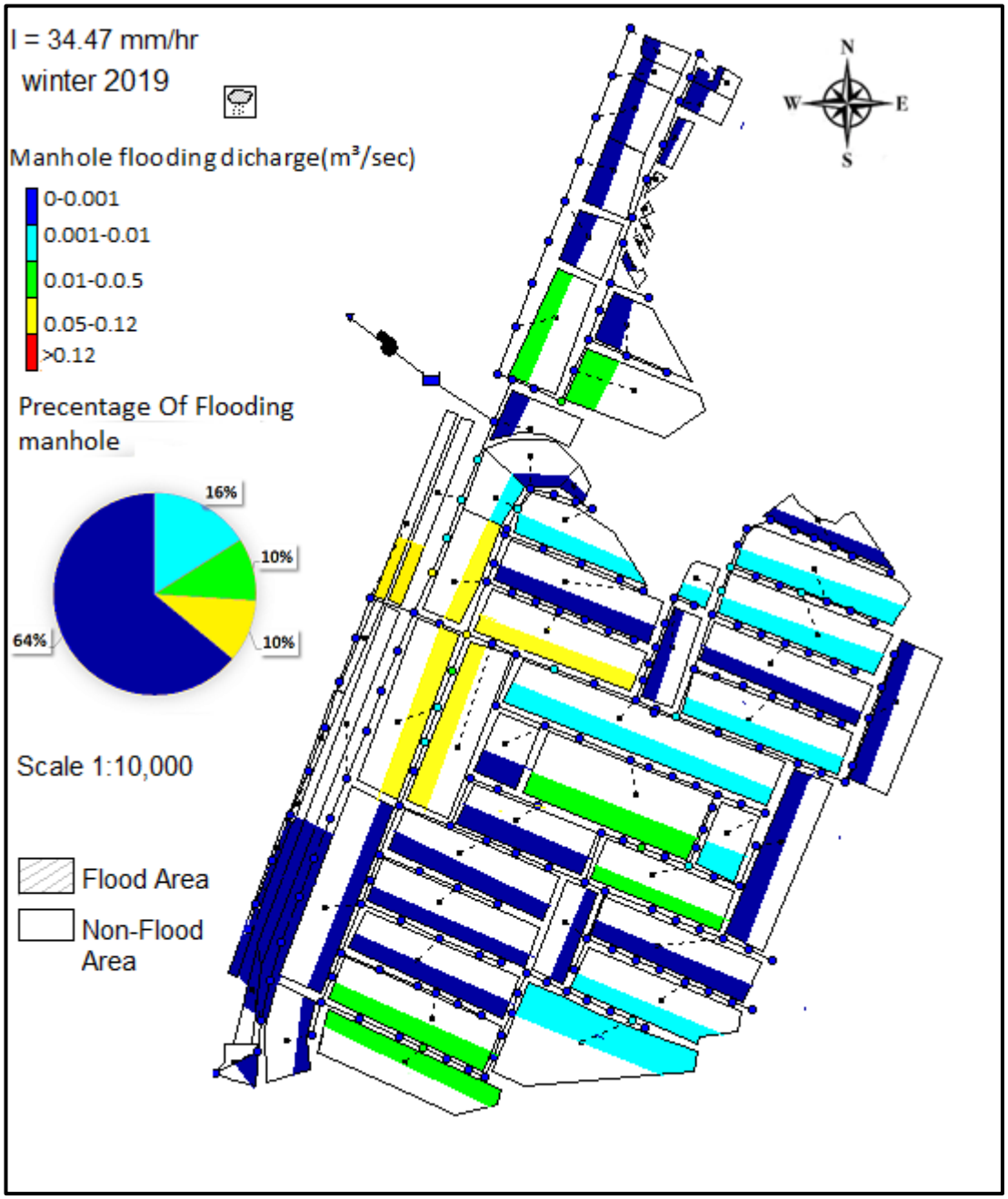

Figure 4-22 The flooding manhole under rainfall intensity (34.74 mm/h) at peak time in winter 2019.

Figure (4.23) Show the behavior of the storm network in winter 2024 with rainfall intensity equal to 28.82mm/h, this value of rainfall intensity

greater than design rainfall intensity with ratio equal to 121%. 73% of the manhole had no flooding (stage 1),14% of the manhole flooding had very light flooding (stage 2), 3% of the manhole had medium flooding (stage 3), and 10% of the manhole flooding had high flooding (stage 4) , the duration of flooding is 45 min .

Also, from the same Figure, it can be observed that flooding discharge condition for year 2024 increase stage 1 with rate about 14%, stage 2 has been decrease with rate about 14.2%, stage 3 decrease to double and stage 4 had no change compared to year 2019.

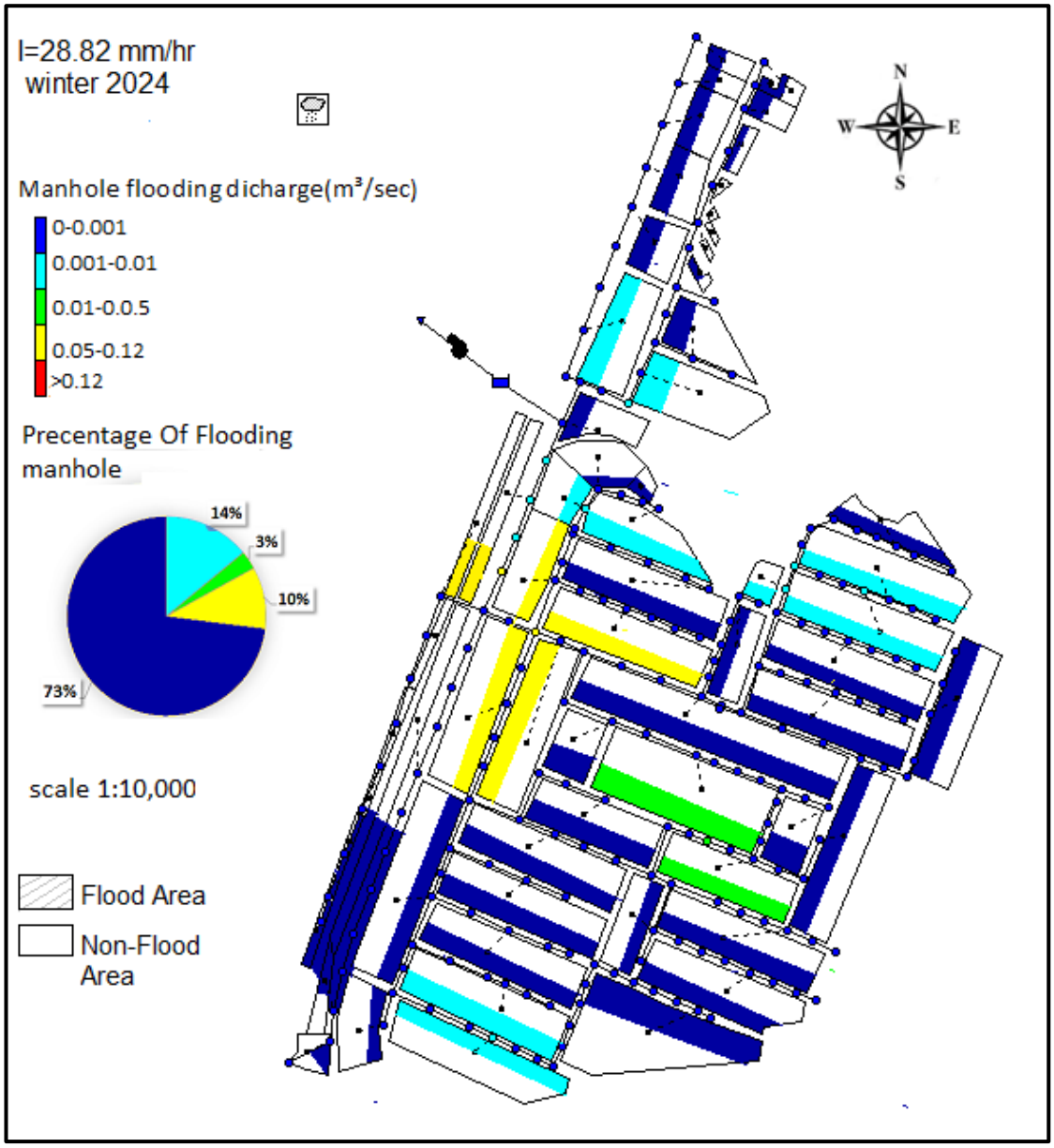

Figure 4-23 The flooding manhole under rainfall intensity (28.82 mm/h) at peak time in winter 2024.

Figure (4.24) Show the behavior of the storm network in winter 2028 with rainfall intensity equal to 29.62mm/h, this value of rainfall intensity greater than design rainfall intensity with ratio equal to 127%. 86% of the manhole had no flooding (stage 1), 13% of the manhole flooding had very light flooding (stage 2) and 1% of the manhole flooding had high flooding (stage 4) , the duration of flooding is 50 min .

Also, from the same Figure, it can be observed that flooding discharge condition for year 2028 increase stage 1 with rate about 1.3%, stage 2 has been decrease with rate about 7.6% , stage 3 and stage 4 had no change compared to year 2024. No significant change has been occurred during this interval since the period too close.

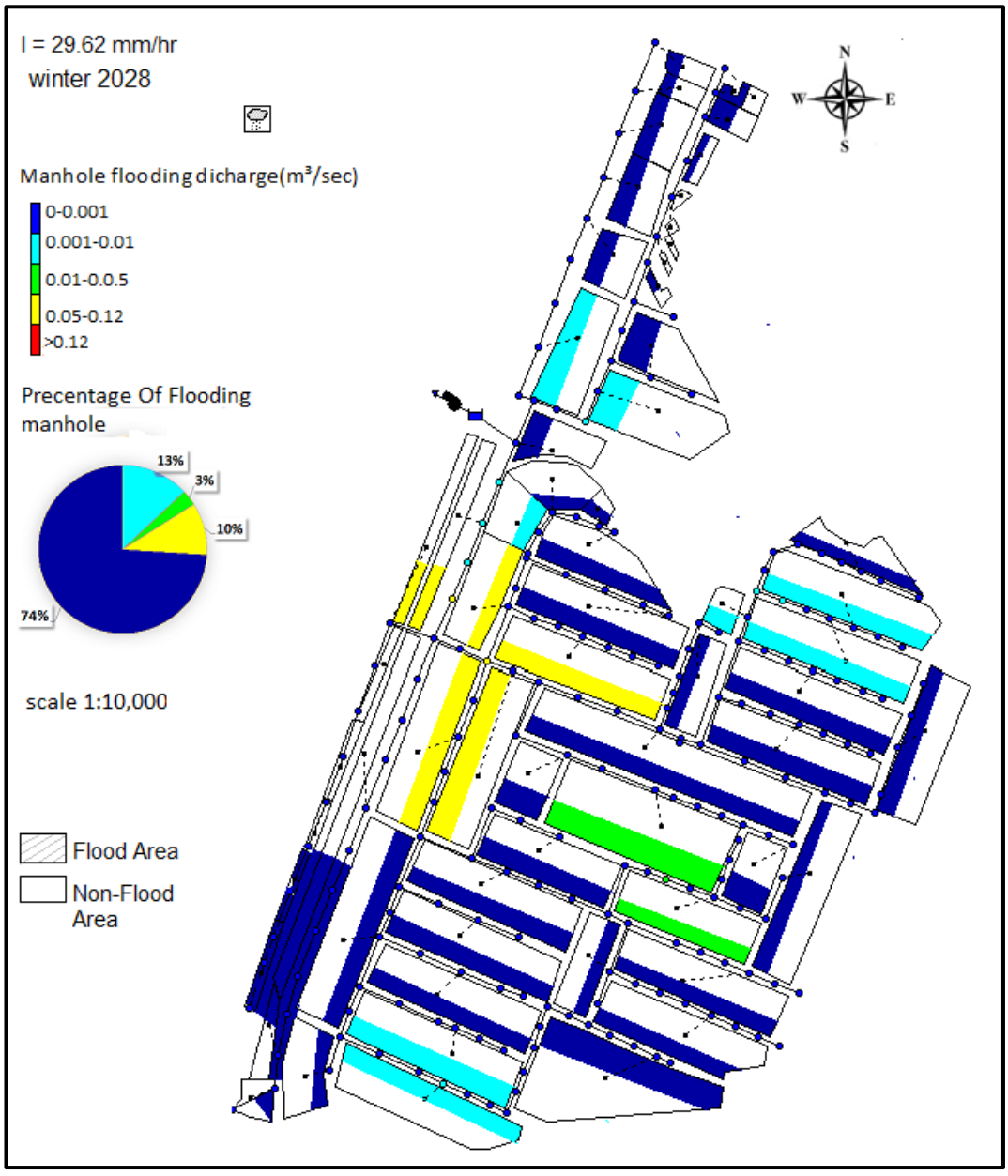

Figure 4-24 The flooding manhole under rainfall intensity (29.62 mm/h) at peak time in winter 2028.

Figure (4.25) show the behavior of the storm network in winter 2037 with rainfall intensity equal to 25.28mm/h, this value of rainfall intensity greater than design rainfall intensity with ratio equal to 94%. 74% of the manhole had no flooding (stage 1), 13% of the manhole had had very light flooding (stage 2) ,8% of the manhole had medium flooding (stage 3)and, 5% of the manhole had very high flooding (stage 5) ,the duration of flooding is 50 min.

Also, from the same Figure, it can be observed that flooding discharge condition for year 2037increase stage 1, stage 2 have been no change , stage 3 has increase with rate about 1.6%, and stage 4 has been decrease once time to year 2028. No significant change has been occurred during this interval since the period too close.

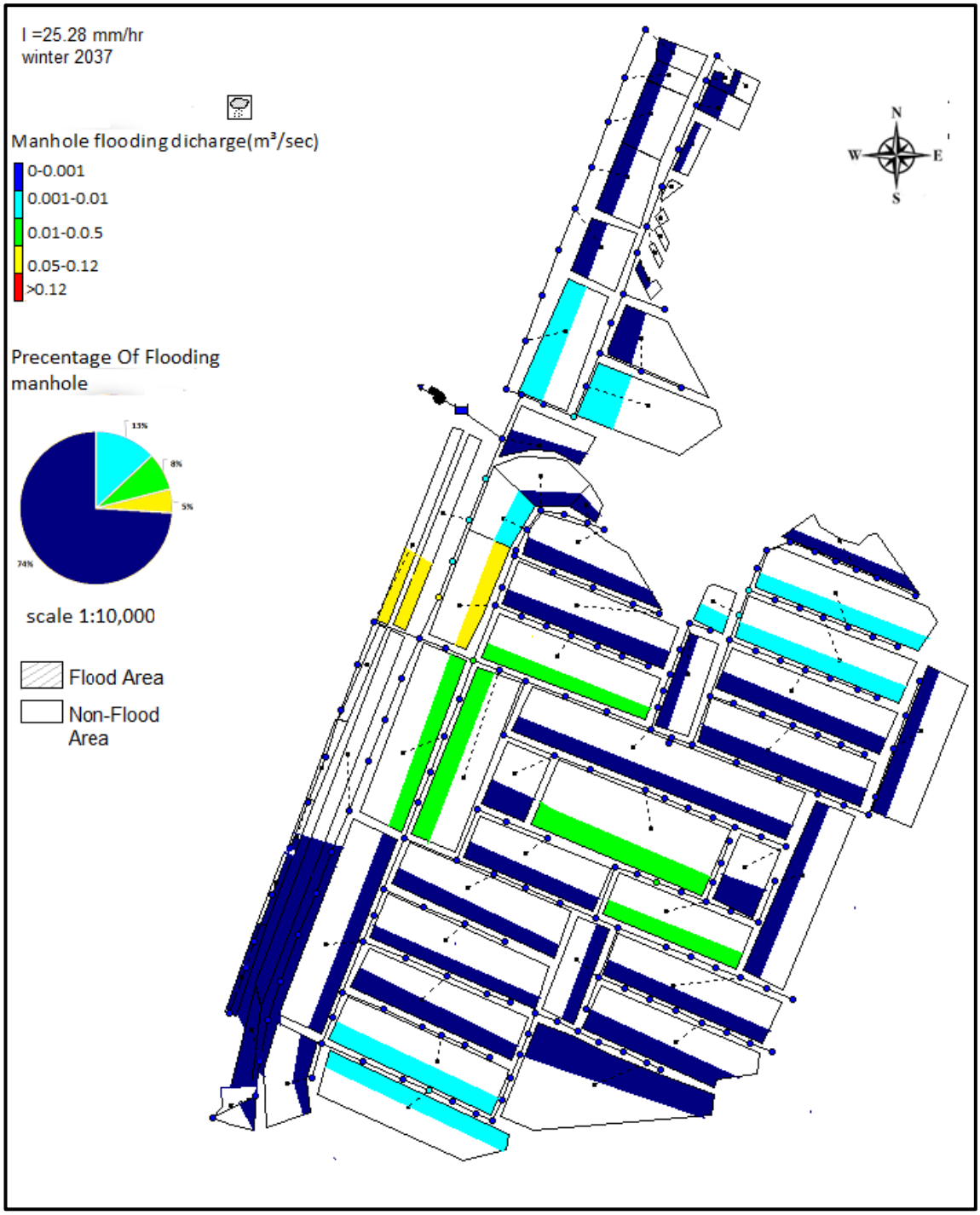

Figure 4-25 The flooding manhole under rainfall intensity (25.28 mm/h) at peak time in winter 2037.

Figure (4.26) show the behavior of the storm network in winter 2042 with rainfall intensity equal to 26.34mm/h, this value of rainfall intensity greater than design rainfall intensity with ratio equal to 103%. 76% of the manhole

had no flooding (stage 1), 11% of the manhole had had very light flooding (stage 2) ,8% of the manhole had medium flooding (stage 3)and, 5% of the manhole had very high flooding (stage 5) ,the duration of flooding is 45 min.

Also, from the same Figure, it can be observed that flooding discharge condition for year 2042 increase stage 1 with rate about 2.7%, stage 2 has been decrease with rate about 18.1%, stage 3 and stage 4 had no change compared to year 2037. No significant change has been occurred during this interval since the period too close.

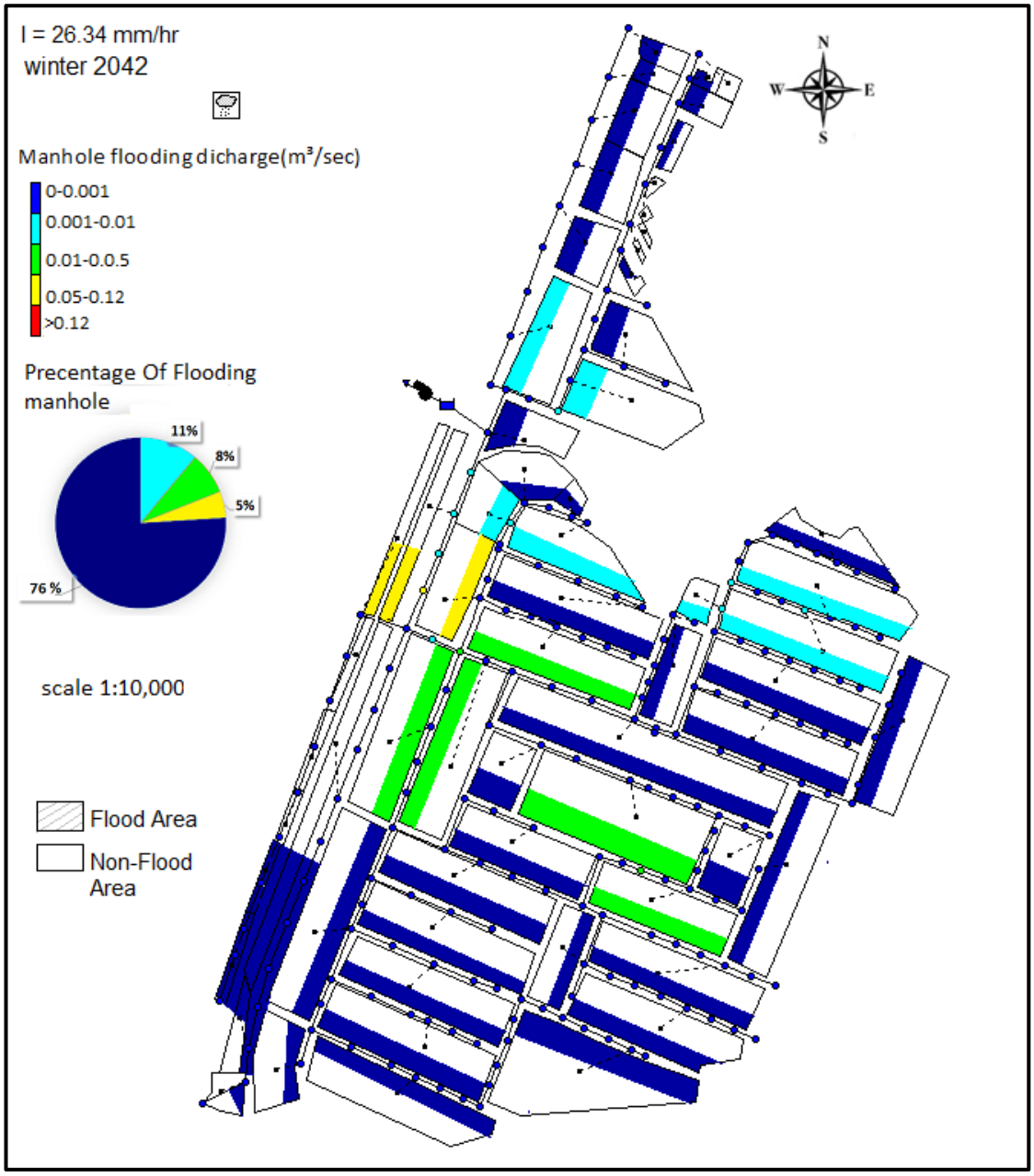

Figure 4-26 The flooding manhole under rainfall intensity (26.34 mm/h) at peak time in winter 2042.

Figure (4.27) show the behavior of the storm network in winter 2055 with rainfall intensity equal to 45.98mm/h, this value of rainfall intensity greater than design rainfall intensity with ratio equal to 254%.56% of the manhole had no flooding (stage 1), 14% of the manhole had very light flooding (stage 2), 21% of the manhole had medium flooding (stage 3), 3% of the

manhole flooding had high flooding (stage 4) and, 6% of the manhole had very high flooding (stage 5), the duration of flooding is 20 min.

Also, from the same Figure, it can be observed that flooding discharge condition for year 2055 decrease stage 1 with rate about 35.7%, stage 2 has been increase with rate about 27.2% , stage 3 has been increase with rate about 1.6 time , stage 4 has been decrease with rate about 66.6%,and stage 5 has been increase with rate about 6% compared to year 2042.

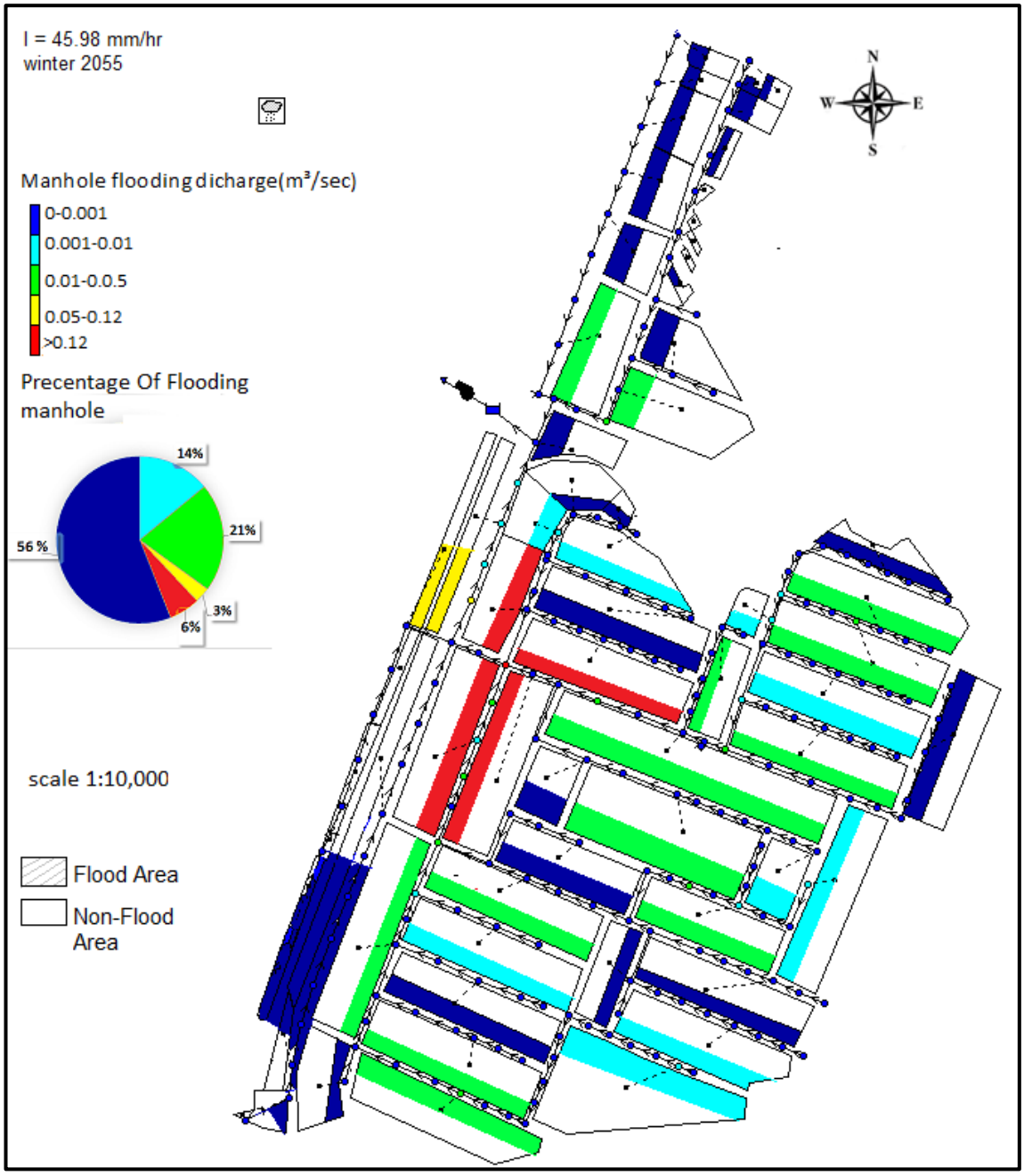

Figure 4-27 The flooding manhole under rainfall intensity (45.98 mm/h) at peak time in winter 2055.

Figure (4.28)show the behavior of the storm network in winter 2060 with rainfall intensity equal to 44.9mm/h, this value of rainfall intensity greater than design rainfall intensity with ratio equal to 245%.60% of the manhole had no flooding (stage 1), 11% of the manhole had had very light flooding (stage 2) ,20% of the manhole had medium flooding (stage 3), 3% of the

manhole flooding had high flooding (stage 4) ,and, 6% of the manhole had very high flooding (stage 5) ,the duration of flooding is 35min.

Also, from the same Figure, it can be observed that flooding discharge condition for year2060 increase stage 1 with rate about 6.1%, stage 2 has been decrease with rate about 27.2% , stage 3 has been decrease with rate about 5% , stage 4 has been increase about once time ,and stage 5 has been decrease about 6% once time compared to year 2055.

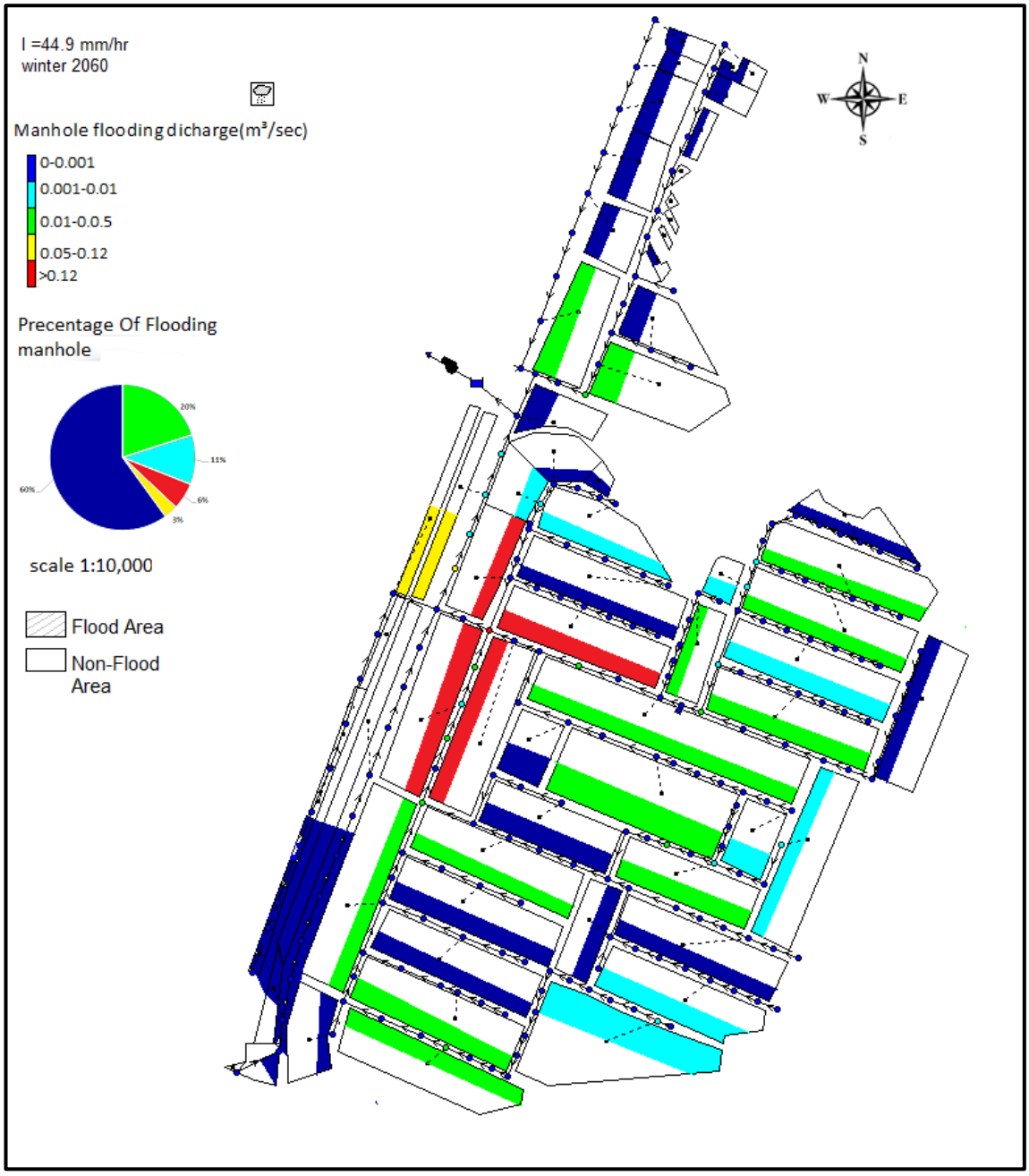

Figure 4-28 The flooding manhole under rainfall intensity (44.9 mm/h) at peak time.

Figure (4.29) show the behavior of the storm network in winter 2067 under maximum rainfall intensity equal to 46.48mm/h, this value of rainfall intensity greater than design rainfall intensity with ratio equal to 257%.59% of the manhole had no flooding (stage 1), 16% of the manhole had very light flooding (stage 2), 19% of the manhole had medium flooding (stage 3)

and, 6% of the manhole had very high flooding (stage 5), the duration of flooding is 45 min.

Also, from the same Figure, it can be observed that flooding discharge condition for year 2067 decrease stage 1 with rate about 7.1%, stage 2 has been increase with rate about 27.2%, stage 3 has been increase with rate about 5%, stage 4 has been decrease about one time, and stage 5 has been increase about once time compared to year 2060.

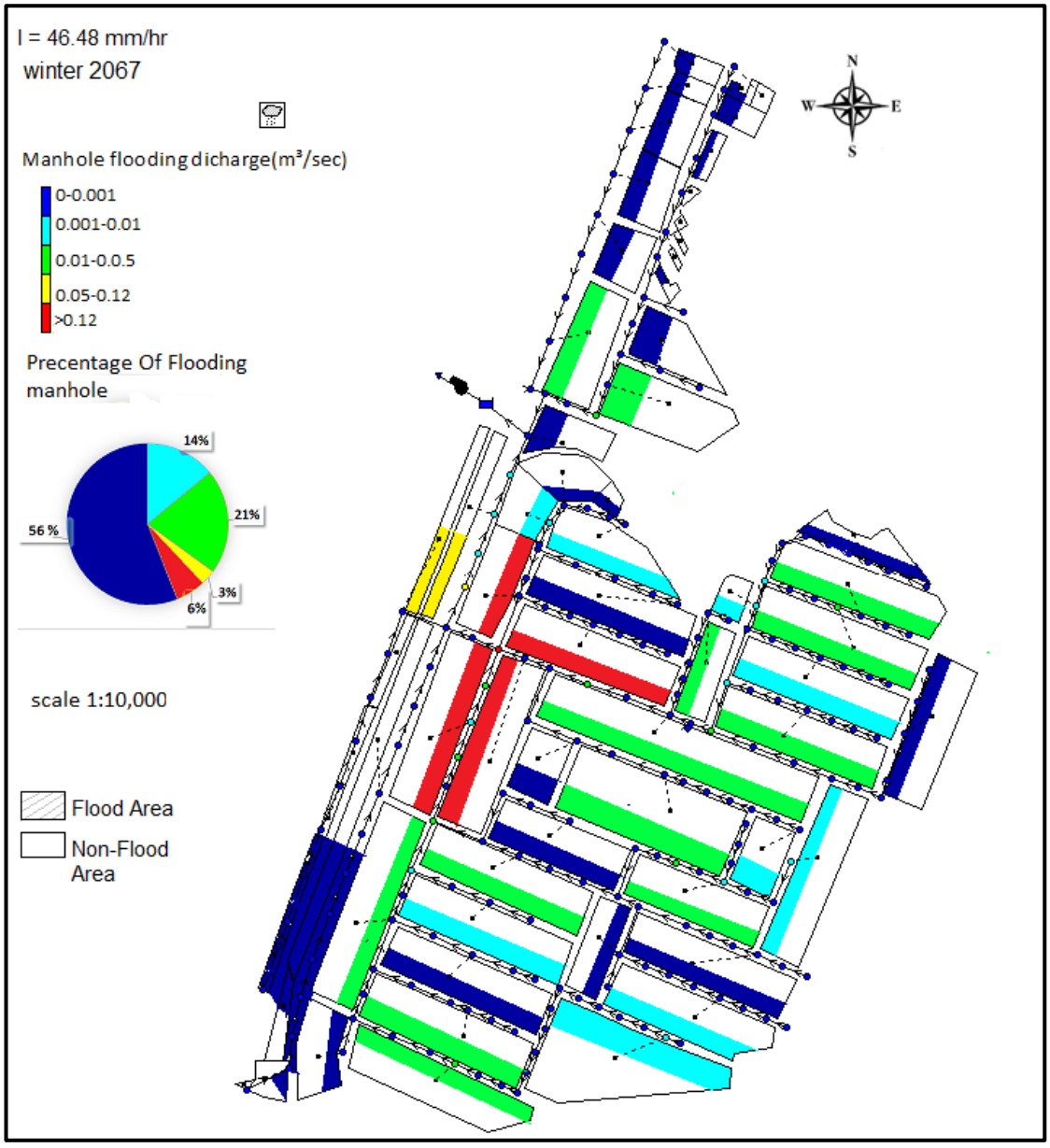

Figure 4-29 The flooding manhole under maximum rainfall intensity (46.48 mm/h) at peak time in winter2067 .

Figure (4.30) show the behavior of the storm network in winter 2070 with rainfall intensity equal to 46.42mm/h, this value of rainfall intensity greater than design rainfall intensity with ratio equal to 257%.56% of the manhole had no flooding (stage 1), 14% of the manhole had very light flooding (stage 2), 21% of the manhole had medium flooding (stage 3), 3% of the manhole flooding had high flooding (stage 4) and, 6% of the

manhole had very high flooding (stage 5), the duration of flooding is 45 min.

Also, from the same Figure, it can be observed that flooding discharge condition for year 2070 decrease stage 1 , stage 2, stage 3, stage 4, and stage 5 have been no change compared to year 2067. No significant change has been occurred during this interval since the period too close.

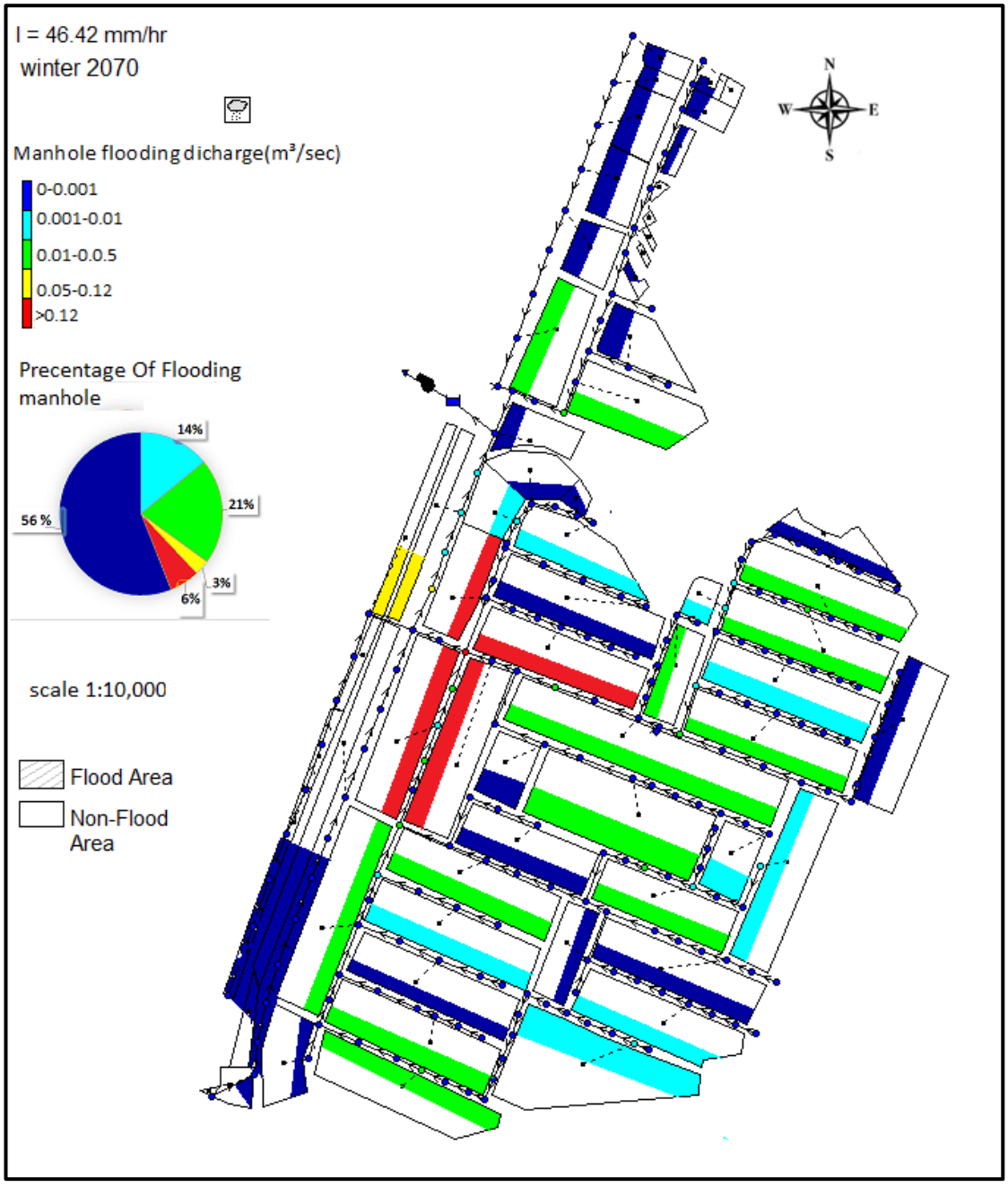

Figure 4-30 The flooding manhole under rainfall intensity (46.42 mm/h) at peak time in winter 2070.

For the cases above there are decrease and increase in the flooding discharge manhole rate with progress of time, but originally flooding discharge increase when compared the end design period (2070) with beginning design period (2017) stage 1 has been decrease with rate about 39.2%, stage 2 has been increase with rate about 14.2%, stage3 has been

increase about 6 times, stage 4 has no change, and stage 5 increase with rate about 6%.

4.4 Result of Suggested scenario

The result of suggestion shall cover the future additional land use area (up to 2070) that surrounding the end life span of Karbala master plan (2050). Figure (4.31) clarifies the proposed future additional land use area and flooding discharge.

Figure (4.31) contains variation of flooding discharge from 2017 until 2070, in addition to current flooding discharge. The current flooding discharge (2017) is about 2.75 m^3/sec. The value of flooding discharge manhole at the end period of master plan (2050) reach to 11.48 m^3/sec, which is increasing about three times of the current flooding discharge (2017). At the end of design period (2070) the value of flooding discharge manhole reach to 16.83 m^3/sec, the rate of increase reach to five time the current one.

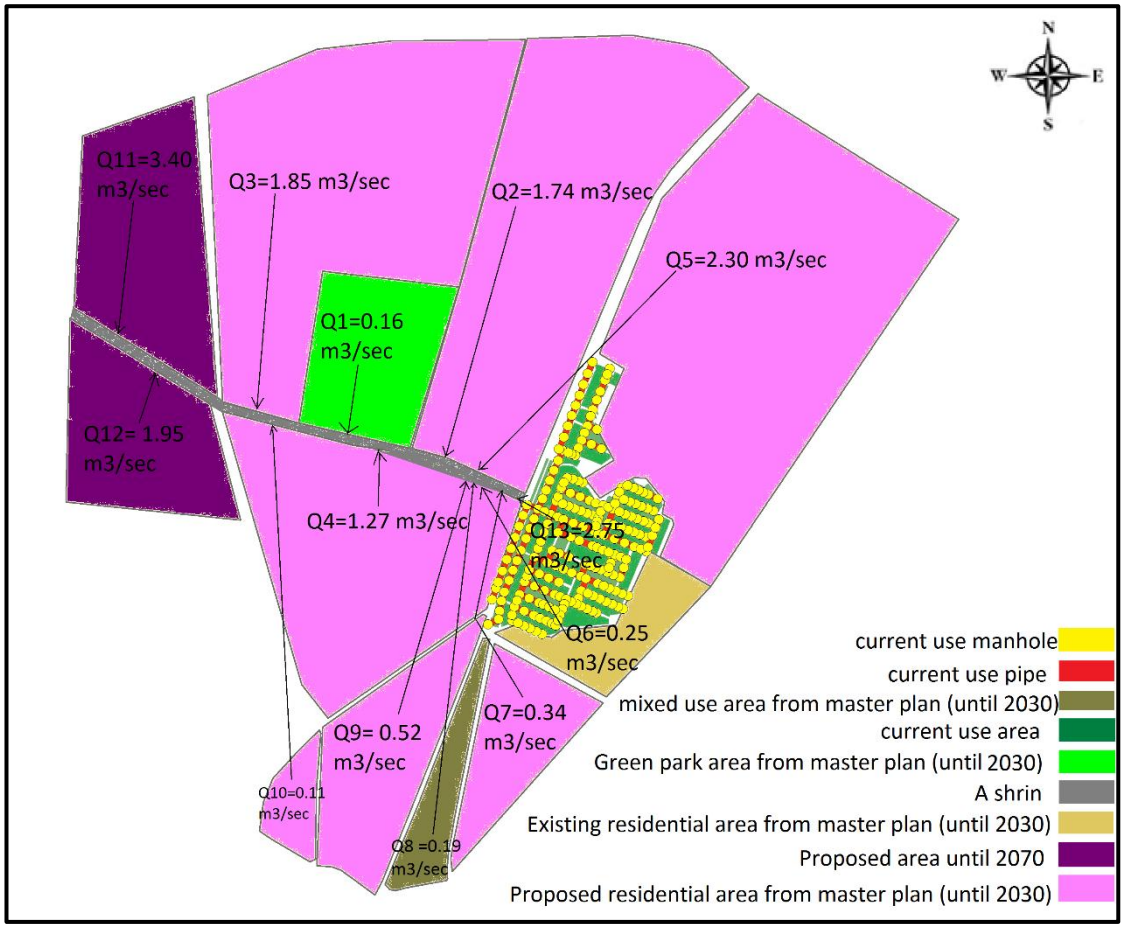

Figure 4-31 suggestion scenario for future flooding occurance forecasting (2070).

Chapter Five

CONCLSION AND FUTURE RECOMMENDATIONS

5.1 Introduction

This study aimed to extrapolate the rainfall intensity depend on climate change and determine the flooding ratio in storm network of the case study.

ANN model was used to extrapolate the rainfall intensity depend on different climate change parameters. The results of analysis was very accurate, flexibility and reduce the length of the time spent in calibration.

5.2 Conclusion

The conclusion depended on the result can be summarized below:

1. The calibration of ANN model depend on R^2 and RMSE, the best models would have least RMSE(1.67 , 3.46), and greater R^2(0.722 , 0.64).
2. The result of ANN model indicate that the rainfall intensity increase with progress of time reach to 46.48 mm/h in winter 2067.
3. There are many factor of climate change that effect on the ANN model include : rainfall , wind speed , sun shine , humidity , min and max temperature ,but the most factor of climate change effect is the rainfall.

4. SWMM model was used to evaluate the storm drainage system in Al-Abbas quarter, Karbala, Iraq as a case study, it was very effective in the analysis of the flooding problem.The calibration of SWMM model for six rainfall event with rainfall intensity (7.86 ,27.5, 19.86, 11.66, 21.28, and 7.24)mm/hr was very good where the cross validation results show that the mean square error (MSE) for all events are very close to zero (0.000021). Moreover, root mean square error (RMSE) is very low as compared to the variance of the observed data for all events (0.0045).The correlation coefficient (R^2) equal to (0.83).
5. This study show the behavior of the drainage system of the study area under various rainfall intensities and the predictable flooding discharge for the flooding area.
6. The SWMM analysis storm drainage system met rainfall intensity greater than design intensity (13 mm/h) with peak rainfall intensity equal to 29.62 mm/h in winter 2028, with flooding duration 50 min and reach to stage 4 (from 0.05-0.12) m^3/s with ratio 1%.
7. The SWMM analysis storm drainage system met rainfall intensity greater than design intensity (13 mm/h) with peak rainfall intensity equal to 45.98 mm/h in winter 2055, with flooding duration 20 min and reach to stage 5 (greater than 0.12) m^3/s with ratio 6%.
8. The SWMM analysis storm drainage system met rainfall intensity greater than design intensity (13 mm/h) with peak rainfall intensity equal to 44.9 mm/h in winter 2060, with flooding duration 35 min and reach to stage 5 (greater than 0.12) m^3/s with ratio 6%.

9. The SWMM analysis storm drainage system met rainfall intensity greater than design intensity (13 mm/h) with peak rainfall intensity equal to 46.48 mm/h in winter 2067, that maximum intensity happened in future period (2017-2070), with flooding duration 45 min and reach to stage 5 (greater than 0.12) m^3/s with ratio 6%.
10. The percentage of flooding manhole at 2017 reach to stage 4 (0.05-0.12) m^3/s with ratio 3% while the percentage of flooding manhole at 2070 reach to stage 5 (greater than 0.12) m^3/s with ratio 6%.

5.3 Recommendation

The proposed mechanism to deal with the flood situation are:

1. Increase the diameter of the pipes to capacity the quantity of water.
2. Add second outlet to rid network from the flooding.

5.4 Further research

1. Using another program to analysis the climate change to predict rainfall intensity.
2. Take another case study in the region.

APPENDIX A – GIS STORM NETWORK DATA

OBJECTID	Upstream In	Downstream	Diameter	Slope	Install Date	Sector No_H	Length	القضا	sector	SHAPE_Length
1	25.93	25.8	315	0.003175	1/1/2007	العباس	50	المركز	باب بغداد	49.99999
2	25.96	25.8	315	0.003175	1/1/2007	العباس	41	المركز	باب بغداد	40.99996
3	26.1	25.96	315	0.003175	1/1/2007	العباس	28	المركز	باب بغداد	28.00003
4	0	0	315	0.003175	1/1/2007	العباس	2	المركز	باب بغداد	1.99995
5	26.05	25.93	315	0.003175	1/1/2007	العباس	50	المركز	باب بغداد	49.99998
6	25.8	25.71	400	0.0025	1/1/2007	العباس	31.2	المركز	باب بغداد	31.20007
7	25.71	25.625	400	0.0025	1/1/2007	العباس	30.3	المركز	باب بغداد	30.30004
8	25.83	25.625	315	0.003175	1/1/2007	العباس	49.2	المركز	باب بغداد	49.19996
9	25.951	25.83	315	0.003175	1/1/2007	العباس	49.4	المركز	باب بغداد	49.40001
10	25.625	25.536	400	0.0025	1/1/2007	العباس	63	المركز	باب بغداد	63.00004
11	25.646	25.536	315	0.003175	1/1/2007	العباس	51.8	المركز	باب بغداد	51.79998
12	25.736	25.646	315	0.003175	1/1/2007	العباس	50.6	المركز	باب بغداد	50.60004
13	25.856	25.736	315	0.003175	1/1/2007	العباس	50.3	المركز	باب بغداد	50.29999
14	25.926	25.856	315	0.003175	1/1/2007	العباس	28	المركز	باب بغداد	27.99997
15	25.536	25.466	400	0.0025	1/1/2007	العباس	30.6	المركز	باب بغداد	30.60002
16	25.466	25.4	400	0.0025	1/1/2007	العباس	31.6	المركز	باب بغداد	31.59998
17	25.561	25.4	315	0.003175	1/1/2007	العباس	50	المركز	باب بغداد	50
18	25.691	25.561	315	0.003175	1/1/2007	العباس	49.5	المركز	باب بغداد	49.50003
19	25.841	25.691	315	0.003175	1/1/2007	العباس	50.6	المركز	باب بغداد	50.59999
20	25.4	25.226	400	0.0025	1/1/2007	العباس	63	المركز	باب بغداد	62.99995
21	25.326	25.226	500	0.002	1/1/2007	العباس	64.5	المركز	باب بغداد	64.49996
22	25.49	25.326	400	0.0025	1/1/2007	العباس	62.2	المركز	باب بغداد	62.20001
23	25.61	25.49	400	0.0025	1/1/2007	العباس	35.7	المركز	باب بغداد	35.70002
24	25.72	25.61	400	0.0025	1/1/2007	العباس	50.3	المركز	باب بغداد	50.29995
25	25.496	25.326	400	0.0025	1/1/2007	العباس	44.4	المركز	باب بغداد	44.39997
26	25.566	25.496	400	0.0025	1/1/2007	العباس	39.2	المركز	باب بغداد	39.20005
27	25.661	25.566	400	0.0025	1/1/2007	العباس	42	المركز	باب بغداد	42.00002
28	25.906	25.661	315	0.003175	1/1/2007	العباس	44.8	المركز	باب بغداد	44.80004
29	26.046	25.906	315	0.003175	1/1/2007	العباس	60	المركز	باب بغداد	59.97993
30	25.996	25.906	315	0.003175	1/1/2007	العباس	26.4	المركز	باب بغداد	26.4
31	26.086	25.996	315	0.003175	1/1/2007	العباس	60.1	المركز	باب بغداد	60.11929
32	26.166	25.996	315	0.003175	1/1/2007	العباس	60.7	المركز	باب بغداد	60.65559
33	26.336	26.166	315	0.003175	1/1/2007	العباس	39.3	المركز	باب بغداد	39.34447
34	25.226	25.156	500	0.002	1/1/2007	العباس	43.2	المركز	باب بغداد	43.20001
35	25.156	25.101	500	0.002	1/1/2007	العباس	37.3	المركز	باب بغداد	37.30004

36	25.101	25.041	500	0.002	1/1/2007	العباس	43.7	المركز	باب بغداد	43.7
37	25.041	24.961	500	0.002	1/1/2007	العباس	45.2	المركز	باب بغداد	45.20002
38	24.961	24.889	500	0.002	1/1/2007	العباس	46	المركز	باب بغداد	45.99997
39	24.889	24.759	500	0.002	1/1/2007	العباس	34	المركز	باب بغداد	34.00004
40	24.759	24.629	500	0.002	1/1/2007	العباس	32	المركز	باب بغداد	32.00004
41	24.889	24.675	500	0.002	1/1/2007	العباس	32	المركز	باب بغداد	32.00001
42	24.813	24.675	500	0.002	1/1/2007	العباس	32	المركز	باب بغداد	32.00003
43	25.159	24.813	315	0.003175	1/1/2007	العباس	66	المركز	باب بغداد	66.00006
44	25.27	25.159	315	0.003175	1/1/2007	العباس	62.6	المركز	باب بغداد	62.59998
45	25.385	25.27	315	0.003175	1/1/2007	العباس	43.7	المركز	باب بغداد	43.70003
46	25.52	25.385	315	0.003175	1/1/2007	العباس	66.4	المركز	باب بغداد	66.36421
47	24.973	24.813	400	0.0025	1/1/2007	العباس	48	المركز	باب بغداد	48
48	25.119	24.973	400	0.0025	1/1/2007	العباس	49	المركز	باب بغداد	49.00001
49	25.279	25.119	400	0.0025	1/1/2007	العباس	54	المركز	باب بغداد	54.00003
50	25.413	25.279	315	0.003175	1/1/2007	العباس	26	المركز	باب بغداد	25.99996
51	0	0	315	0.003175	1/1/2007	العباس	6	المركز	باب بغداد	5.999977
52	25.479	25.413	315	0.003175	1/1/2007	العباس	25	المركز	باب بغداد	24.99997
53	25.619	25.479	315	0.003175	1/1/2007	العباس	53	المركز	باب بغداد	52.99999
54	25.729	25.619	315	0.003175	1/1/2007	العباس	52	المركز	باب بغداد	51.99998
55	25.831	25.729	315	0.003175	1/1/2007	العباس	48	المركز	باب بغداد	48.00002
56	25.61	25.479	315	0.003175	1/1/2007	العباس	59	المركز	باب بغداد	59.00006
57	25.056	24.966	400	0.0025	1/1/2007	العباس	22.6	المركز	باب بغداد	22.58902
58	25.126	25.056	400	0.0025	1/1/2007	العباس	38.5	المركز	باب بغداد	38.49996
59	24.965	24.629	500	0.002	1/1/2007	العباس	50	المركز	باب بغداد	49.99999
60	25.05	24.965	500	0.002	1/1/2007	العباس	49.5	المركز	باب بغداد	49.50005
61	25.13	25.05	500	0.002	1/1/2007	العباس	50.5	المركز	باب بغداد	50.50003
62	25.23	25.13	500	0.002	1/1/2007	العباس	60.6	المركز	باب بغداد	60.59996
63	25.31	25.23	500	0.002	1/1/2007	العباس	51.7	المركز	باب بغداد	51.70002
64	25.41	25.31	500	0.002	1/1/2007	العباس	49.5	المركز	باب بغداد	49.5
65	25.5	25.41	500	0.002	1/1/2007	العباس	50.7	المركز	باب بغداد	50.70002
66	25.58	25.5	500	0.002	1/1/2007	العباس	57.6	المركز	باب بغداد	57.60005
67	25.66	25.58	500	0.002	1/1/2007	العباس	45.5	المركز	باب بغداد	45.50002
68	25.75	25.66	500	0.002	1/1/2007	العباس	48.4	المركز	باب بغداد	48.40001
69	25.83	25.75	500	0.002	1/1/2007	العباس	38	المركز	باب بغداد	38.00002
70	25.9	25.83	500	0.002	1/1/2007	الهيابي	55	المركز	باب بغداد	54.99997
71	25.885	24.629	315	0.003175	1/1/2007	العباس	55	المركز	باب بغداد	54.99997
72	25.955	25.885	315	0.003175	1/1/2007	العباس	52	المركز	باب بغداد	52.00002
73	26.136	25.955	315	0.003175	1/1/2007	العباس	55	المركز	باب بغداد	54.99997
74	26.318	26.136	315	0.003175	1/1/2007	العباس	55	المركز	باب بغداد	55.00003

75	26.499	26.318	315	0.003175	1/1/2007	العباس	56	المركز	باب بغداد	55.99999
76	26.681	26.499	315	0.003175	1/1/2007	العباس	55	المركز	باب بغداد	55.00002
77	26.862	26.681	315	0.003175	1/1/2007	العباس	57	المركز	باب بغداد	57.00001
78	27.044	26.862	315	0.003175	1/1/2007	العباس	57	المركز	باب بغداد	57.00001
79	27.225	27.044	315	0.003175	1/1/2007	العباس	31	المركز	باب بغداد	30.99999
80	25.196	25.126	400	0.0025	1/1/2007	العباس	48.3	المركز	باب بغداد	48.29996
81	25.306	25.196	315	0.003175	1/1/2007	العباس	49	المركز	باب بغداد	48.99995
82	25.456	25.306	315	0.003175	1/1/2007	العباس	48	المركز	باب بغداد	48.00003
83	25.595	25.456	315	0.003175	1/1/2007	العباس	31.5	المركز	باب بغداد	31.50002
84	0	0	400	0.0025	1/1/2007	العباس	6	المركز	باب بغداد	5.999984
85	23.886	23.738	315	0.003175	1/1/2007	العباس	38	المركز	باب بغداد	37.99998
86	24.253	23.886	315	0.003175	1/1/2007	العباس	40	المركز	باب بغداد	39.99998
87	24.633	24.253	315	0.003175	1/1/2007	العباس	50	المركز	باب بغداد	49.99997
88	24.783	24.633	315	0.003175	1/1/2007	العباس	50	المركز	باب بغداد	50.00001
89	24.376	24.253	315	0.003175	1/1/2007	العباس	37	المركز	باب بغداد	37.00006
90	24.496	24.376	315	0.003175	1/1/2007	العباس	35	المركز	باب بغداد	35.00003
91	25.046	24.496	315	0.003175	1/1/2007	العباس	49	المركز	باب بغداد	48.99994
92	24.606	24.496	315	0.003175	1/1/2007	العباس	49	المركز	باب بغداد	48.99996
93	24.746	24.606	315	0.003175	1/1/2007	العباس	32	المركز	باب بغداد	31.99995
94	24.856	24.746	315	0.003175	1/1/2007	العباس	49	المركز	باب بغداد	49.00003
95	25	24.856	315	0.003175	1/1/2007	العباس	45	المركز	باب بغداد	44.99999
96	25.185	25	315	0.003175	1/1/2007	العباس	55	المركز	باب بغداد	54.99996
97	25.355	25.185	315	0.003175	1/1/2007	العباس	30	المركز	باب بغداد	29.99995
98	25.495	25.355	315	0.003175	1/1/2007	العباس	30	المركز	باب بغداد	30.00002
99	25.68	25.645	315	0.003175	1/1/2004	العباس	18.1	المركز	باب بغداد	18.0791
100	25.83	25.68	315	0.003175	1/1/2007	العباس	59.4	المركز	باب بغداد	59.42456
101	25.98	25.83	315	0.003175	1/1/2007	العباس	55	المركز	باب بغداد	55.00003
102	26.13	25.98	315	0.003175	1/1/2007	العباس	54	المركز	باب بغداد	53.99998
103	26.28	26.13	315	0.003175	1/1/2007	العباس	50	المركز	باب بغداد	50.00002
104	26.4	26.28	315	0.003175	1/1/2007	العباس	51	المركز	باب بغداد	50.99999
105	26.56	26.4	315	0.003175	1/1/2007	العباس	54	المركز	باب بغداد	53.99995
106	26.725	26.56	315	0.003175	1/1/2007	العباس	54	المركز	باب بغداد	53.99996
107	26.87	26.725	315	0.003175	1/1/2007	العباس	59	المركز	باب بغداد	59.00001
126	0	0	315	0.003175	1/1/2007	العباس	32	المركز	باب بغداد	31.99999
127	0	0	315	0.003175	1/1/2004	العباس	30	المركز	باب بغداد	30.00001
128	0	0	315	0.003175	1/1/2004	العباس	30	المركز	باب بغداد	30.00004
129	0	0	315	0.003175	1/1/2004	العباس	20.4	المركز	باب بغداد	20.37663
130	0	0	315	0.003175	1/1/2004	العباس	26	المركز	باب بغداد	25.99998
131	0	0	315	0.003175	1/1/2004	العباس	26	المركز	باب بغداد	25.99998

132	0	0	315	0.003175	1/1/2004	العباس	30	المركز	باب بغداد	30.00004
133	0	0	315	0.003175	1/1/2004	العباس	25	المركز	باب بغداد	25.00001
134	0	0	315	0.003175	1/1/2004	العباس	25	المركز	باب بغداد	25
135	0	0	315	0.003175	1/1/2004	العباس	26	المركز	باب بغداد	25.99997
136	0	0	315	0.003175	1/1/2004	العباس	26	المركز	باب بغداد	25.99999
137	0	0	315	0.003175	1/1/2004	العباس	26.5	المركز	باب بغداد	26.50003
138	0	0	315	0.003175	1/1/2004	العباس	30	المركز	باب بغداد	29.99995
139	0	0	315	0.003175	1/1/2004	العباس	30	المركز	باب بغداد	30.00001
140	0	0	315	0.003175	1/1/2004	العباس	17	المركز	باب بغداد	17.00001
141	0	0	315	0.003175	1/1/2007	العباس	32.4	المركز	باب بغداد	32.39996
142	0	0	315	0.003175	1/1/2004	العباس	30	المركز	باب بغداد	29.99997
143	0	0	315	0.003175	1/1/2004	العباس	32	المركز	باب بغداد	31.99998
144	0	0	315	0.003175	1/1/2004	العباس	33	المركز	باب بغداد	33.00002
145	0	0	315	0.003175	1/1/2004	العباس	30	المركز	باب بغداد	30.00004
146	0	0	315	0.003175	1/1/2004	العباس	30	المركز	باب بغداد	29.99999
147	0	0	315	0.003175	1/1/2004	العباس	26	المركز	باب بغداد	26.00005
148	0	0	315	0.003175	1/1/2004	العباس	31	المركز	باب بغداد	31.00002
149	0	0	315	0.003175	1/1/2004	العباس	32	المركز	باب بغداد	32.00001
150	0	0	315	0.003175	1/1/2004	العباس	31	المركز	باب بغداد	30.99997
151	0	0	315	0.003175	1/1/2004	العباس	30	المركز	باب بغداد	30.00011
152	0	0	315	0.003175	1/1/2004	العباس	30	المركز	باب بغداد	29.99998
153	0	0	315	0.003175	1/1/2004	العباس	26	المركز	باب بغداد	26.00001
154	0	0	315	0.003175	1/1/2004	العباس	24	المركز	باب بغداد	24.00001
155	0	0	315	0.003175	1/1/2004	العباس	30	المركز	باب بغداد	30.00004
156	0	0	315	0.003175	1/1/2004	العباس	30	المركز	باب بغداد	30.00004
157	0	0	315	0.003175	1/1/2004	العباس	31	المركز	باب بغداد	31
158	0	0	315	0.003175	1/1/2004	العباس	33	المركز	باب بغداد	33.00005
159	0	0	315	0.003175	1/1/2004	العباس	51	المركز	باب بغداد	51.00003
160	0	0	315	0.003175	1/1/2004	العباس	23	المركز	باب بغداد	23
161	0	0	315	0.003175	1/1/2004	العباس	24	المركز	باب بغداد	23.99999
162	0	0	315	0.003175	1/1/2004	العباس	26	المركز	باب بغداد	25.99999
163	0	0	315	0.003175	1/1/2004	العباس	31	المركز	باب بغداد	31.00007
164	0	0	315	0.003175	1/1/2004	العباس	30	المركز	باب بغداد	29.99987
165	0	0	315	0.003175	1/1/2004	العباس	28	المركز	باب بغداد	27.99994
166	0	0	315	0.003175	1/1/2004	العباس	29	المركز	باب بغداد	29.00008
167	0	0	315	0.003175	1/1/2004	العباس	30	المركز	باب بغداد	29.99997
168	0	0	315	0.003175	1/1/2004	العباس	23	المركز	باب بغداد	22.99996
169	0	0	315	0.003175	1/1/2004	العباس	32	المركز	باب بغداد	32.00001
170	0	0	315	0.003175	1/1/2004	العباس	30	المركز	باب بغداد	30.00004

171	24.966	24.889	400	0.0025	1/1/2007	العباس	67	المركز	باب بغداد	67.01099
172	0	0	315	0.003175	1/1/2007	العباس	33	المركز	باب بغداد	32.99997
173	0	0	315	0.003175	1/1/2004	العباس	30	المركز	باب بغداد	30.00003
174	0	0	315	0.003175	1/1/2004	العباس	30	المركز	باب بغداد	29.99998
175	0	0	315	0.003175	1/1/2004	العباس	32	المركز	باب بغداد	32.00002
176	0	0	315	0.003175	1/1/2004	العباس	30	المركز	باب بغداد	30.00001
177	0	0	315	0.003175	1/1/2004	العباس	31	المركز	باب بغداد	30.99998
178	0	0	315	0.003175	1/1/2004	العباس	20	المركز	باب بغداد	20.00004
179	0	0	315	0.003175	1/1/2004	العباس	20	المركز	باب بغداد	20.00002
180	0	0	315	0.003175	1/1/2007	العباس	25.4	المركز	باب بغداد	25.40811
181	0	0	315	0.003175	1/1/2004	العباس	31	المركز	باب بغداد	31.00006
182	0	0	315	0.003175	1/1/2004	العباس	32	المركز	باب بغداد	32.00001
183	0	0	315	0.003175	1/1/2004	العباس	25	المركز	باب بغداد	24.99999
184	0	0	315	0.003175	1/1/2007	العباس	27	المركز	باب بغداد	27.00001
185	0	0	315	0.003175	1/1/2004	العباس	27	المركز	باب بغداد	26.99999
186	0	0	315	0.003175	1/1/2004	العباس	28	المركز	باب بغداد	28.00002
187	0	0	315	0.003175	1/1/2004	العباس	28	المركز	باب بغداد	27.99997
188	0	0	315	0.003175	1/1/2004	العباس	20	المركز	باب بغداد	20
189	25.759	25.61	315	0.003175	1/1/2007	العباس	67.3	المركز	باب بغداد	67.27319
190	0	0	315	0.003175	1/1/2007	العباس	28	المركز	باب بغداد	28
191	0	0	315	0.003175	1/1/2004	العباس	35	المركز	باب بغداد	35.00002
192	0	0	315	0.003175	1/1/2004	العباس	36	المركز	باب بغداد	36.00004
193	0	0	315	0.003175	1/1/2004	العباس	30	المركز	باب بغداد	30.00003
194	0	0	315	0.003175	1/1/2004	العباس	29	المركز	باب بغداد	28.99997
195	0	0	315	0.003175	1/1/2004	العباس	29	المركز	باب بغداد	29.00003
196	0	0	315	0.003175	1/1/2004	العباس	32.1	المركز	باب بغداد	32.10246
197	0	0	315	0.003175	1/1/2004	العباس	30	المركز	باب بغداد	30
198	0	0	315	0.003175	1/1/2004	العباس	30	المركز	باب بغداد	30.00003
199	0	0	315	0.003175	1/1/2004	العباس	30	المركز	باب بغداد	29.99998
200	0	0	315	0.003175	1/1/2004	العباس	33	المركز	باب بغداد	33
201	0	0	315	0.003175	1/1/2004	العباس	24	المركز	باب بغداد	23.99999
202	0	0	315	0.003175	1/1/2004	العباس	30	المركز	باب بغداد	29.99996
203	0	0	315	0.003175	1/1/2004	العباس	31	المركز	باب بغداد	31.00001
204	0	0	315	0.003175	1/1/2004	العباس	26	المركز	باب بغداد	25.99998
205	0	0	315	0.003175	1/1/2004	العباس	23.5	المركز	باب بغداد	23.49997
206	0	0	315	0.003175	1/1/2007	العباس	22	المركز	باب بغداد	21.99995
207	0	0	315	0.003175	1/1/2004	العباس	30	المركز	باب بغداد	29.99993
208	0	0	315	0.003175	1/1/2004	العباس	31	المركز	باب بغداد	31.00004
209	0	0	315	0.003175	1/1/2004	العباس	41	المركز	باب بغداد	41.00001

210	0	0	315	0.003175	1/1/2004	العباس	40	المركز	باب بغداد	40.00003
211	0	0	315	0.003175	1/1/2004	العباس	58	المركز	باب بغداد	57.99996
212	0	0	315	0.003175	1/1/2004	العباس	21.6	المركز	باب بغداد	21.63831
213	0	0	315	0.003175	1/1/2004	العباس	31	المركز	باب بغداد	30.99995
214	0	0	315	0.003175	1/1/2004	العباس	30	المركز	باب بغداد	29.99999
215	0	0	315	0.003175	1/1/2004	العباس	29	المركز	باب بغداد	28.99997
216	0	0	315	0.003175	1/1/2004	العباس	30	المركز	باب بغداد	29.99998
217	0	0	315	0.003175	1/1/2004	العباس	30	المركز	باب بغداد	30.00001
218	0	0	315	0.003175	1/1/2004	العباس	30	المركز	باب بغداد	29.99998
219	0	0	315	0.003175	1/1/2004	العباس	29	المركز	باب بغداد	29.00001
220	0	0	315	0.003175	1/1/2004	العباس	30	المركز	باب بغداد	30.00001
221	0	0	315	0.003175	1/1/2004	العباس	26	المركز	باب بغداد	25.99998
222	0	0	315	0.003175	1/1/2004	العباس	25	المركز	باب بغداد	24.99999
223	0	0	315	0.003175	1/1/2004	العباس	25	المركز	باب بغداد	25.00004
224	0	0	315	0.003175	1/1/2004	العباس	48	المركز	باب بغداد	48.00002
225	0	0	315	0.003175	1/1/2007	العباس	26	المركز	باب بغداد	26.00008
226	0	0	315	0.003175	1/1/2004	العباس	32	المركز	باب بغداد	31.99987
227	0	0	315	0.003175	1/1/2004	العباس	30	المركز	باب بغداد	30.00003
228	0	0	315	0.003175	1/1/2004	العباس	32	المركز	باب بغداد	31.99992
229	0	0	315	0.003175	1/1/2004	العباس	32	المركز	باب بغداد	32.00004
230	0	0	315	0.003175	1/1/2004	العباس	28	المركز	باب بغداد	27.99996
231	0	0	315	0.003175	1/1/2004	العباس	17	المركز	باب بغداد	16.9672
232	0	0	315	0.003175	1/1/2007	العباس	19	المركز	باب بغداد	19.00004
233	0	0	315	0.003175	1/1/2004	العباس	10	المركز	باب بغداد	10.00002
234	0	0	600	0.001667	1/1/2004	العباس	53	المركز	باب بغداد	52.99997
235	0	0	600	0.001667	1/1/2004	العباس	50	المركز	باب بغداد	50.00003
236	0	0	600	0.001667	1/1/2004	العباس	50	المركز	باب بغداد	49.99996
237	0	0	600	0.001667	1/1/2004	العباس	50	المركز	باب بغداد	50.00002
238	0	0	600	0.001667	1/1/2004	العباس	44	المركز	باب بغداد	44
239	0	0	600	0.001667	1/1/2007	العباس	51.2	المركز	باب بغداد	51.19109
244	0	0	315	0	1/1/2007	العباس	0	المركز	باب بغداد	55.2471

List of Reference

AL-ANSARI, N., ABDELLATIF, M., ALI, S. S. & KNUTSSON, S. 2014. Long term effect of climate change on rainfall in northwest Iraq. *Central European Journal of Engineering,* 4**,** 250-263.

ALFATLAWI, T. J. & ALSHAKLI, H. I. 2015. Prediction the Coefficient of Discharge for Stepped Morning Glory Spillway Using ANN and MNLR Approaches.

BIJLSMA, L., EHLER, C., KLEIN, R., KULSHRESTHA, S., MCLEAN, R., MIMURA, N., NICHOLLS, R., NURSE, L., NIETO, H. P. & STAKHIV, E. 1996. Coastal zones and small islands. Cambridge University Press, Cambridge, United Kingdom and New York, NY, USA.

BOIX, A. P. 2017. towerd sustained cities through an envormental ,ecnomic and eco-effeciency and drainage system

BOUZERIA, H., GHENIM, A. N. & KHANCHOUL, K. 2017. Using artificial neural network (ANN) for prediction of sediment loads, application to the Mellah catchment, northeast Algeria. *Journal of Water and Land development,* 33**,** 47-55.

CYBENKO, G. 1989. Approximation by superpositions of a sigmoidal function. *Mathematics of control, signals and systems,* 2**,** 303-314.

DAWSON, C. W. & WILBY, R. 1998. An artificial neural network approach to rainfall-runoff modelling. *Hydrological Sciences Journal,* 43**,** 47-66.

DENAULT, C., MILLAR, R. G. & LENCE, B. J. 2006. Assessment of possible impacts of climate change in an urban catchment. *JAWRA Journal of the American Water Resources Association,* 42**,** 685-697.

EVANS, J. P. 2009. 21st century climate change in the Middle East. *Climatic Change,* 92**,** 417-432.

G.A.A.S.O 2018. General Authority for Aeronautical and Seismic Observations

GIRONÁS, J., ROESNER, L. A., DAVIS, J., ROSSMAN, L. A. & SUPPLY, W. 2009. *Storm water management model applications manual,* National Risk Management Research

Laboratory, Office of Research and Development, US Environmental Protection Agency Cincinnati, OH.

GIRONÁS, J., ROESNER, L. A., ROSSMAN, L. A. & DAVIS, J. 2010. A new applications manual for the Storm Water Management Model (SWMM). *Environmental Modelling & Software,* 25**,** 813-814.

GIUSEPPE CIABURRO, B. V. & SEPTEMBER 2017
Neural network with R

HASSAN, W. H., NILE, B. K. & AL-MASODY, B. A. 2017. Study the climate change effect on storm drainage networks by storm water management model [SWMM].

HINTON, G. E., OSINDERO, S. & TEH, Y.-W. 2006. A fast learning algorithm for deep belief nets. *Neural computation,* 18**,** 1527-1554.

HORNIK, K. 1991. Approximation capabilities of multilayer feedforward networks. *Neural networks,* 4**,** 251-257.

HOUGHTON, J. T. 1996. *Climate change 1995: The science of climate change: contribution of working group I to the second assessment report of the Intergovernmental Panel on Climate Change*, Cambridge University Press.

HUONG, H. & PATHIRANA, A. 2013. Urbanization and climate change impacts on future urban flooding in Can Tho city, Vietnam. *Hydrology and Earth System Sciences,* 17**,** 379-394.

I.A.C.D 2018. Iraqi Agromet Center Data

JAIN, S., DAS, A. & SRIVASTAVA, D. 1999. Application of ANN for reservoir inflow prediction and operation. *Journal of water resources planning and management,* 125**,** 263-271.

JENG, D., CHA, D. & BLUMENSTEIN, M. Application of neural network in civil engineering problems. Proceedings of the International Conference on Advances in the Internet, Processing, Systems and Interdisciplinary Research, 2003.

JIANG, L., CHEN, Y. & WANG, H. 2015. Urban flood simulation based on the SWMM model. *Proceedings of the International Association of Hydrological Sciences,* 368**,** 186-191.

JUNG, M., KIM, H., MALLARI, K., PAK, G. & YOON, J. 2015. Analysis of effects of climate change on runoff in an urban drainage system: a case study from Seoul, Korea. *Water Science and Technology*, 71**,** 653-660.

LUK, K. C., BALL, J. E. & SHARMA, A. 2001. An application of artificial neural networks for rainfall forecasting. *Mathematical and Computer modelling*, 33**,** 683-693.

MLNNOTEBOOK 2017. A Simple Neural Network - Transfer Functions. 08 Mar 2017.

MURATA, N., YOSHIZAWA, S. & AMARI, S.-I. 1994. Network information criterion-determining the number of hidden units for an artificial neural network model. *IEEE Transactions on Neural Networks*, 5**,** 865-872.

NIE, L., LINDHOLM, O., LINDHOLM, G. & SYVERSEN, E. 2009. Impacts of climate change on urban drainage systems–a case study in Fredrikstad, Norway. *Urban Water Journal*, 6**,** 323-332.

NIRUPAMA, N. & SIMONOVIC, S. P. 2007. Increase of flood risk due to urbanisation: a Canadian example. *Natural Hazards*, 40**,** 25.

OSMAN, Y. 2017. Climate Change and Future Precipitation in Arid Environment of Middle East: Case study of Iraq: Climate Change and Future Precipitation in Arid Environment of Middle East: Case study of Iraq. *Journal of Environmental Hydrology*, 25**,** 1-18.

PITT, R., LILBURN, M., NIX, S., DURRANS, S., BURIAN, S., VOORHEES, J. & MARTINSON, J. 1999. Guidance Manual for Integrated Wet Weather Flow (WWF) Collection and Treatment Systems for Newly Urbanized Areas (New WWF Systems). *Current and Future Design Practices*.

RAWLS, W. J., BRAKENSIEK, D. L. & MILLER, N. 1983. Green-ampt Infiltration Parameters from Soils Data. *Journal of Hydraulic Engineering*, 109**,** 62-70.

REYNARD, N. S., PRUDHOMME, C. & CROOKS, S. M. 2001. The flood characteristics of large UK rivers: potential effects of changing climate and land use. *Climatic change*, 48**,** 343-359.

ROSSMAN, L. A. 2010. *Storm water management model user's manual, version 5.0*, National Risk Management Research Laboratory, Office of Research and Development, US Environmental Protection Agency Cincinnati.

SAGHAFIAN, B., FARAZJOO, H., BOZORGY, B. & YAZDANDOOST, F. 2008. Flood intensification due to changes in land use. *Water resources management*, 22**,** 1051-1067.

SANSOM, J. & RENWICK, J. A. 2007. Climate change scenarios for New Zealand rainfall. *Journal of Applied Meteorology and Climatology,* 46**,** 573-590.

SCHREIDER, S. Y., SMITH, D. & JAKEMAN, A. 2000. Climate change impacts on urban flooding. *Climatic Change,* 47**,** 91-115.

SEMADENI-DAVIES, A., HERNEBRING, C., SVENSSON, G. & GUSTAFSSON, L.-G. 2008. The impacts of climate change and urbanisation on drainage in Helsingborg, Sweden: Suburban stormwater. *Journal of hydrology,* 350**,** 114-125.

SUJANA PRAJITHKUMAR, D., VERMA, S. & MAHAJAN, B. Application of ANN model for the prediction of Water Quality Index. *International Journal of Engineering Research and General Science,* 3.

TOKAR, A. S. & JOHNSON, P. A. 1999. Rainfall-runoff modeling using artificial neural networks. *Journal of Hydrologic Engineering,* 4**,** 232-239.

USGS 2018. U.S. Geological Survey

الخلاصة

يحدث فيضان شبكة مياه الأمطار بسبب تغير المناخ وتغير استخدام الأراضي وزيادة التمدن والسكان على نطاق أوسع. تتناول هذه الدراسة تطوير نماذج لتنبئ التغيير المستقبلي في أحداث هطول الأمطار من أجل حماية البنى التحتية لشبكة مياه الأمطار من الفيضانات. تم اختيار حي العباس في مدينة كربلاء ، العراق كدراسة حالة. بالنسبة للتحليل الأول ، فإن تأثير تغير المناخ على كثافة الأمطار المتوقعة للفترة المستقبلية (٢٠١٧-٢٠٧٠) يعتمد على البيانات التاريخية للفترة ١٩٨٠ - ٢٠١٦. وقد تم إجراء هذا باستخدام نموذج الشبكة العصبية الاصطناعية (ANN).تتضمن طبقات الدخول التي تدخل في نموذج ANN عوامل التغير المناخي وتشمل (هطول الأمطار شهريًا ودرجة الحرارة ودرجة الحرارة القصوى وسرعة الرياح والرطوبة وأشعة الشمس). هذه البيانات مقسمة إلى بيانات التدريب تمثل ٩٥ ٪ من البيانات وبيانات الاختبار تمثل ٥ ٪ لعملية المعايرة. عوامل الاخراج تشمل كثافة هطول الأمطار. بعد ذلك ، تم بناء نموذج إدارة مياه العواصف (SWMM) من أجل تقييم ظروف الفيضان في منطقة الدراسة لكثافة الأمطار المتوقعة. تشير النتائج إلى أن الحد الأقصى لكثافة الأمطار سيبلغ ٤٦.٤٨ ملم / ساعة. في عام ٢٠٦٧. تمثل هذه القيمة ثلاث مرات من كثافة التصميم. وتزداد نسبة فيضان المنهولات مع تقدم الوقت. في نهاية فترة التصميم (٢٠٧٠) تم تخفيض المرحلة الأولى بمعدل حوالي ٣٩.٢٪ ، وتمت زيادة المرحلة الثانية بمعدل ١٤.٢٪ ، وتمتاز المرحلة الثالثة بزيادة ٦ مرات ، والمرحلة لا تتغير ، والمرحلة الخامسة تزيد مع معدل ٦٪ مقارنة بفترة البداية (٢٠١٧).

جمهورية العراق
وزارة التعليم العالي والبحث العلمي
جامعة كربلاء
كلية الهندسة
قسم الهندسة المدنية

تأثير تغير المناخ في نظام شبكة مياه الامطار:
دراسة الحالة في كربلاء

رسالـــــــــة

مقدمة إلى كلية الهندسة في جامعة كربلاء

وهي جزء من متطلبات نيل درجة ماجستير في الهندسة المدنية

(هندسة البنى التحتية)

من قبل :

غفران عبدالحسين محمدحسن علي

(بكالوريوس في علوم الهندسة المدنية ٢٠١٥)

بإشراف:

أ.د. باسم خليل نايل

أ.م.د. واقد حميد حسن

2019